Chapter 4: Observations: Cryosphere

Coordinating Lead Authors: Josefino C. Comiso (USA), David G. Vaughan (UK)

Lead Authors: Ian Allison (Australia), Jorge Carrasco (Chile), Georg Kaser (Austria), Ronald Kwok (USA), Philip Mote (USA), Tavi Murray (UK), Frank Paul (Switzerland), Jiawen Ren (China), Eric Rignot (USA), Olga Solomina (Russia), Koni Steffen (USA), Tingjun Zhang (USA)

Contributing Authors: Anthony A. Arendt (USA), David B. Bahr (USA), Michiel van den Broeke, (Netherlands), Ross Brown (Canada), J. Graham Cogley (Canada), Alex S. Gardner (USA), Stephan Gruber (Switzerland), Christian Haas (Canada), Jon Ove Hagen (Norway), Regine Hock (USA), David Holland, (USA), Thorsten Markus (USA), Rob Massom (Australia), Pier Paul Overduin (Germany), W. Tad Pfeffer (USA), Terry Prowse (Canada), Valentina Radic (Canada), David Robinson (USA), Martin Sharp (Canada), K. Shikomanov (USA), Sharon Stammerjohn (USA), Isabella Velicogna, (USA), Anthony Worby (Australia), L. Zhao (China)

Review Editors: Jonathan Bamber (UK), Philippe Huybrechts (Belgium), Peter Lemke (Germany)

Date of Draft: 16 December 2011

Notes: TSU Compiled Version

Table of Contents

Executive Summary

The cryosphere, comprising snow, river and lake ice, sea ice, glaciers, ice shelves and ice sheets, and frozen ground, plays a major role in the Earth's system through its impact on the surface energy budget, sea level change, water cycle, primary productivity and surface gas exchange, and is thus a fundamental control on physical, biological and social environment over substantial areas of the Earth's surface. Given the inherent temperature-sensitivity of all components of the cryosphere on a wide range of time scales, the cryosphere is a natural integrator of climate variability that provides some of the most visible signatures of change in the Earth climate system. Since the AR4, observational technology has improved, and key time-series of measurements have been lengthened, such that our measurement of changes and trends in all components of the cryosphere has been substantially improved and our understanding of the specific processes governing their responses has been refined.

The highlights of observed changes in sea ice, land ice, snow cover and permafrost are as follows:

- The significant retreat in the extent of Arctic sea ice, in all seasons, that was documented by AR4 has continued. Since 1979, the annual average extent of ice in the Arctic has decreased by 4% per decade. The decline in extent at the end of summer has been even greater at 12% per decade, and the decadal average extent of the September minimum Arctic ice cover has decreased each decade since satellite records commenced. Submarine and satellite records provide robust evidence that the thickness of Arctic ice, and hence the total mass of ice, has been decreasing since the 1980s. This is the result of the loss of the thicker multiyear ice due to melt and export from the Arctic Basin. Approximately 17% of this ice has been lost per decade between 1979 and 1999, and another 40% has been lost since 1999. In contrast, the total extent of Antarctic sea ice has increased slightly over the same 30-year period (1.3% per decade), but there are strong regional differences in the changes around the Antarctic. There are no measurements of Antarctic sea ice thickness over time, and we do not know whether the total volume (or mass) of Antarctic sea ice is decreasing, steady, or increasing.

- Retreat of glaciers in mountain is highly visible and widespread. Length variations of a few individual valley glaciers are among the longest directly-observed climate system variables dating even back to the 16th or 17th Century. Overall, these glaciers have lost considerable mass since about 1850 with spatially and temporally varying rates. Since about 1960, mass budget measurements show different regional patterns with the highest variance in rates of mass changes in regions with maritime climates. Cold high latitude regions, generally have less negative rates of mass change. Mass changes of Central Europe show a strong linear trend of increasing loss and a recently increased loss has also been observed for Alaska, the Canadian Arctic, and the Southern Andes. Contribution to sea level rise is strongest from Alaska and the glaciers in Antarctica and Sub-Antarctica, most recently also from the Canadian Arctic, followed by northern Central Asia. Globally, present glacier mass loss rates are at about 1 mm SLE per year, slightly lower than for the five-year period 2001–2005.

- Confidence in the measurement of mass change in the polar ice sheets (Antarctica and Greenland) has increased considerably since AR4 as new technologies and measurement technique have been used more widely and as measurements become available over longer time periods. Independent techniques of assessment of ice sheet change give consistent (robust) evidence that parts of the Antarctic and Greenland ice sheets are losing mass. The same techniques indicate that the mass loss has been increasing with time over the last two decades on record. Overall, the ice sheets in Greenland and Antarctica have certainly been contributing to sea level rise over 1992 to 2011. Uncertainty in the estimation of ice sheet mass losses has reduced considerably so that there is strong agreement in the rates of mass loss for Greenland and moderate agreement for Antarctica. Over the period 1992–2011, Greenland lost on average 120 ± 30 Gt yr^{-1} (6–7 mm of sea level equivalent) and Antarctica lost 75 ± 20 Gt yr^{-1} (4 mm of sea level equivalent). In the GRACE period 2002–2011, the losses were higher in Greenland (230 ± 30Gt yr^{-1}) and Antarctica (175 ± 70 Gt yr^{-1}). The major part of the signal was very likely caused by changes in ice flow in Antarctica, and certainly by a mix of changes in ice flow and increases in snow/ice melt in Greenland.

- The judicious combination of in situ observations with satellite-derived snow cover extent indicates a decline in snow cover extent in most months over the 1922–2010 period of record; the largest declines (8%) occur in spring and are strongly correlated with atmospheric temperature and precipitation. Studies based on station observations reveal trends that vary considerably from one region to another but tend to indicate less snow at warmer locations which are also sensitive to spring melting, and more snow in very cold locations (such as, high mountains or high latitudes) where an increase in temperature is correlated with an increase in snowfall.

- During the past three decades, significant degradation of the permafrost has been observed. The average temperature of the permafrost has increased by up to 3°C since the late-1970s in some regions of the Arctic. The areal extent of permafrost is declining because the permafrost boundary has been moving towards higher latitudes and higher elevations, in part because the thin permafrost component is disappearing. The active layer thickness (ALT) has increased by several centimetres to more than one meter during the past two to three decades with strong regional differences. The thickness of seasonally frozen ground has decreased by about 32 cm from 1930 through 2000 across Russia with minimal changes during the 2000s, and by 20 to 40 cm from 1960 to the present on the Qinghai-Xizang (Tibetan) Plateau. Satellite records show that the thaw season has expanded by more than two weeks from 1988 through 2007 across central and eastern Asia.

4.1 Introduction

The cryosphere is the collective term for the components of the Earth system that comprise a substantial fraction of water in the frozen state (Table 4.1). The cryosphere comprises several components: snow, river and lake ice; sea ice; glaciers in mountainous regions, ice caps and ice sheets; and finally, frozen ground which exists, both on land and beneath the oceans (Figure 4.1). The lifespan of each components is very different. River and lake ice, for example, are transient features that generally do not survive from winter to summer; sea ice advances and retreats with the seasons but especially in the Arctic can survive to become multi-year ice, lasting several years: the East Antarctic ice sheet, on the other hand, is believed to have survived for more than 30 Million years (DeConto and Pollard, 2003). Nevertheless, all components of the cryosphere are inherently sensitive to changes in surface temperature and hence to a changing climate (see Chapter 2).

[INSERT FIGURE 4.1 HERE]

Figure 4.1: The cryosphere in the Northern and Southern Hemispheres in polar projection. The map of the Northern Hemisphere shows the sea ice cover during minimum extent (9th September 2011). The yellow line is the average location of the ice edge (15% ice concentration) for the yearly minima for 1979 to 2011. Areas of continuous permafrost are shown in darker pink, discontinuous permafrost in lighter pink. The shaded area over land and permafrost shows snow cover as derived from MODIS data (July 2009 to March 2010) with the greatest extent during that period represented by the white line. The Greenland ice sheet (white) and locations of glaciers (yellow) are also shown, but the glaciers within the ice sheet are shown as part of the ice sheet. The map of the Southern Hemisphere shows approximately the maximum sea ice cover during an austral winter (9th September 2011). The yellow line shows the average ice edge (15% ice concentration) during maximum extents of the sea ice cover for 1979 to 2011. Some of the elements (e.g., some glaciers and snow) located at low latitudes are not visible in this projection (see Figure 4.8). The source of the data for sea ice, permafrost, snow and ice sheet are datasets held at the National Snow and Ice Data Center (NSIDC), University of Colorado, on behalf of the North American Atlas, Instituto Nacional de Estadstica Geografa e Informatica, Natural Resources Canada, U.S. Geological Survey, Government of Canada, Canada Centre for Remote Sensing and The Atlas of Canada. Sources of glacier outlines: Weidick et al. (1992); Zheltyhina (2005). Figure courtesy of the NASA Visualization Group.

Changes in the long-lived components of the cryosphere (e.g., glaciers) are the result of an integrated response to climate, and they are often referred to as 'natural thermometers', but as our understanding of the complexity of this response has grown, it is becoming increasingly clear that elements of the cryopshere should rather be considered as 'natural climate-meters', responsive not only to temperature, but also to other climate variables (e.g.; precipitation). However, it remains the case that the highly visible nature of the changing cryosphere (in particular; sea ice, glaciers and ice sheets) means they are frequently used emblems of the impact of changing climate, and for this reason, it is imperative that we understand the context of current change within the framework of past changes and natural variability.

The cryosphere is, however, not simply a passive indicator of climate change; changes in each component of the cryosphere have a significant and lasting impact on physical, biological and social systems. Ice sheets and glaciers (Figure 4.2) exert a major control on global sea level (see WGII Chapter 5), and the loss of glaciers may have direct impacts on water resources used by many populations (see WGII Chapter 24). Similarly, reduced sea ice extent has, and may in future, altered ocean circulation, ocean productivity and regional climate, and will have direct impacts on shipping and mineral and oil explorations (see WGII Chapter 24). Furthermore, declines in snow cover and sea ice will amplify regional warming through the ice albedo feedback effect (see Chapter 9). Finally, changes in frozen ground (in particular, permafrost) will damage arctic infrastructure (see WGII Chapter 28), and could substantially alter the carbon budget across through the release of methane (see Chapter 6).

[INSERT FIGURE 4.2 HERE]

Figure 4.2: Block diagram showing the progression of characteristics from glaciers in mountainous regions, which exist across a wide range of latitudes, through tidewater and marine glaciers, to polar ice sheets which occur exclusively in polar regions. (Drafted by J. Oliver, BAS)

Since the AR4, substantial progress has been made throughout cryospheric research. Satellite technologies now permit rather precise estimates of regional and temporal changes in the volume and mass of the ice sheets. The longer time-series now available enable more accurate assessments of trends and anomalies in sea ice cover and rapid identification of unusual events such as the dramatic decline of perennial sea ice in

2007. Similarly, sea ice thickness can now be measured using satellite altimetry, allowing pan-Arctic measurements of changes in volume and mass. A nearly complete glacier inventory covers now almost all glaciers worldwide (42% in AR4) and allows for better estimates of the total ice volume. Remote measurements of regional glacier volume are also now available and modelling of glacier mass change has improved considerably. Finally, fluctuations in the cryosphere in distant and recent past have been mapped with increasing certainty, demonstrating the potential for rapid loss, compared to slow recovery, particularly when related to sea level rise.

This chapter describes the current state and observed variability of the cryosphere with a focus on recent improvements in understanding, addressing each of the important components of the cryosphere in turn. Given space constraints, less important but nonetheless significant components are not discussed, even though they may show changes that could be related to climate. Although observed trends are presented, projections of future cryospheric changes are discussed elsewhere (e.g., Chapter 13). Earlier IPCC reports used cryospheric terms that have specific scientific meanings (see Cogley et al., 2011), but have rather different meanings in everyday language. To avoid confusion, this chapter uses the term "glaciers" for what has previously termed, "glaciers and ice caps" (e.g., IPCC, 2007). For the largest glaciers, those covering Greenland and Antarctica, we use "ice sheet". For simplicity, we use units such as Gigatonnes (Gt, 10^{12} tonnes, or 10^{15} kg). One Gt is roughly equal to cubic kilometre of water (1.1 km^3 of ice), and 362 Gt of ice removed from the land and immersed in the oceans will cause roughly 1 mm of global sea level rise.

Table 4.1: Cryospheric components, sensitivity to climate and potential impacts.

Ice on land		% of global land surface [j]	Sea level equivalent [k] (m)
	Antarctic ice sheet [a]	8.3%	56.6
	Greenland ice sheet [b]	1.2%	7.4
	Glaciers [c]	0.4%	0.5
	Permafrost [d]	*15.5%*	*0.03–0.10*
	Seasonally frozen ground [e]	33%	0.0
	Seasonal snow cover (seasonally variable) [f]	1.3% to 30.6%	0.001–0.01
	Total	**30.6% to 57.9%**	**64.6 m**
Ice in the ocean		**% of global ocean area [j]**	**Volume [l] (10^3 km^3)**
	Antarctic ice shelves [g]	0.21%	~761
	Antarctic sea ice (seasonally variable)	0.8% to 5.2%	4.5–19.0
	Arctic sea ice (seasonally variable)	1.7% to 3.9%	18.0–35.0
	Sub-sea permafrost	???	???
	Total	**5.1% to 7.3%**	**37.7 to 40.2**

Notes:
[a] Lythe et al., 2001
[b] Griggs and Bamber, 2011a
[c] Dyuergerov and Meier, 2005; excludes glaciers around Greenland and Antarctica
[d] Zhang and al., 1999; excluding permafrost under ocean, ice sheets and glaciers and the permafrost in the Southern Hemisphere
[e] Zhang and al., 2003; excludes Southern Hemisphere
[f] Lemke et al., 2007
[g] Values derived from published data (Griggs and Bamber, 2011b)
[j] Assuming a global land area of 147.6 Million km^2, and ocean area of 362.5 Million km^2
[k] Assuming an ice density of 917 kg m^{-3}, a seawater density of 1,028 kg m^{-3}, with seawater replacing currently ice below sea level
[l] Calculated assuming average Antarctic austral summer (winter) thicknesses of 1.0 (1.5) m, and average Arctic boreal summer (winter) thickness of 2.5 (3.0) m (Kwok et al., 2009)

4.2 Sea Ice

4.2.1 Background

Sea ice is an important component of the climate system. A sea ice cover on the ocean changes the surface albedo, insulates the ocean from heat loss, and provides a barrier to the exchange of momentum and gases such as water vapour and CO2 between the ocean and atmosphere. Salt ejected by growing sea ice alters the density structure and modifies the circulation of the ocean. Regional climate changes affect the sea ice characteristics and the ice changes can feed back on the climate system, both regionally and globally. Sea ice is also a major component of polar ecosystems; plants and animals at all trophic levels use sea ice as their habitat.

Most sea ice exists as pack ice, and wind and ocean currents drive the drift of individual pieces of ice (called floes). Divergent pack-ice motion creates areas of open water where, during colder months, new ice can quickly form and grow. On the other hand, convergent ice motion causes the ice cover to thicken by deformation. Two relatively thin floes colliding with each other can "raft", stacking on top of each other and thickening the ice. When thicker ice collide, thick ridges may be built from broken pieces, with a height above the surface (ridge sail) of 2 m or more, and a much greater thickness (~10 m) and width below the surface (ridge keel).

Sea ice thickness also increases during winter months by basal freezing. But the thicker the ice becomes the more it insulates heat loss from the ocean to the atmosphere and the slower the basal growth is: there is an equilibrium thickness for basal ice growth that is dependent on the air temperature, and on any source of heat from the deep ocean below. Snow cover on the ice provides additional insulation, as well as altering the surface albedo and aerodynamic roughness. But, particularly in the Antarctic, a heavy snow load on thin ice can depress the ice surface and allow seawater to flood the snow. This saturated snow layer freezes quickly to form "snow ice" (see FAQ 4.2).

Because sea ice is formed from seawater it contains sea salt in small pockets of concentrated brine. The total salt content in newly formed sea ice is only 25–50% of that in the parent seawater, and the residual salt ejected as the ice forms impacts the ocean density and stability. The salinity of the ice decreases as it ages, particularly for multiyear ice where melt ponds can form on the surface in summer and subsequently drain through and flush the ice. The salinity of sea ice affects its mechanical strength, its thermal properties and its electrical properties – the latter being very important for remote sensing.

Geographical constraints play a large (but not complete) role in determining the quite different characteristics of sea ice in the Arctic and the Antarctic (see FAQ 4.2). This is one of the reasons why the sea ice in both hemispheres is changing differently. We also have much more information on Arctic sea ice thickness than we do on Antarctic sea ice thickness. Hence we treat the Arctic and Antarctic separately in this assessment.

4.2.2 Arctic Sea Ice

Regional sea ice observations, which span more than a century, have revealed significant inter-annual changes in sea ice coverage (Walsh and Chapman, 2001). Since the advent of satellite passive microwave imaging systems, which now provide more than 32 years of continuous coverage, it has been possible to monitor the entire extent of sea ice at a temporal resolution of a few days. A number of procedures have been used to convert the observed microwave brightness temperature into sea ice concentration – the fractional area of the ocean covered by ice (Comiso and Nishio, 2008; Markus and Cavalieri, 2000) – and thence to derive sea ice extent and ice area. Sea ice extent is defined as the integral sum of ice covered areas with concentrations of at least 15% while ice area is the product of the ice concentration and area of each data element within the ice extent. Ice concentrations and trends in extent and area derived from different procedures are generally consistent (Parkinson and Comiso, 2008), and the results presented in this report are solely based on techniques described by Comiso and Nishio (2008).

Arctic sea ice cover is seasonal, with the average ice extent varying between about 6 x 10^6 km^2 in the summer and 15 x 10^6 km^2 in the winter (Comiso and Nishio, 2008; Gloersen et al., 1992). The summer ice cover is confined to mainly the Arctic basin, while winter sea ice reaches as far south as 44°N, into the peripheral seas. The relatively extensive Arctic ice cover at the end of summer consists primarily of thick, old and ridged ice types. Interannual variability is largely determined by the extent of the ice cover in the peripheral seas in winter, and by the ice cover that survives the summer melt in the Arctic basin.

4.2.2.1 Total Arctic Sea Ice Extent and Concentration

Figure 4.3 (derived from passive microwave data) shows both the seasonality of the Arctic sea ice cover, and the large decadal changes that have occurred over the last 32 years. Typically, Arctic sea ice reaches its maximum seasonal extent in February or March while the minimum occurs in September at the end of summer-melt. Decadal changes in Arctic ice extent are higher in summer than in winter. The change in winter extent between 1979–1988 and 1989–1998 was negligible. Between 1989–1998 and 1999–2008, there was a decrease in winter extent of around 0.6 x 10^6 km^2. This can be contrasted to a decrease in ice extent at the end of the summer (September) of 0.5 x 10^6 km^2 between 1979–1988 and 1989–1998, followed by a further decrease of 1.2 x 10^6 km^2 between 1989–1998 and 1999–2008. Figure 4.3 also shows that the change in extent from 1979–1988 to 1989–1998 was significant mainly in spring and summer while the change from 1989–1998 to 1999–2008 was significant during all seasons. The largest interannual changes occur during the summer minima, and mainly to the perennial ice (Comiso, 2011; Comiso et al., 2008).

Changes have been large in the last five years: the average extent for 2007–2011 is below the other periods in all seasons, especially summer, and the summer minimum extent was at a record low in 2007 (Comiso et al., 2008; Stroeve et al., 2007). The ice extents for each day of the growth season from December 2010 to March 2011 were significantly lower than those in previous years, and the values for most days were at record lows for the satellite era. The 2011 extent in the spring and summer was comparable to the 2007 record low.

Although relatively short as a climate record, the 32-year satellite record is long enough to provide significant and consistent trends in monthly anomalies (i.e., difference between the monthly and the record averages) of ice extent, area and concentration. The trends in ice concentration for the winter, spring, summer and autumn are shown in Figure 4.3 b, c, d, and e, respectively, for the period November 1978 to December 2010. The seasonal trends for different regions, except the Bering Sea, are predominantly negative. Ice cover changes are relatively large in the eastern Arctic basin in winter and spring, while in the western basin they are more pronounced in summer and spring. Changes also occur in the peripheral seas and near the ice edge zones.

From the monthly anomaly data, the trend in sea ice cover in the Northern Hemisphere for 1979–2010 is –4.0 ± 0.18% per decade (see FAQ 4.2). The trends for different regions vary greatly, ranging from +4% per decade in the Bering Sea to –8% per decade in the Greenland Sea. This large spatial variability is associated with the complexity of the atmospheric circulation system as influenced by the Arctic Oscillation. The trends also change with season (Comiso, 2010): for the entire Northern Hemisphere, the trends in ice extent are –2.32 ± 0.39, –2.28 ± 0.37, –5.87 ± 0.74, and –6.50 ± 0.90% per decade in winter, spring, summer and autumn, respectively. The corresponding trends in ice area are –2.81 ± 0.37, –2.68 ± 0.38, –7.20 ± 0.84, and –7.28 ± 0.90% per decade. The trends for ice extent and ice area are comparable except in the summer and autumn when the trend in ice area is significantly more than that in ice extent. This implies increasing open water areas within the pack that may be caused by more frequent storms and more divergence in the summer (Simmonds et al., 2008; Comiso, 2010) The trends are larger in the summer and autumn mainly because of the rapid decline of the multiyear ice cover as discussed below.

[INSERT FIGURE 4.3 HERE]

Figure 4.3: (a) Plots of decadal averages of daily sea ice extent in the Arctic (1979 to 1988 in red, 1989 to 1998 in blue, 1999 to 2008 in gold) and a five-year average daily ice extent from 2007 to 2011; ice concentration trends (1979–2010) in (b) winter, (c) spring, (d) summer and (e) autumn (Comiso and Nishio, 2008).

[INSERT FIGURE 4.4 HERE]

Figure 4.4: Yearly perennial (blue) and multiyear (green) ice extent (a) and ice area (b) in the Central Arctic for each year from 1979 to 2011 as derived from satellite passive microwave data. Perennial ice values are derived from summer

ice minimum values, while the multiyear ice values are averages of December, January and February data. The gray lines (after 2002) are derived from AMSR-E data (Comiso, 2011).

4.2.2.2 Multiyear/Seasonal Ice Coverage

The winter extent and area of the perennial and multiyear ice cover in the Central Arctic (i.e., excluding Greenland Sea multiyear ice) for the period 1979–2010 are shown in Figure 4.4. Perennial ice is ice that survives the summer and the extent at summer minimum has been used as a measure of its coverage (Comiso, 2002). Multiyear ice (as defined by World Meteorological Organization) is ice that has survived at least two summers. Generally, that ice is less salty and has a distinct microwave signature compared to seasonal ice, and thus can be monitored with satellite radiometers (Comiso, 2011; Johannessen et al., 1999; Zwally and Gloersen, 2008).

Figure 4.4 shows large but similar interannual variability for perennial and multiyear ice. The extent of the perennial ice cover, which was about 8 x 10^6 km^2 in the early-1980s, decreased to about 5 x 10^6 km^2 in the latter part of the 2000s. Similarly, the multiyear ice extent decreased from about 6.2 x 10^6 km^2 in the 1980s to about 3.5 x 10^6 km^2 in the late-2000s. The trends in perennial ice extent and ice area were strongly negative at –13.0 ± 1.5 and -14.4 ± 1.5% per decade respectively. These values indicate an increased decline from the –9% per decade reported by Comiso (2002) for the 1979 to 2000 period. The trends in multiyear ice extent and area are even more negative, at –15.6 ± 1.9 and –17.5 ± 2.4% per decade, respectively, for the period from 1981 to 2011 (Comiso, 2011). The higher negative trend in ice area compared to that in ice extent indicates that the average ice concentration of multiyear ice in the Central Arctic has also been declining. The rate of decline in the extent and area of multiyear ice cover is consistent with the observed decline of old ice types from the analysis of ice drift and ice age by Maslanik et al. (2007), confirming that older and thicker ice types in the Arctic have been declining significantly. The higher negative trend for the thicker multiyear ice area than that for the perennial ice area implies that the average thickness of the ice, and hence the ice volume, has also been declining.

Drastic changes in the multiyear ice coverage from QuikScat (scatterometer) data, validated using high resolution SAR data (Kwok, 2004; Nghiem et al., 2007), have also been reported. Some of these changes have been attributed to the near zero replenishment of the Arctic multiyear ice cover during the summer (Kwok, 2007).

4.2.2.3 Ice Thickness and Volume

For the Arctic there are several different techniques available for estimating the ice thickness distribution. These show strong and broadly consistent decreases in Arctic sea ice thickness over recent years.

4.2.2.3.1 Submarine ice draft

Data collected by upward-looking sonar on submarines operating beneath the Arctic pack ice provided the first evidence of 'basin-wide' decreases in ice thickness. Sonar measurements are of draft (the submerged portion of sea ice), which is converted to thickness by assuming an average density for the measured floe, including its snow cover. Rothrock et al. (1999) found that ice draft in the mid-1990s was less than that measured between 1958 and 1977 at each of six locations within the basin. The change was least (–0.9 m) in the southern Canada Basin and greatest (–1.7 m) in the Eurasian Basin (with an estimated overall error of less than 0.3 m). The decline averaged about 42% of the average 1958 to 1977 thickness.

A subsequent analysis (Rothrock et al., 2008) used a much richer data set from 34 submarine cruises within a data release area that covered almost 38% of the area of the Arctic Ocean, rather than just select locations. These cruises are equally distributed in spring and autumn over a 25-year period from 1975 to 2000. Multiple regression was employed to separate the interannual change, the annual cycle, and the spatial distribution of draft. They show that the annual mean ice draft declined from a peak of 3.1 m in 1980 to a minimum of 2.0 m in 2000, a decrease of 1.1 m (1.2 m in thickness). Over the period, the steepest rate of decrease is –0.08 m yr^{-1} in 1990.

4.2.2.3.2 Satellite freeboard and thickness

Satellite altimetry techniques are now capable of mapping sea ice freeboard to provide a spatially comprehensive distribution of Arctic sea ice thickness. Like ice draft, satellite measured freeboard (the floating portion of sea ice) is converted to thickness, assuming an average density of the ice and snow cover. The principal challenges to accurate thickness estimation are in the discrimination of ice and open water, and in estimating snow cover thickness.

Radar altimeters on the ESA ERS and Envisat satellites have provided circum-Arctic observations south of 81.5°N. Although the ERS1 estimates (Laxon et al., 2003) showed no observable trend in the derived winter sea ice thickness between 1993 and 2001, the data showed significant (9%) interannual variability in this region of mixed seasonal and multiyear ice. Their data also reveal a realistic geographic variation in thickness (increasing from about 2 m near Siberia to 4.5 m off the coasts of the Canadian Archipelago and Greenland). Envisat observations between 2002 and 2008 showed a large decrease (0.25 m) following the September 2007 ice extent minimum (Giles et al., 2008b). However, this decline in thickness was regionally confined to the Beaufort and Chukchi Seas, with no significant changes found in the eastern Arctic. Results from the NASA ICESat laser altimeter over the same region also show thinning between 2007 and 2008, although these data suggest stronger interannual variability (Figure 4.2, Kwok, 2009). A large decrease in thickness due to the 2007 record minimum in summer ice is clearly seen in both the radar and lidar thickness estimates.

The lidar altimeter on ICESat (which ceased operation in 2009) provided a broader picture of the Arctic Basin as the coverage extends to 86°N. ICESat thickness estimates also provided seasonal contrast between the spring and autumn. Data from five winter ICESat campaigns between 2003 and 2008 show remarkable thinning and volume loss of the Arctic Ocean ice cover (Kwok, 2009). Regions covered by multiyear ice thinned by ~0.6 m over four years (Figure 4.5) while the average thickness of the first-year ice in mid-winter (~2 m) exhibited a negligible trend. Together with the 42% decline in the area of MY ice since 2005, the total MY ice volume in the winter experienced a net loss of 6300 km^3 (>40%) in the four years since 2005. Over this period, first-year ice became the dominant ice type of the Arctic Ocean, increasing in both area and volume. The average winter sea ice volume over the period was ~14,000 km^3.

[INSERT FIGURE 4.5 HERE]

Figure 4.5: The distribution of winter sea ice thickness in the Arctic and the trends in average, first-year (FY) ice, and multiyear (MY) ice thickness derived from ICESat records, 2004–2008 (Kwok, 2009).

4.2.2.3.2 Airborne electro-magnetic (EM) sounding

EM sounding measures the distance between an EM instrument and the ice/water interface. The technique is based on the amplitude and phase of a secondary EM field induced in the seawater relative to the primary field generated by the instrument deployed on an airborne platform. Repeat EM surveys, even though limited in time and space, have provided a regional view of the changing ice cover. From repeat ground-based and helicopter-borne EM surveys, Haas et al. (2008) found significant thinning in the region of the Transpolar Drift. Between 1991 and 2004, modal thicknesses decreased from 2.5 m to 2.2 m, and then dropped to 0.9 m in 2007. Mean thicknesses also decreased strongly. This thinning was associated with reductions of the age of the ice, and replacement of second-year ice by first-year ice in 2007 seen in satellite observations.

4.2.2.4 Arctic Sea Ice Drift

Pack ice motion influences ice mass locally, through deformation and creation of open water areas; regionally, through advection of ice from one area to another; and globally, through export of ice from polar seas to lower latitudes where it melts. The drift and deformation of sea ice is primarily forced by winds and ocean currents, but depends also on ice strength, top/bottom surface roughness, and regional ice concentration. On time scales of days to weeks, winds are responsible for most of the variance in sea ice motion. On longer time scales, the patterns of ice motion follow surface currents and the evolving patterns of wind forcing.

4.2.2.4.1 Drift speed

Drifting buoys have been used to measure Arctic Ocean ice displacements over the last 29 years. From these data Rampal et al. (2009) found an increase in average drift speed between 1978 and 2007 of +17% per decade in winter and +8.5% in summer. Spreen et al. (2011) used daily satellite ice motion fields, which provide a better regional depiction, to show that between 1992 and 2008, the spatially averaged trend in winter ice drift speed was +10.5% per decade, but varied regionally between −4 and +16 % per decade. Increases in drift speed are seen over much of the Arctic except in areas with thicker ice (e.g., north of Greenland and the Canadian Archipelago). The largest increases occurred during the second half of the period, coinciding with the years of rapid ice thinning. From examination of wind fields in atmospheric reanalyses, both of these investigations concluded that the observed spatial trends suggest a weaker and thinner ice cover, especially during the period after 2005, rather than stronger winds.

4.2.2.4.2 Ice export

Sea ice export through the Fram Strait, together with growth and melt, is a major component of the Arctic Ocean ice mass balance, annually exporting approximately 10% of the area of Arctic Ocean ice. Over a 31-year satellite record (1979–2010), the mean annual area outflow through Fram Strait was ~699 ± 112 x 10^3 km^2 with a peak in 1994/1995 (Kwok, 2009). But there has been no significant decadal trend in Fram Strait area flux in the satellite records. Decadal trend in ice volume export – a more definitive measure of changes in mass balance – is far less certain due to the lack of an extended record of the thickness of ice exported through Fram Strait. Comparison of recent estimates of volume outflow (Spreen et al., 2009) with earlier estimates by Kwok and Rothrock (1999) and Vinje et al. (2001) (~2,200–2,900 km^3) show no discernible change.

4.2.2.4.3 Export versus in-situ melt

More than a third of the thicker and older sea ice lost between 2005 and 2008 occurred by transport of multiyear ice (typically found west of the Canadian Archipelago) into the southern Beaufort Sea where it melted during the summer (Kwok and Cunningham, 2010). There remains some uncertainty of the relative contributions of in-basin melt and export to the observed Arctic ice loss. It has also been shown that thicker/older MY ice can be exported through Nares Strait (Kwok, 2005), which could account for a small fraction of the volume loss.

4.2.2.5 Time of Arctic Sea Ice Advance, Retreat and Ice Season Duration; Length of Arctic Melt Season

Seasonality collectively describes the annual timing of sea ice advance, retreat and resultant duration. It is derived from the daily satellite ice-concentration records, which have been used to determine, for each year and each satellite pixel location, the day sea ice advanced to that location and the day it retreated from that location. Maps of the timing of sea ice advance, retreat and ice season duration (the time between day of advance and retreat), as well as maps of trends over time are derived from these data (for detail methods see Parkinson, 2002; Stammerjohn et al., 2008).

Most regions in the Arctic show trends towards shorter ice season duration. However, the strongest seasonal trends were found in an area extending from the East Siberian Sea to the western Beaufort Sea. Here, over 1979/1980–2006/2007, sea ice advance has become 26 ± 7 days later (at +0.93 ± 0.20 days yr^{-1}), sea ice retreat 35 ± 8 days earlier (at –1.25 ± 0.30 days yr^{-1}), and ice season duration 59 ± 11 days shorter (at –2.09 ± 0.41 days yr^{-1}) . There has been a nearly 2-month lengthening of the summer ice-free season. (Stammerjohn et al., in submission).

The timing of melt onset during spring, and freeze-up in autumn, can be derived from satellite passive microwave brightness temperature (Belchansky et al., 2004; Drobot and Anderson, 2001; Smith, 1998) as the emissivity of the surface changes significantly with snow melt. The length of a melt season is the number of days between the onset of surface melt in spring and the onset of surface freeze in autumn. The amount of solar energy absorbed by the ice cover increases with the length of the melt season. Longer melt seasons with lower albedo surfaces (wet snow, melt ponds, and open water) increase absorption of incoming shortwave and melt, thus enhancing the ice albedo feedback. The satellite record (Markus et al., 2009) shows trends toward earlier melt and later freeze-up nearly everywhere in the Arctic. Over the last 30 years, the mean melt season over the Arctic ice cover has increased by about 20 days. The largest and most significant trends (at the 99% level) of >10 days per decade are seen in the coastal margins and peripheral seas: Hudson Bay, the East Greenland Sea, the Laptev/East Siberian seas, and the Chukchi/Beaufort seas.

4.2.2.6 Arctic Polynyas and the Odden

The Odden sea ice feature is a tongue of sea ice, related to cold surface waters, that extends more than 1000 km eastward from the normal east Greenland ice edge at about 73°N. Time series (1951–2005) of the Odden ice extent have been analyzed in the context of sea level pressure, surface wind, air temperature, cloud, and energy flux variations using NCEP-NCAR reanalyses (Rogers and Hung, 2008). The Odden was a recurring winter feature in 1966–1972, during the Great Salinity Anomaly (GSA), appeared occasionally in the 1980s and 1990s, but has occurred rarely since 2000.

High ice production in coastal polynyas (anomalous regions of open water or low ice concentration) over the continental shelves of the Arctic Ocean is responsible for the formation of cold saline water, which contributes to the maintenance of the Arctic Ocean halocline. A new passive microwave algorithm has been used to estimate thin sea ice thicknesses (<0.15 m) in the Arctic Ocean (Tamura and Ohshima, 2011), providing the first circumpolar mapping of sea ice production in coastal polynyas. High ice production is confined to most persistent Arctic coastal polynyas, with the highest ice production rate being in the North Water Polynya. Ice production in the 10 major Arctic polynyas decreased by 462 km^3 between 1992 and 2007.

4.2.3 Antarctic Sea Ice

The Antarctic sea ice cover is more seasonal than that in the Arctic, with average extent varying from a minimum of about 3 x 10^6 km^2 in February to a maximum of about 18 x 10^6 km^2 in September (Comiso, 2010; Zwally et al., 2002). The relatively small fraction of Antarctic sea ice that survives the summer is found mostly in the Weddell Sea, but with some perennial ice also surviving on the western side of the Antarctic Peninsula and in small patches around the coast. As well as being mostly first-year, Antarctic sea ice is also on average thinner, warmer, more saline and more mobile than Arctic ice. These characteristics, which affect some remote sensing capabilities, plus its more distant location from inhabited continents, result in far less being known about the properties of Antarctic sea ice than of that in the north.

4.2.3.1 Total Antarctic Sea Ice Extent and Concentration

Figure 4.6 shows the seasonal variability of Antarctic sea ice extent from 32 years of satellite passive microwave data. In contrast to the Arctic, decadal monthly averages almost overlap with each other, and the seasonality of the total Antarctic sea ice cover has not changed much over the period. In winter, the values for the 1999–2008 decade were slightly higher than those of the other decades while in autumn, the values for 1989–1998 and 1999–2008 decades are higher than those of 1979–1988. The plot for 2007–2011 shows more seasonal variability than the decadal plots with relatively high values in late autumn, winter and spring.

Trend maps for winter, spring, summer and autumn extent are presented in Figures 4.6 b, c, d, and e respectively. The seasonal trends are significant mainly near the ice edge, with the values alternating between positive and negative around Antarctica. Such an alternating pattern has been described previously and associated with the influence of the Antarctic Circumpolar Wave (White and Peterson, 1996). In the Austral winter, negative trends are evident at the tip of the Antarctic Peninsula and also at the opposite side of the continent, while positive trends are prevalent in the Weddell and Ross seas. The patterns in Austral spring are very similar to those of winter while in summer and autumn, negative trends are mainly confined to the Bellingshausen/Amundsen Seas, while positive trends are dominant in the Ross Sea.

The regression trend in the Antarctic sea ice cover monthly anomalies from 1978 to 2011 is slightly positive, at 1.2 ± 0.19% per decade (see FAQ 4.2). For the seasonal trends in ice extent in winter, spring, summer and autumn Comiso (2010) reports –0.77 ± 0.39, 0.73 ± 0.36, 1.03 ± 1.41, and 3.08 ± 1.33% per decade, respectively. The corresponding trends in ice area are 1.43 ± 0.42, 1.22 ± 0.42, 2.10 ± 1.64, and 4.66 ± 1.54% per decade. The values are all positive except for a negative but insignificant trend in winter extent. The trends are consistently higher for ice area than ice extent, indicating less open water (possibly due to less divergence and storms) within the pack in later years. The overall inter-annual trends for the various sectors are given in FAQ 4.2, but such trends have to be interpreted carefully because of an atmospheric circulation pattern that is influenced strongly by the Southern Annular Mode and the Antarctic Circumpolar Wave.

[INSERT FIGURE 4.6 HERE]

Figure 4.6: (a) Plots of decadal averages of daily sea ice extent in the Antarctic (1979 to 1988 in red, 1989 to 1998 in blue, 1999 to 2008 in gold) and yearly values of daily ice extents in 2007, 2010 and 2011; ice concentration trends (1979–2010) in (b) winter, (c) spring, (d) summer and (e) autumn.

4.2.3.2 Antarctic Sea Ice Thickness and Volume

Since AR4, advances have been made in determining the thickness of Antarctic sea ice, particularly in the use of ship-based observations and satellite altimetry. However there remains an ongoing lack of data providing routine global coverage for monitoring and no information on large-scale Antarctic ice thickness change. Worby et al. (2008) compiled 25 years of ship-based data from 83 Antarctic voyages on which routine observations of ice and snow properties were made. Their compilation included a gridded data set that reflects the regional differences in sea ice thickness. A subset of these ship observations, and ice charts, was used by DeLiberty et al. (2011) to estimate the annual cycle of sea ice thickness and volume in the Ross Sea, and to investigate the relationship between ice thickness and extent. They found lag in the timing of maximum sea ice volume from maximum extent. While ice advects to the northern edge and melts, the interior is supplied with ice from higher latitudes and continues to thicken by thermodynamic growth and deformation. Satellite retrievals of freeboard and thickness in the Antarctic (Mahoney et al., 2007; Xie et al., 2011; Zwally et al., 2008) are under development but progress is limited by our present knowledge of snow thickness and the paucity of suitable validation data sets.

4.2.3.3 Antarctic Sea Ice Drift

[PLACEHOLDER FOR SECOND ORDER DRAFT: Recent changes in atmospheric circulation and the associated changes in sea ice drift will be reported in articles to be submitted prior to deadline.]

4.2.3.4 Time of Antarctic Sea Ice Advance, Retreat and Ice Season Duration

There have been contrasting regional patterns of change in the Antarctic ice duration. In the northeast and west Antarctic Peninsula and southern Bellingshausen Sea region, later ice advance (48 ± 11 days later) and earlier retreat (35 ± 9 days earlier) has shortened the ice season by 83 ± 23 days over the period 1979/1980–2006/2007 (a trend of –2.97 ± 0.81 days yr^{-1}). The opposite is true in the adjacent western Ross Sea, where the ice season has lengthened by 57 ± 13 days (at +2.02 ± 0.46 days yr^{-1}) due to earlier advance (29 ± 7 days earlier) and later retreat (28 ± 6 days later) (Stammerjohn et al., in submission).

The magnitude of the seasonal/regional sea ice changes in both the Arctic and Antarctic point to strong positive feedbacks. However, the asymmetric seasonal response appears to indicate different sensitivities and underlying mechanisms. For example, an earlier sea ice retreat is consistent with an ice albedo feedback (e.g., Perovich et al., 2008), while a delayed sea ice advance is consistent with an enhanced ocean heat feedback (e.g., Steele et al., 2008). Additionally, changes in winds can also affect the ice-edge advance and retreat (Massom et al., 2008). Thus, different atmosphere-ocean forcings and sea ice sensitivities are likely present in different regions and seasons, but we currently lack the data to fully resolve these differences.

4.2.3.5 Antarctic Polynyas

Polynyas are commonly found along the coasts of Antarctica. An increase in the extent of coastal polynyas in the Ross Sea caused enhanced ice production that is primarily responsible for the positive trend in ice extent in the Antarctic (Comiso et al., 2011). Variability in the ice cover in this region is linked to changes in the Southern Annular Mode (SAM) and secondarily to the Antarctic Circumpolar Wave. Ocean convection that injected relatively warm deep water into the surface layer was observed between 1974–1976 creating the large Weddell Sea Polynya, but since the late-1970s the SAM has been negative or slightly positive, resulting in warmer and wetter condition forestalling the Weddell Polynya (Gordon et al., 2007). A recent study shows that the net ice export equals the polynya ice production of approximately 400 km^3 in 1992 for the Ross Sea in Antarctica, with an annual increase in ice production of 21 km^3 per year to 2008, whereas the ice production, which is three times less in the Weddell Sea, has decreased by 8 km^3 per year over the same time period (Drucker et al., 2011).

4.2.3.6 Antarctic Land-Fast Ice

Landfast ice (or "fast ice") occurs in both the Arctic and Antarctic, but is more extensive in the Antarctic. Around East Antarctica, where it typically occurs in narrow coastal bands of varying width up to 150 km from the coast and in water depths of up to 400–500 m, it is generally between 5% (winter) and 30% (summer) of the overall sea ice area (Fraser et al., in press), and a greater fraction of ice volume (Giles et al., 2008a). In contrast, fast ice in the Arctic is typically grounded in shallow water, with the seaward edge around the 20–30 m isobath (Mahoney et al., 2007).

Variability in the distribution and extent of fast ice is sensitive to processes of ice formation and to climate-related processes (such as ocean swell and waves, and strong wind events) that cause the fast ice to break-up. Historical records of Antarctic fast ice extent, such as that of Kozlovsky et al. (1977) covering 0° to 160°E, were limited by sparse and sporadic sampling. But using cloud-free MODIS composite images, Fraser et al. (in press) derive a high resolution time series of landfast sea ice extent along the East Antarctic coast, showing a statistically-significant increase (1.43 ± 0.30% yr^{-1}) between March 2000 and December 2008. There is a strong increase in the Indian Ocean sector (20°E to 90°E, 4.07 ± 0.42% yr^{-1}), and a non-significant decrease in the Western Pacific Ocean sector (90 °E to 160 °E, -0.40 ±0.37 % yr^{-1}). An apparent shift from a negative to a positive trend was noted in the Indian Ocean sector from 2004, which coincided with greater interannual variability. Although significant changes are observed, this record is only 9 years in length.

4.2.4 Synthesis of Sea Ice Changes

The strong and significant decrease in Arctic sea ice extent and area reported in AR4 has continued, and is accompanied by many other changes in the characteristics of the Arctic sea ice cover. These changes are robust and in high agreement.

The average decadal extent of the ice has decreased in every season and in every successive decade since satellite observations commenced. The overall anomaly trend in extent over the period 1979–2010 has been -4% per decade (–0.47 million square kilometres per decade; Figure 4.7), with larger changes occurring in summer and autumn, and the largest changes of all to the perennial ice (the summer minimum extent; –12.2 % per decade) and multiyear ice (more than 2 years old; –15.6 % per decade; Figure 4.7c). The rate of decrease in ice area has been greater than that in extent because the ice concentration has also decreased (Figure 4.7a).

The decrease in perennial and multiyear ice coverage has resulted in a strong decrease in ice thickness, and hence in ice volume. Within the data release area of declassified submarine sonar measurements (covering ~38% of the Arctic Ocean), the overall mean winter thickness of 3.64 m in 1980 decreased by 1.75 m to only 1.89 m during 2009. Between 1975 and 2000, the steepest rate of decrease was –0.08 m yr^{-1} in 1990 compared to a slightly higher winter/summer rate of –0.10/–0.20 m yr^{-1} in the five-year ICESat record (2003–2008) (Kwok and Rothrock, 2009). This combined analysis (Figure 4.7b) shows a long-term trend of sea ice thinning that spans five decades. The decrease of thickness means that Arctic ice is becoming increasingly seasonal and would take at least several years for any recovery because of the time taken to form multiyear ice.

The decrease in both concentration and thickness means that the ice has less resistance to wind forcing, and the rate of ice drift has also increased (Figure 4.7e). Other significant changes to the Arctic Ocean sea ice include lengthening in the duration of the surface melt on perennial ice of 6 days per decade (Figure 4.7d) and a nearly 2-month lengthening of the ice-free season in the region from the East Siberian Sea to the western Beaufort Sea.

The status of change to many of these sea ice characteristics in the Antarctic is not known. There has been a small but significant increase in total ice extent of 1.1% per decade between 1979 and 2010, and a greater increase in ice area, indicating an increase in concentration. But there are strong regional differences within this total, with some regions increasing in extent/area and some decreasing. There are also contrasting regions around the Antarctic where the ice-free season has lengthened, and others where it has decreased over the satellite period. There are still inadequate data to make any assessment of changes to Antarctic sea ice thickness and volume.

[INSERT FIGURE 4.7 HERE]

Figure 4.7: Summary of linear decadal trends (red) in: (a) Arctic ice extent and concentration from satellite passive microwave observations (Comiso and Nishio, 2008); (b) sea ice thickness from submarine (blue), satellites (black), and in-situ/EM surveys (circles); trend in submarine ice thickness is from multiple regression of available observations to separate the interannual changes, the annual cycle, and the spatial field of thickness within the data release area (Haas et al., 2008; Kwok and Rothrock, 2009); (c) multiyear sea ice coverage from analysis of QuikSCAT (Kwok et al., 2009); (d) length of melt season (Markus et al., 2009); and (e) satellite-derived drift speed (Spreen et al., 2011).

4.3 Glaciers

Much of the discussion in AR4 was underpinned by an incomplete inventory that contained less than 42% of the world's glaciers. Considerable effort to improve the coverage and quality of this inventory has since been undertaken, however while completion is expected by the end of 2011, most of the work on which this chapter is written is based on an early version of that inventory containing 48% of the complete inventory (Arendt and Al, 2011)[*].

4.3.1 Background

Glaciers show some of the most visible recent changes of all components in the climate system and records of length variations on a few valley glaciers dating back to the 16th and 17th century are among the longest directly observed climate system variables. There is robust evidence and high agreement in the observations that, globally, glaciers shrank considerably since about 1850. By their nature, glaciers are sensitive indicators of climate change, act as seasonal to long-term hydrologic reservoirs that are significant on regional scales and, on a global scale, are contributors to sea level rise. Yet, changes in glaciers occur across spatial and temporal scales and it is non-trivial to attribute them to specific climate drivers (see Chapter 10). The impact of glacier change on regional water supply depends strongly on the respective regional climate (see Chapter 3).

Glaciers occur where climate conditions and relief allows snow and ice to accumulate over several years and then flow downward to warmer elevations where various processes of ablation occur. The relief modifies atmospheric conditions and hence also influences accumulation and ablation processes. Accumulation is mainly due to solid precipitation, wind-driven and avalanche deposition of snow, and refreezing of liquid water. Ablation is mostly due to runoff of melt-water and, for some glaciers, calving of icebergs; but sublimation and loss of wind-blown snow also contributes to ablation. Energy and mass fluxes across the glacier surface are directly linked to atmospheric conditions and determine the 'climatic mass budget'. Changes in internal or basal processes, as well as mechanical ones (calving, avalanches), may also be related to climate, but the relationship is more complex (e.g., Cogley et al., 2011). Changes in glacier length, area, mass and volume are regularly measured from a wide range of observation techniques that are summarized in Table 4.2.

Table 4.2: Typical characteristics of the observational database for the determination of glacier changes.

Para-meter	Method	Techniques	Number of glaciers	Glacier area (km^2)	Repeat interval (years)	Earliest data	Accuracy	References
Length	Various	Reconstruction		?	5–50	1600	100 m	(e.g., WGMS, 2008)
	Field	Tradition and modern survey	~600	1–100	1	1894	1 m	
Area	Maps	Cartographic	1–1,000	0.02–1,000	10	1900	<10%	(Maisch, 2000)
	Remote sensing	Inventory / GIS	10–10,000	0.02–1,000	10	1984	<5%	(Paul et al., 2004)
Mass	Field	Tradition and modern survey	~50 10	1–10 –	0.5–1 –	1947 1908	0.2 m we	(WGMS, 2008)

[*] *Refined values, based on the completed inventory, will be available for the inclusion in the second order draft, although it is unlikely that substantive statements will require modification.*

Remote sensing	Laser and radar profiling	~100 >1,000	10–1,000 10–1,000	5–10 0.5	1990s 2000–2010	0.05 m 0.1 m	(Arendt et al., 2006)
Remote sensing	DEM differencing	~10 (aerial) >100 (space)	0.1–100 1–1,000	10–50 10–50	1920s 1960s	0.2 m we 0.5 m we	(Larsen et al., 2007)
Remote sensing	Gravimetry (GRACE)	not resolved	>10,000	1	2000	Large regions	(Luthcke et al., 2008)

In AR4 (Lemke et al., 2007), glacier mass changes were up-scaled from varying numbers of directly measured glaciers (climatic mass budget) to regional and global estimates, with uncertainties quantified from statistics within and between four different extrapolation methods. Strongest ice loss per unit area was reported in Patagonia, Alaska and northwest USA and southwest Canada. The largest contributions to sea level rise came from Alaska, the Arctic and the Asian high mountains. A large uncertainty resulted from an incomplete glacier inventory, with total areas estimated from up-scaling methods. The applied extrapolation of mass budgets could have resulted in an overestimation of ice loss in high mountain ranges, where small glaciers are most frequently monitored. Furthermore, for logistic and practical reasons, mass change measurements were available for very few calving glaciers (Cogley, 2009c).

4.3.2 Current Glacier Extent

Since the AR4 projections, Cogley (2009b) and Radic and Hock (2010) extended the global inventory to approximately 48% of estimated global glacier-covered area, and produced a new estimate of global glacier area and volume, including glaciers surrounding the Greenland and Antarctic ice sheets (Table 4.3). Notably absent from these, were details about glacier areas in heavily glacierized regions of Alaska, Canada (Rocky Mts. and Arctic), the Himalaya and local glaciers around the Greenland the ice sheet (Cogley, 2009b). More recent estimates have used statistical extrapolation to reduce the gaps in coverage (Ohmura, 2009; Radic and Hock, 2010). For AR5, a new global glacier inventory is derived from a wide range of data sources (Arendt and Al, 2011). The results of this inventory, subdivided into 19 large regions to reflect different climatic zones, is illustrated in Figure 4.8 with the totals* listed in Table 4.3 alongside earlier estimates.

Thickness data, and thus volumes measurements, are only available for a few glaciers worlwide. The up-scaling of these measurements to unmeasured glaciers results in a considerable uncertainty. A volume-area power-law scaling, based on geometric and ice-dynamic considerations is frequently applied to estimate glacier volume (Bahr et al., 1997). New approaches also consider features of glacier geometry that can be derived from terrain information and basic glaciological principles (Farinotti et al., 2009; Huilin et al., 2011; Paul and Linsbauer, in press). Values* from both approaches are shown in Figure 4.8 and listed in Table 4.3.

[INSERT FIGURE 4.8 HERE]

Figure 4.8: Total glacier area in 1,000 km^2 (white) subdivided into the 19 regions (green numbers in italics) used throughout the Section 4.3. The size of each circle is equivalent to the glaciated area in each region. The glacier areas are based on the new calculations (Arendt et al., 2011). The regions are: 1 Alaska, 2 Western Canada and US, 3 Arctic Canada (North), 4 Arctic Canada (South), 5 Greenland, 6 Iceland, 7 Svalbard, 8 Scandinavia, 9 Russian Arctic, 10 North Asia, 11 Central Europe, 12 Caucasus and Middle East, 13 Central Asia (North), 14 Central Asia (West), 15 Central Asia (South), 16 Low-Latitudes, 17 Southern Andes, 18 New Zealand, and 19 Antarctic and Sub-Antarctic. Yellow dots illustrate schematically locations of glaciers. The total area for region 19 is derived from various sources (Arendt et al., 2011) but data for digital overlay on this map are not yet available.

Table 4.3: Global glacier area and volume* according to various published sources.

Reference	Area [10^3 km^2]		Volume [10^3 km^3]		Sea Level Equivalent [m]	
	Excluding	Including	Excluding	Including	Excluding	Including
AR4 (Lemke et al., 2007)	546	795	133	260	0.37	0.72
Radic and Hock (2010)	518 ± 2	741 ± 68	166 ± 10	241 ± 29	0.41 ± 0.03	0.60 ± 0.07
By end of 2011 (new inventory)	504	683	*	*	*	*

4.3.3 Observed Changes in Glacier Length, Area and Mass

Length variations of glaciers are obtained from annually repeated measurements or are reconstructed from maps, photographs and dated moraines. Being relatively easy to obtain, some records go back in to the 16th and 17th Century (WGMS (ICSI-IAHS), various years; Zemp et al., 2011). Whereas glacier mass changes are an immediate and direct response to the annual atmospheric conditions, length variations are modified by glacier dynamics, so they are smoothed and delayed – but can also be strongly magnified; for example, a length change of 100 m or more may result from a temperature change of only 0.1°C (e.g., Leysinger Vieli and Gudmundsson, 2004).

Despite their high variability due to different response times and local conditions (see FAQ 4.2), records of glacier length provide a largely homogenous signal (Figure 4.9) giving robust evidence that glaciers retreated strongly worldwide (up to several kilometres) since their last Holocene maximum extent in the 17th to 19th century. The general retreat was interrupted by intermediate phases of stagnation, or even glacier advance, around the 1890s, 1920s and 1970s (1990s in Norway) (UNEP, 2007). The long-term records have also been used to determine the contribution of glaciers to sea level rise (Leclercq et al., 2011), or to model the mean annual mass budget of glaciers in the European Alps (Hoelzle et al., 2003). In Figure 4.9 the observed cumulative front variations for glaciers of different size in seven selected regions of the world are compiled (WGMS, 2008). Besides the clear overall trend in glacier-terminus retreat, intermittent advances that are not globally synchronous can be seen. In some areas, these advances are related to regional atmospheric conditions (e.g., in Scandinavia and New Zealand), while in others they are likely more related to dynamical instabilities than to climate change (e.g., in the Karakoram).

[INSERT FIGURE 4.9 HERE]

Figure 4.9: Cumulative glacier length changes as measured in the field for seven different regions. Data from WGMS (2008).

Glacier area changes are increasingly reported from the comparison of repeat satellite imagery in all parts of the world (WGMS, 2008). Though area changes are difficult to correlate with climatic change, annual area-loss rates are globally available and the observed geometric changes often provide evidence for other processes, e.g., surface lowering is expressed by separation of tributaries and emerging rock outcrops (Paul et al., 2007; Pelto, 2010). The calculated relative area changes are dependent on glacier size, but as the mean relative area loss always includes the entire sample of glaciers in the respective region, they show a regional characteristic. These mean annual area-loss rates are shown in Figure 4.10 for selected regions globally. The studies reveal that loss rates have increased recently, and are now up to 2–4% yr^{-1} in some regions and over shorter time periods.

[INSERT FIGURE 4.10 HERE]

Figure 4.10: Mean annual area-loss rates for 14 out of the 19 regions depicted in Figure 4.8. Each line refers to the observed relative area loss from a specific publication and its length is related to the period used for averaging. The publications considered for each subregion (in brackets) are: (**1**) Le Bris et al., 2011; (**2**) Bolch et al., 2010a; Debeer and Sharp, 2007; Jiskoot et al., 2009; (**3**) Huss et al., 2008; (**4**) Paul and Kaab, 2005; (**7**) Kaab, 2008; (**8**) Andreassen et al., 2008; Paul and Andreassen, 2009; (**10**) Shahgedanova et al., 2010; (**11**) Abermann et al., 2009; Lambrecht and Kuhn, 2007; Paul et al., 2004; (**13**) Aizen et al., 2007; Bolch et al., 2010b; Cia et al., 2005; Kutuzov and Shahgedanova, 2009; Li et al., 2006; Surazakov et al., 2007; Wang et al., 2009; Ye et al., 2006a; Ye et al., 2006b; Zhou et al., 2009; (**14**) Bolch, 2007; Khromova et al., 2006; Narama et al., 2006; (**15**) Bolch et al., 2008; Kulkarni et al., 2007; Nie et al., 2010; (**16**) Cullen et al., 2006; Klein and Kincaid, 2006; Peduzzi et al., 2010; Racoviteanu et al., 2008; Silverio and Jaquet, 2005; (**17**) Rivera et al., 2005; Rivera et al., 2007; Schneider et al., 2007; (**19**) Berthier et al., 2009; Thost and Truffer, 2008. Data compilation by Matthias Mahrer, University of Zurich.

Glacier mass changes are traditionally obtained from stake and pit measurements of seasonal mass gains and losses, summed to give the net annual climatic mass budget. This method is, however, generally restricted to a limited number of accessible glaciers: uninterrupted time series spanning more than 40 years are only available from 37 glaciers worldwide, and long-term mass budget measurement programs are being reduced (Zemp et al., 2009). Glaciers with calving fronts are usually excluded from such measurements, but can be estimated by repeat measurements of surface topography that are converted to total mass change, usually over intervals of a decade. Overall regional or even global values of glacier-mass change are then obtained by applying spatial extrapolations that add uncertainty to that arising from the measurement technique. At present, it is not possible to objectively quantify all sources of uncertainty in overall mass budgets extrapolated from single-glacier measurements. Regional sample sizes are commonly too small to yield reliable estimates of spatial variability, and in some cases also of temporal variability. Indeed, in several regions a pentadal (5-year) sample as applied by (Cogley, 2009c) is often close to zero. In such cases, there is, strictly speaking, no better estimate of the regional mass budget than the corresponding global estimate. Two alternative approaches, with attendant uncertainties of their own, show promise for addressing this problem. First, regional-scale measurements of surface-elevation change are growing in number and value, and second, models of mass balance that rely on temperature and other meteorological variables are improving in fidelity and physical completeness (see Figure 4.11 caption for references). A series of studies provide both regional (Figure 4.11) and global estimates of glacier mass changes (Figure 4.12).

[INSERT FIGURE 4.11 HERE]

Figure 4.11: Glacier mass change rates in [kg m^{-2} yr^{-1}] for the 19 regions from Figure 4.8. Values are either from regional measurements (Abdalati et al., 2004; Arendt et al., 2002; Berthier et al., 2010; Chen et al., 2007; Gardner et al., 2011; Glazovsky and Macheret, 2006; Ivins et al., 2011; Luthcke et al., 2008; Magnusson et al., 2005; Matsuo and Heki, 2010; Moholdt et al., submitted; Moholdt et al., 2010; Nuth et al., 2010; Paul and Haeberli, 2008; Peltier, 2009; Rignot et al., 2003; Schiefer et al., 2007; Schrama and Wouters, 2011; Wu et al., 2010), extrapolation from single glacier measurements (Cogley, 2009c; Huss, 2011; Lambrecht and Kuhn, 2007), and modelling with atmospheric input variables (Hirabayashi et al., 2010; Marzeion et al., 2011). Incomplete regional measurements are up-scaled. Uncertainties, if not provided by the authors, are given as a random error of 500 kg m^{-2} for non-elevation difference studies and as a cumulative error of 5 m for elevation change studies. Conversions from area specific 1,000 kg m^{-2} into mm SLE are given for each region below the region names. Figure compilation: Alex S. Gardner, Atmospheric, Oceanic & Space Sciences, University of Michigan.

4.3.4 Regional Synthesis

Not all regions are equally rich in data, and estimates of glacier mass changes and the different methods applied are not necessarily comparable. Yet, they give *robust evidence* of a considerable ice loss (Figure 4.11) and glacier-shrinkage (Figure 4.10) and, with some delay, glacier-front recessions (Figure 4.9.) During the past two decades, **glacier fronts** retreated strongly in North and South America, the European Alps, Equatorial Africa, Northern Asia. In other regions, terminus positions were rather stable (e.g., Central Asia West) or individual glaciers advanced (e.g Norway, New Zealand, Karakoram). However, in each region, the length variations show a typical pattern, with the largest glaciers displaying more or less continuous retreat and strong overall changes, medium-sized mountain glaciers showing decadal fluctuations, and smaller glaciers showing little overall variability but a clear retreat. A modifying factor on many large valley glacier tongues is a debris-covered surface, which strongly reduces melt compared to clean ice (e.g., Benn and Lehmkuhl, 2000). Strongest **area losses** are reported from several mid-latitude (e.g., 2% yr^{-1} in the Alps, 3% yr^{-1} in Norway) and low-latitude mountain ranges (East Africa, Indonesia, Peru). Mean loss-rates from 0.3 to 1% yr^{-1} over the period 1960–2000 are found in all regions, including the Arctic and regions in a cold/dry continental climate in Asia.

Glacier mass loss rates are of two different types showing the total mass loss (geodetic, and modeled plus calving) and the climatic mass loss (directly measured or modeled). In general, extrapolations from single glacier observations (Cogley, 2009a) tend to agree with the total mass loss (see discussion of global curves, Figure 4.12) and the climatic mass loss rates show regional similarities for the past five decades. However, the study by Hock et al. (2009) shows, in most regions, generally greater mass loss even than some geodetic observations (e.g., Southern Andes). There are few long-term measurements of glacier mass changes for Arctic Canada South (4), Greenland (5), Central Asia (13, 14, 15), Antarctic & Subantarctic (19), Low Latitudes (16), and New Zealand (18) and, therefore, uncertainty in long-term rates of mass change in these regions is highest. In general, cold high latitude regions [Arctic Canada (3 & 4), Greenland (5), Svalbard (7), Russian Arctic (9), and Antarctic & Subantarctic (19)] have less negative rates of mass change with resent sharp decreases in mass observed for Arctic Canada (3 & 4). Regions that experience a more maritime climate [Alaska (1), Western Canada and US (2), Iceland (6), Scandinavia (8), Low Latitudes (16), Southern Andes (17), and New Zealand (18)] have the highest variance in rates of mass changes as these regions have larger annual mass turnover. Mass changes of Central Europe (11) glaciers are very well constrained and show a strong linear trend of increasing loss. Recent increased glacier mass loss has also been observed for Alaska (1) and the Southern Andes (17).

While the mass change rates in [kg m^{-2} yr^{-1}] in Figure 4.11 are indicative for climate signal manifested in glacier changes, only the product of these rates with the respective total glacier area of a region shows its contribution potential to sea level rise (the glacier areas are displayed in Figure 4.8 and the respective conversion numbers are given in each of the regional plots in Figure 4.11 below the region name). Accordingly, the recent climate effect on glacier contributions to sea level rise is strongest in Alaska (1) and the glaciers in Antarctica and Sub-Antarctica, most recently also in the Canadian Arctic (3 and 4), followed by Central Asia North (13). Studies of recent glacier velocity change (Azam et al., submitted; Heid and Kääb, 2011), length versus mass change (Luethi et al., 2010) and comparisons of accumulation areas under present and equilibrium conditions (Bahr et al., 2009), show that the world's glaciers are currently strongly out of balance with the present climate and thus committed to lose considerable ice in the near future, even without further increasing temperatures.

[INSERT FIGURE 4.12 HERE]

Figure 4.12: The global glaciers' cumulative (top graphs) and annual (lower graphs) mass change 1800–2010 and 1960–2010 in panel (a) and (b) respectively. Different cumulative estimates are all set to zero mm SLE with their 1961–1990 average. Estimates are from glacier length variations (Leclercq et al., 2011), from arithmetic means and area weighted extrapolations of individual glaciers directly and geodetically measured mass budgets (extended from Cogley, 2009c; Kaser, 2006), and modelling with atmospheric variables as input (Hirabayashi et al., 2010; Marzeion et al., 2011). Figure drawn by Ursula Blumthaler, Institute of Meteorology and Geophysics, University of Innsbruck.

*4.3.5 Global Synthesis**

Four recent studies provide evidence of global glacier mass changes (Figure 4.12). Leclercq et al. (2011) use length variations from 349 glaciers worldwide to estimate glacier mass-loss since 1800. For a recent global extrapolation, Cogley (2009c) compiled 4,146 annually directly measured mass budgets from 344 glaciers, and 16,383 annual values from 754 volume change measurements from an additional 327 glaciers, and assembled these data in pentades (5-year periods). By adding geodetically to the directly measured changes from earlier estimates (Kaser et al., 2006a; Lemke et al., 2007), the proportion of calving glaciers was increased from 7 to 31% which may not yet fully meet reality but gets definitely closer to it. Whereas after 1961 an area weighted extrapolation was possible, earlier global estimates could only be obtained from arithmetic means of small numbers of glaciers. The values as obtained for the glaciers excluding those around the ice sheets are up-scaled to a total by applying a scaling factor described in Kaser et al. (2006). The other cumulative curves and rates in Figure 4.12 are from modelling the climatic mass balance only by simulating surface mass changes from daily or monthly mean air temperatures and precipitation sums. While Hirabayashi et al. (2010) upscale daily from example glaciers over a grid raster, extended from Marzeion et al. (2011) calculated monthly mass changes for each individual glacier as available from the present inventory. An obvious bias towards negative values as shown in the respective validation plots (Hirabayashi et al., 2010, Figures 3 & 4) may explain the relative high mass losses. As for sea level contribution best confidence is in the values extracted from Cogley's (2009c) area weighted extrapolations which are up-scaled from the present area inventory including the glaciers in the peripheries of the two ice sheets (bold in Table 4.4). The two curves extended from Marzeion et al. (2011) indicate that a considerable climate-driven signal comes from these glaciers. As for the longest period in question, 1901 to 1990, the arithmetic mean values from Cogley (2009c) with respective large error bars are suggested.

The sea level contribution rates from glaciers have gradually increased since about 1985 with a slight decrease in the most recent years. Comparing the curves derived by different approaches indicates that glaciers are strongly out of balance with the present climate (SLE derived from terminus variations lag considerably behind others, particularly since mass losses increased around 1985).

Table 4.4: Average annual rates of global mass loss for different time periods as obtained from Cogley (2009c) up-scaled to all glaciers including those around the Greenland and Antarctic ice sheets following Kaser et al. (2006b). The 1901–1990 value comes from arithmetic means, the others from area weighted extrapolations.

	Gt yr^{-1}	mm SLE yr^{-1}
1901–1990	182.7 ± 93.6	0.50 ± 0.26

1971–2009	261.4 ± 13.9	0.72 ± 0.04
1993–2009	342.0 ± 15.9	0.94 ± 0.04
2005–2009	334.9 ± 17.8	0.92 ± 0.05

[START BOX 4.1 HERE]

Box 4.1: Interaction of Snow with the Cryosphere

Snow has important and at the same time very different effects on the components of the cryosphere. While snowfall is essential for the genesis and survival of most cryospheric components, snow cover can also diminish permafrost. Both snowfall and the persistence of snow cover are strongly dependent on atmospheric temperature and highly variable precipitation events and thus climate, and snow cover also has a high spatio-temporal variability.

The two most important physical properties of snow for Earth's climate in general, and the cryospheric components on which it falls, are its high albedo (reflectivity for solar radiation) and the strong insulation it can provide as a result of its high air-content. When snow is present, both factors can dramatically alter the flux of energy into or out of the material below. In this regard, snow mediates the physical fluxes of mass and energy between the atmosphere and the cryosphere.

The high albedo of snow has a large impact on the radiative energy balance of all surfaces on which it lies, most of which are normally much less reflective. For example, the albedo of bare glacier or sea ice is typically 20–30%; the other 70–80% of solar radiation is absorbed at the surface. For ice at the melting point, this energy melts the ice. With a snow cover over the bare ice, the albedo changes to 80% or higher and melting is greatly reduced. The effect is similar for other land surfaces – bare soil, frozen ground, low-lying vegetation – but here snow cover protects the ground from warming rather than from melting. Because such large regions are covered by seasonal snow in the northern hemisphere, snow also has a major impact on the total energy balance of the Earth's surface.

For frozen ground, the second characteristic of snow is also important since the insulating effect of even a thin snow cover can be significant. If the air above is colder than the material on which it lies, the presence of snow will reduce heat transfer upwards. This could, for example, reduce the thickening of lake and sea ice. Alternatively, if the air is warmer than the material beneath the snow, heat transfer downwards from the air would be reduced. Thus snow can both reduce the cooling of frozen ground or protect permafrost from thawing depending on season.

For these reasons, the timing of the snowfall and the persistence of snow cover is of major importance. Whereas snow falling on glaciers in summer has a strongly positive (sustaining) effect on the mass budget, an early snow cover over frozen ground can prevent cooling of the seasonally unfrozen surface layer (also called active layer) and potentially contribute to its long-term thawing. During winter, snowfall is the most important source of nourishment for glaciers but radiative cooling of frozen ground under a thick snow cover is strongly reduced, thereby contributing to an increase of its temperature.

[END BOX 4.1 HERE]

4.4 Ice Sheets

4.4.1 Background

Today, the vast polar ice sheets in Greenland and Antarctica are shrinking as our climate becomes warmer. In Greenland, warm summers extend the zone and intensity of summer melting to higher elevation and have doubled meltwater runoff since the 1980s. In both Greenland and Antarctica, some glaciers are accelerating, and their floating extensions are thinning and even breaking up. As a result of these processes net losses from both ice sheets are very likely increasing. At some locations, glacier acceleration is likely due to the presence of warm ocean waters at the ice-ocean boundary that melts the submerged ice and contributes to increased ice-discharge into the ocean.

4.4.2 Changes in Mass of Ice Sheets

The current state of mass balance of the Greenland and Antarctic ice sheets is discussed here, focusing on improvements in techniques of measurement and understanding of the change made since AR4 (Cazenave et al., 2009; Chen et al., 2011; IPCC, 2007)

4.4.2.1 Techniques

There are broadly three techniques for measuring ice sheet mass balance. All have been applied to both ice sheets by multiple groups, and over time scales ranging from multiple years to decades (Figures 4.13 to 4.17).

[INSERT FIGURE 4.13 HERE]
Figure 4.13: Temporal pattern of ice loss in Greenland from GRACE time-variable gravity in cm of water per year for the periods (a) 2002 to 2006, (b) 2006 to 2011 and (c) 2002 to 2011, color coded red (loss) to blue (gain) (Velicogna, 2009). Circles in c) indicate average ice loss (Gt/yr) from GRACE (red = mass budget (Rignot et al., 2011b); orange = GRACE (Velicogna, 2009); and blue = ICESat (Sorensen et al., 2011)); (d) surface mass balance for years 1957–2009 (Ettema et al., 2009); (e) ice velocity from satellite radar interferometry data for years 2007–2009, and (f) ice-thinning rates from ICESat data for years 2003–2008 (Pritchard et al., 2009).

[INSERT FIGURE 4.14 HERE]
Figure 4.14: Temporal evolution of ice loss in Antarctica from GRACE time-variable gravity in cm of water per year for the periods (a) 2002 to 2006, (b) 2006 to 2011 and (c) 2002 to 2011, color coded red (loss) to blue (gain) (Velicogna, 2009). Circles in (c) indicate average ice loss (Gt/yr) for 2002–2011 for the Antarctic Peninsula (red = flux (Rignot et al., 2011b); orange = GRACE (Ivins et al., 2011)), the West Antarctic Ice Sheet (red = flux (Rignot et al., 2011b)), orange = GRACE (Velicogna, 2009) and East Antarctica (red = flux (Rignot et al., 2008b)), orange = GRACE (Chen et al., 2009)); no regional estimates are available from altimetry for that time period; (d) surface mass balance in Antarctica for years 1989–2004 (van den Broeke et al., 2006); (e) ice sheet velocity for 2007–2009 showing fastest flow in red, fast flow in blue, and slower flow in green and yellow (Rignot et al., 2011a); (f) ice thinning rates from ICESat for years 2003–2008 with thinning in red to thickening in blue (Pritchard et al., 2009).

4.4.2.1.1 Mass budget method
The mass budget method relies on estimating the difference between surface mass balance (input) and perimeter fluxes (output). It compares two very large numbers, and even small errors in either may result in large errors in total mass balance. However, advances since AR4 have provided increasing reliability.

For ice discharge, improvements include more complete mapping of perimeter fluxes for both ice sheets (Rignot et al., 2011a), more complete ice-thickness data (Griggs and Bamber, 2009) and velocity data from satellite radar interferometry (Joughin et al., 2010b; Rignot et al., 2011a). However, incomplete ice thickness mapping still causes uncertainties in ice discharge at several percent.

For surface mass balance, regional atmospheric climate models are increasingly used to produce estimates that are verified using independent in situ data. Surface mass balance in Antarctica averaged 2,080 Gt yr^{-1} in 1989–2009 (Arthern et al., 2006; Monaghan et al., 2006) with interannual variability of 300 Gt yr^{-1} (6%), and an average uncertainty of 5% or 90 Gt yr^{-1} (Figure 4.14). In Antarctica runoff is negligible, however, interannual variability in surface mass balance in Greenland is mostly caused by variation in runoff. Surface mass balance ranges from 300 to 600 Gt yr^{-1} with an average uncertainty of 40 Gt yr^{-1} (7%) (Hanna et al., 2008) (Figure 4.13). Combining uncorrelated errors in input and output, current mass budget uncertainties are about 101 Gt yr^{-1} in Antarctica and 51 Gt yr^{-1} in Greenland.

4.4.2.1.2 Repeated altimetry
Repeat altimetry measures rates of surface-elevation change with time (dS/dt), revealing changes in ice sheet mass after correction for changes in snow density and bed elevation, or if the ice is floating, from tides and sea level.

Satellite radar altimetry (SRALT) has been widely used (e.g., Thomas et al., 2008b; Wingham et al., 2009) together with laser altimetry from airplanes (Krabill et al., 2002; Thomas et al., 2009) and satellites (Abdalati et al., 2010; Pritchard et al., 2009; Zwally et al., 2011), but with significant challenges. The surface footprint of early SRALT sensors was 20 km, and interpretation is complex over ice sheets with undulating surfaces or significant slopes. Estimates are also affected by surface characteristics, e.g., wetness (Thomas et al., 2008b). The ESA CryoSat-2 radar altimeter promises to be another valuable tool, although the first release of data is too recent to assess its impact (Wingham et al., 2006b).

Laser altimeters have been used from aircraft for many years, but satellite laser altimetry, available for the first time from NASA's ICESat satellite launched in 2003, provides a major advance in capability since AR4. Laser altimetry is easier to validate and interpret than radar data; the footprint is small (1 m for airborne laser, 60 m for ICESat), and there is negligible penetration into the ice. However, clouds limit spaceborne data acquisition, accuracy is affected by atmospheric conditions, laser-pointing errors, and data scarcity. Laser surveys over Greenland yield elevation estimates accurate to 10 cm along survey tracks for airborne platforms (Krabill et al., 1999; Thomas et al., 2011) and 15 cm for ICESat (Siegfried et al., 2011).

4.4.2.1.3 Temporal variations in earth gravity field

Since 2002, the GRACE (Gravity Recovery and Climate Experiment) satellite mission has surveyed Earth's time-variable gravity field. Time-variable gravity provides a direct estimate of the ice-mass change. GRACE data yielded early estimates of 'secular' ice-mass changes over the Greenland and Antarctic ice sheets (Luthcke et al., 2006; Velicogna and Wahr, 2006a, 2006b) and confirmed regions of ice loss in East Greenland and West Antarctica. With extended time series, now more than nine years, GRACE results have lower uncertainties than in AR4. The ice loss signal is also more distinct due to the increased rate of ice sheet loss (e.g., Cazenave et al., 2009; Chen et al., 2009; Velicogna, 2009; Wouters et al., 2008). GRACE ice loss estimates vary among published studies. Some of the difference is caused by the time-variable nature of the signal. Additional differences are caused by: (1) errors introduced by data-centre specific processing, (2) post-processing errors due specific methods used to calculate the mass change, and (3) post-processing errors due to contamination by other signals within the ice sheet (e.g., glacial isostatic adjustment or GIA) or outside the ice sheet (continental hydrology, ocean).

In Antarctica, the GIA signal is of the same order as the ice loss signal, with an uncertainty of 80 Gt yr^{-1} (Riva et al., 2009; Velicogna, 2009; Velicogna and Wahr, 2006a). The GIA signal is allowed for using numerical models, (e.g., Ivins and James, 2005; Paulson et al., 2007; Peltier, 2009). In Greenland, only a small GIA correction is required, with a contribution of less than 10% of the GRACE signal and an error of 19 Gt yr^{-1}. However, since the GIA rate is constant over the satellite's lifetime, GIA uncertainty does not affect the estimate of change in the rate of ice mass-loss.

In addition to GRACE, measurements of the elastic response of the crustal deformation shown in GPS measurements of uplift rates confirm increasing rates of ice loss in Greenland (Khan et al., 2010) and Antarctica (Thomas et al., 2011). Analysis of a 34-year time series of Earth's oblateness (J2) by satellite laser ranging also suggests that ice loss from Greenland and Antarctica has progressively dominated the J2 trend since the 1990s (Nerem and Wahr, 2011).

4.4.2.2 Greenland

There is robust evidence and strong agreement between the methods described above that the Greenland Ice Sheet has been losing ice and contributing to sea level rise over recent years. Recent GRACE results are in better agreement than in AR4 as discussed above (Baur et al., 2009; Chen et al., 2011; Pritchard et al., 2009; Schrama and Wouters, 2011; Thomas et al., 2006; Velicogna, 2009; Wu et al., 2010). Altimetry missions report slightly lower losses than other methods (Zwally et al., 2011)) but sampling is sparser along the coast where much of the loss is concentrated (Figure 4.13f).

[INSERT FIGURE 4.15 HERE]

Figure 4.15: Cumulative sea level rise (and ice loss equivalent) from Greenland derived from the weighted average of 12 recent studies (see Table 4.5 and Appendix 4.A) (Baur et al., 2009; Cazenave et al., 2009; Chen et al., 2011; Pritchard et al., 2010; Rignot et al., 2011b; Sasgen and others, In review; Schrama and Wouters, 2011; Slobbe et al., 2009; Sorensen et al., 2011; Velicogna, 2009; Wu et al., 2010; Zwally et al., 2011). The studies selected are the latest made by 12 different research groups, for Greenland, and do not include earlier estimates from the same researchers

when those have been updated by more recent analyses using extended data. In calculating the average, each estimate has been weighted based on an assessment of its reliability: High reliability = weighting of 1.0, Medium = 0.5, Low = 0.2. The number of estimates used in this composite varies with time, with only 2 per year in the 1990s and up to 12 per year after 2002. The plotted values are the cumulative sea level contribution at the end of the year on the x-axis, starting at an arbitrary zero on January 1st 1992. Since yearly estimates from different studies do not overlap within the uncertainties quoted by the authors, the errors shown are based on the maximum and minimum estimate for each year within uncertainty ranges cited in the original studies. The cumulative error is weighted by $1/\sqrt{n}$, where n is the number of years accumulated.

Despite year-to-year differences between the various original analyses, the multi-study assessment provides robust evidence that Greenland has lost mass over the last two decades, and that the rate of loss has increased. This increase is also shown in many individual studies (Chen et al., 2011; Rignot et al., 2011b; Velicogna, 2009; Zwally et al., 2011) (Figure 4.13a-c). The total sea level contribution from the Greenland ice sheet has been 5.9 mm (±1.1 mm) over the period 1992–2009, and 4.5 mm (±1.0 mm) between 2002 and 2009.

Partitioning of ice loss

The mass budget method shows the partitioning of ice loss from the ice sheet is about 50% surface mass balance (i.e., runoff) and 50% glacier discharge (van den Broeke et al., 2009) (Figure 4.13d).

Surface mass balance

Altimetric measurements of surface height suggest slight inland thickening (Thomas et al., 2006, 2009) that is not confirmed by regional atmospheric climate models (Ettema et al., 2009). Probable changes in accumulation are however exceeded by the increased runoff especially since 2006 (Box et al., 2006; van den Broeke et al., 2009). The total melt area has continued to increase since AR4 and has accelerated in the past few years (Fettweis et al., 2011; Tedesco et al., 2011). Five of the highest runoff years over the last 49 years occurred since 2001 (Hanna et al., 2008).

Regional changes

There are significant differences in the relative importance of ice-discharge and surface mass balance in various regions of Greenland (Howat et al., 2007; Pritchard et al., 2009; Sasgen and others, in review; van den Broeke et al., 2009). Dynamic losses dominate in South-East and North-West Greenland; changes in SMB dominate in the central north, southwest and northeast sectors. In the northwest, the acceleration in ice loss from 1996–2006 to 2006–2010 was caused by a high accumulation in the late 1990s (Sasgen and others, in review), whereas in the southeast the reduction in ice loss after year 2005 is caused by a slowdown of many glaciers (Howat et al., 2007).

GRACE results show ice loss was concentrated in South-East Greenland during 2005 and increased in the northwest after 2007 (Chen et al., 2011; Khan et al., 2010; Schrama and Wouters, 2011). Subsequent to 2005, ice loss decreased in the southeast. These GRACE results agree with measurements of ice discharge from the major glaciers that confirm the dominance of dynamic losses in these regions (van den Broeke et al., 2009). In particular, a major glacier speed up occurred in Central East, South-East and Central West Greenland between 1996–2000 (Howat et al., 2008; Rignot and Kanagaratnam, 2006) and in 2003–2005 (Joughin et al., 2010b): in the southeast many glaciers slowed after 2005 (Howat et al., 2007), with many flow speeds decreasing back towards those of the early 2000s (Murray et al., 2010), although most are still flowing faster than they did in 1996.

4.4.2.3 Antarctica

Antarctic results from the gravity method are also now more numerous and consistent than in AR4 (Figure 4.14a-c). Methods combining GPS and GRACE indicate the Antarctic Peninsula is certainly losing ice (Ivins et al., 2011). In other areas, large uncertainties remain in the GRACE-GPS combined approach (Wu et al., 2010).

Results from the mass budget method have improved significantly since AR4 (Lenaerts et al., in press; Rignot et al., 2011b; Rignot et al., 2008b; van den Broeke et al., 2006). Reconstructed snowfall from regional atmospheric climate models indicates higher accumulation along the wet coastal sectors than in prior maps, but little difference in total snowfall. There is no long-term trend in total accumulation over the past few decades (Bromwich et al., 2011; Monaghan et al., 2006; van den Broeke et al., 2006). Satellite and airborne laser altimetry indicate that ice volume changes are concentrated on outlet glaciers and ice streams, as illustrated by the strong correspondence between areas of thinning (Figure 4.14f) and areas of fast flow (Figure 4.14e).

[INSERT FIGURE 4.16 HERE]

Figure 4.16: Assessment of the cumulative sea level contribution from Antarctica derived from the weighted average of 12 recent analyses (see Table 4.5 and Appendix 4.A) (Cazenave et al., 2009; Chen et al., 2009; Dong-Chen et al., 2009; Horwath and Dietrich, 2009; Ivins et al., 2011; Moore and King, 2008; Rignot et al., 2011b; Shi et al., 2011; Velicogna, 2009; Wingham et al., 2006a; Wu et al., 2010; Zwally et al., 2005). The studies selected are the latest made by 12 different research groups for Antarctica, and do not include earlier estimates from the same researchers when those have been updated by more recent analyses using extended data. In calculating the average, each estimate has been weighted based on an assessment of its reliability: High reliability = weighting of 1.0, Medium = 0.5, Low = 0.2. The number of estimates used in this composite varies with time, with only 2 per year in the 1990s and up to 12 per year after 2002. The plotted values are the cumulative sea level contribution at the end of the year on the x-axis, starting at an arbitrary zero on January 1st 1992. Since yearly estimates from different studies do not overlap within the uncertainties quoted by the authors, the errors shown are based on the maximum and minimum estimate for each year within uncertainty ranges cited in the original studies. The cumulative error is weighted by $1/\sqrt{n}$, where n is the number of years accumulated. See Section 4.4.2.2 for further details.

Overall, the ice sheet is very likely currently losing mass. The total sea level contribution from Antarctica has been 3.4 mm (±1.6 mm) over the period 1992–2009, and 3.0 mm (±1.1 mm) between 2002 and 2009.

Significantly, ice loss is almost certainly increasing with time (Chen et al., 2009; Rignot et al., 2011b; Velicogna, 2009) (Figure 4.16). For GRACE, this conclusion is independent of the GIA signal, which is constant. From the mass budget method, the increase in loss is certainly caused by an increase in glacier flow-speed in West Antarctica (Joughin et al., 2010a; Rignot, 2008; Thomas et al., 2011) and the Antarctic Peninsula (Pritchard and Vaughan, 2007; Rignot, 2006; Rott et al., 2011; Scambos et al., 2004). Comparison of GRACE and the mass budget methods indicate an increase in ice loss of 14 ± 2 Gt yr^{-1} every year for 1992–2010 versus 21 ± 2 Gt yr^{-1} for Greenland during the same time period (Rignot et al., 2011b).

Partitioning of ice loss

In the absence of surface runoff and long-term change in total snowfall, Antarctic long-term changes in grounded ice mass are almost entirely explained by increased glacier speed.

Regional changes

The three mass balance methods are in excellent agreement as to the spatial pattern of ice loss (thinning) and gain (thickening) in Antarctica (Figure 4.14). The largest ice losses are located along the northern tip of the Antarctic Peninsula where ice shelves continue to collapse and in the Amundsen Sea, in West Antarctica (Figure 4.14c). In the Antarctic Peninsula, precipitation is likely to have increased (Thomas et al., 2008a) but the resulting ice-gains are insufficient to counteract the losses (Cook and Vaughan, 2010; Ivins et al., 2011; Wendt et al., 2010). Changes in the Amundsen Sea region are likely due to the thinning of ice shelves by a warm ocean (Jacobs et al., 2011), which caused grounding line retreat (1 km yr^{-1}) (Joughin et al., 2010a) and glacier thinning (Wingham et al., 2009). Indications of dynamic change are also evident from East Antarctica, primarily Totten Glacier, from GRACE (Chen et al., 2009), SRALT (Wingham et al., 2006a) and satellite radar interferometry (Rignot et al., 2008b). The contribution to the total ice loss from these areas is however small and poorly understood.

4.4.2.4 Floating Ice Shelves

As much as 74% of the ice discharged from Antarctica passes through ice shelves and floating ice tongues (Bindschadler and 17 others, 2011). Ice shelves help to buttress and restrain flow of the inland ice (Hulbe et al., 2008; Rignot et al., 2004; Scambos et al., 2004), and so changes in thickness (Pritchard et al., in submission; Shepherd et al., 2003; Shepherd et al., 2010) and extent (Doake and Vaughan, 1991; Scambos et al., 2004; Tedesco et al., 2011) of ice shelves influence current ice sheet change. Indeed, nearly all glaciers experiencing high rates of ice loss are flowing into thinning or disintegrated ice shelves (Pritchard et al., in submission).

Around the Antarctic Peninsula, ice shelf retreat has been ongoing for several decades, and has continued since AR4 with substantial collapse of a section of Wilkins Ice Shelf (Humbert et al., 2010) that had been retreating since the late-1990s (Scambos et al., 2000). Overall, 7 of 12 ice shelves around the Peninsula have retreated in recent decades with a total loss of 28,000 km^2, and a continuing rate of loss of around 6,000 km^2 per decade (Cook and Vaughan, 2010).

4.4.2.5 Total Ice Loss from Both Ice Sheets

The total ice loss from both ice sheets for 1992–2009 (inclusive) has been 3,400 ± 980 Gt, equivalent to 9.4 ± 2.7 mm of sea level rise. The majority of this ice however has been lost in the second half of the period, and the rate of change has increased steadily with time. Over the last three years (2007–2009) it has been equivalent to 1.08 mm yr^{-1} of sea level rise (Figure 4.17)

[INSERT FIGURE 4.17 HERE]

Figure 4.17: Rate of ice sheet contribution to sea level rise averaged over 5 year periods between 1992 and 2009 (the last period is only 3 years). These estimates are derived from the data in Figures 4.15 and 4.16.

Table 4.5: Weighted average of 12 estimates of sea level rise as described in Figures 4.15 and 4.16.

Period	Weighted average of 12 estimates (mm sea level rise /yr)	
Greenland		
1992–2001 (10-yr)	0.14	±0.06
2002–2009 (8-yr)	0.56	±0.13
1992–2009 (18-yr)	0.33	±0.06
Antarctica		
1992–2001 (10-yr)	0.05	±0.12
2002–2009 (8-yr)	0.37	±0.14
1992–2009 (18-yr)	0.19	±0.09
Combined		
1992–2001 (10-yr)	0.19	±0.18
2002–2009 (8-yr)	0.93	±0.27
1992–2009 (18-yr)	0.52	±0.15

4.4.3 Causes of Changes in Ice Sheets

4.4.3.1 Climatic Forcing

4.4.3.1.1 Snowfall and surface temperature

Ice sheets experience large inter-annual variability in snowfall and local trends may deviate significantly from the long-term trend in integrated snowfall, but – as in AR4 – there is very little evidence for long-term change (Bromwich et al., 2011; Ettema et al., 2009; Monaghan et al., 2006; van den Broeke et al., 2010).

Over Greenland, temperature has risen significantly since the early-1990s, reaching values similar to those in the 1930s (Box et al., 2009). The year 2010 was the warmest since 1978 in west Greenland (Tedesco et al., 2011). In Antarctica, in response to ozone depletion, the summertime Southern Annular Mode strengthened from the mid-1950s to the mid-1990s (Thompson et al., 2011). This strengthening has resulted in statistically significant summer warming on the east coast of the northern Antarctic Peninsula (Chapman and Walsh, 2007; Marshall et al., 2006) while East Antarctica has showed summer cooling (Turner et al., 2005). In contrast, the significant winter warming at Faraday/Vernadsky station in the western Antarctic Peninsula is caused by a reduction of sea ice extent (Turner et al., 2005), while winter temperatures in West Antarctica are responding to tropical sea surface temperatures (Ding et al., 2011).

4.4.3.1.2 Ocean thermal forcing

Interaction between ocean waters and the periphery of large ice sheets very likely plays a major role in present ice sheet changes (Bindschadler, 2006) . Ocean waters provide the heat that drives high melt rates beneath ice shelves (Holland and Jenkins, 1999; Jacobs et al., 1992; Rignot and Jacobs, 2002) and at marine-terminating glacier fronts (Holland et al., 2008a; Jacobs et al., 2011; Rignot et al., 2010). The importance of this effect has become increasingly apparent through observations made since AR4.

Wind-driven ocean circulation delivers warm, salty waters originating from lower-latitudes to polar oceans. Variations in wind patterns associated with the North Atlantic Oscillation (Hurrell, 1995; Jacobs et al., 1992) and the Southern Annular Mode (Thompson and Wallace, 2000) are probable drivers of increasing amounts of warm water towards the ice sheet margins. Limited but strong observations have established that warm waters are present beneath some Antarctic ice shelves (Jacobs et al., 1996; Martinson et al., 2008), and that some marine-terminating glacier in Greenland are in contact with warm waters of tropical origin (Christoffersen et al., 2011; Daniault et al., 2011; Myers et al., 2007; Myers et al., 2009; Straneo et al., 2010). The presence of warm waters is a necessary condition for rapid melting but other factors are important, such as the bathymetry of fjords and ice shelf cavities (Jenkins et al., 2010).

Satellite records and *in situ* observations indicate warming of the Southern Ocean (see Chapter 3) since the 1950s (Gille, 2002; Gille, 2008). This warming is confirmed by data from robotic ocean buoys (Boning et al., 2008) but the observational record remains short and close to Antarctica there are only scattered observations from ships (Jacobs et al., 2011), short-duration moorings and data from instrumented seals (Charrassin et al., 2008; Costa et al., 2008).

4.4.3.2 Ice Sheet Processes

4.4.3.2.1 Basal lubrication

In Greenland, abundant summer meltwater on the surface of the ice sheet forms large lakes in many areas. This surface water can drain to the ice sheet bed to lubricate ice flow through conduits created by rapid lake drainage. Such conduits are common in southwest and northeast Greenland, but rare in the most rapidly changing southeast and northwest regions (Selmes et al., 2011). This effect can be seen in diurnal flow variations of some land-terminating regions (Das et al., 2008; Shepherd et al., 2009), and after lake-drainage events, when 50–110% speed-up of flow has been observed. However, the effect is temporally and spatially restricted (Das et al., 2008) and the annual increase in speed is only ~10–20%, and speed increases fall at higher elevations (Bartholomew et al., 2011b). Theory and field studies suggest an initial increase in flow rate with increased surface meltwater supply (Bartholomew et al., 2011a; Palmer et al., 2011), but as melting continues to increase and subglacial drainage becomes more efficient, speed-up eventually becomes less (Schoof, 2010; Sundal et al., 2011; van de Wal et al., 2008). Overall, basal lubrication appears important in modulating flow in some regions, especially southwest Greenland, but it does not explain recent dramatic regional speed-ups that have resulted in rapid increases in ice loss from calving glaciers. Future basal lubrication may, however, cause a progressive increase in the rate of ice loss from land-terminating portions of the ice sheet (Parizek and Alley, 2004).

Percolation of surface meltwater through the ice column via moulins, crevasses and fractures may also affect the thermal regime of the ice sheet (Phillips et al., 2010), causing near-basal ice to soften and become easier to deform, affecting flow on decadal time scales.

4.4.3.2.2 Ice shelf buttressing

Recent changes in marginal regions of the Greenland and Antarctic ice sheets include some thickening and slowdown but mostly thinning and acceleration (Pritchard et al., 2009; Sorensen et al., 2011), with some glacier speeds increasing two to eightfold (Howat et al., 2007; Joughin et al., 2004; Luckman and Murray, 2005; Rignot and Kanagaratnam, 2006; Rignot et al., 2004; Rott et al., 2011; Scambos et al., 2004). Many of the largest and fastest glacier changes appear to be partly in response to ice shelf or floating ice-tongue shrinkage or loss. This glacier response is consistent with classical models of ice shelf buttressing and marine instability proposed 40 years ago (Hughes, 1973; Mercer, 1978; Thomas and Bentley, 1978; Weertman, 1974).

4.4.3.2.3 Ice-ocean interaction

Warm waters at depth melt the periphery of ice sheets in Greenland and Antarctica and very likely play a central role in the evolution of the ice sheets. Numerical models suggest that ice melting is proportional to the product of ocean thermal forcing (difference between ocean temperature and the in-situ freezing point of seawater) and water flow speed at the ice-ocean interface (Holland and Jenkins, 1999). Flow speed may increase with thermal forcing due to greater ice melting increasing the buoyancy of the melt-water plume (Holland et al., 2008a), but observations are not yet sufficient to verify this conclusion.

Ice-ocean interactions are very likely important in Greenland. Melt rates along marine-terminating glacier margins are one to two orders of magnitude greater than for the nearly horizontal faces of ice shelves because of the additional buoyancy forces provided by the discharge of sub-glacial melt water at the glacier base (Jenkins, 2011; Motyka et al., 2003). There is robust evidence from South Greenland that the acceleration of glaciers from the mid-1990s to mid-2000s was likely due to the intrusion of ocean waters of sub-tropical origin into glacial fjords (Christoffersen et al., 2011; Holland et al., 2008b; Howat et al., 2008; Murray et al., 2010; Straneo et al., 2011; Straneo et al., 2010). The increase in ice melting by the ocean most probably contributed to the de-stabilization of the glacier fronts and their acceleration (Nick et al., 2009; Payne et al., 2004; Schoof, 2007; Thomas, 2004).

4.4.3.2.4 Iceberg calving

Calving of icebergs from marine-terminating glaciers and ice-shelves is important in their overall mass balance, but the processes that initiate calving range from seasonal melt-driven processes (Benn et al., 2007), to rare, and hard to predict, break-up events caused by ocean swells and tsunamis (MacAyeal et al., 2006). Some of these processes show strong climate influence, while others do not. Progress in recent times has been argued to be rather limited (Pfeffer, 2011), although there have been recent advances (Amundson et al., 2010; Blaszczyk et al., 2009; Joughin et al., 2008), and continental-scale ice sheet models currently rely on heuristic parameterisations (Alley et al., 2008; Pollard and DeConto, 2009). Recently more realistic models have been developed allowing the dependence of calving and climate to be explicitly investigated (Nick et al., 2010).

4.4.4 Rapid Ice Sheet Changes

The IPCC AR4 Summary for Policy Makers estimates of sea level rise excluded future rapid dynamical changes in ice flow because at that time the feeling was that “understanding of these processes is limited and there is no consensus on their magnitude“. Here, we summarise those processes thought be potential causes of rapid changes in ice flow and outline observational evidence that those processes are currently occurring, emphasizing progress and new observations since AR4. We consider "rapid ice sheet changes" to be changes that are of sufficient speed and magnitude to impact on the rate of sea level rise on timescales of several decades or less. A further consideration is whether and under what circumstances any such changes are ‘irreversible’, i.e., would take several decades to centuries to reverse under a different climate forcing. For example, an effectively irreversible change might be the loss of a significant fraction of the Greenland Ice Sheet, because a feedback between elevation and surface temperature that would prevent thinning of Greenland ice sheet from reversing until there was a significant cooling (Ridley et al., 2010).

Since AR4, new observations in Greenland and Antarctica and theoretical advances suggest that rapid changes are to be expected in those regions of ice sheets that are grounded well below sea level (Figure 4.18). Where this ice meets the ocean, warm waters can increase bottom and ice front melting, causing undercutting, higher calving rates, ice-front retreat (Benn et al., 2007; Motyka et al., 2003; Thomas et al., 2011), speed-up and consequent thinning. These processes can occur in tandem with increased surface melting which increases ice flow, ice fracturing and calving rates. Where ice shelves are present, ice melt by the ocean may cause migration of the grounding line further inland into the deep basin, with a major impact on buttressing, flow speed and thinning rate (Thomas et al., 2011).

[INSERT FIGURE 4.18 HERE]

Figure 4.18: Bed topography for Greenland and Antarctica, derived from (Griggs and Bamber, 2011a; Pritchard et al., 2011) with marine-based parts of the ice sheet highlighted and arrows showing access routes for rapid discharge of marine-based sectors. Figure drawn by P. Fretwell, BAS.

The influence of the ocean on the ice sheets is controlled by the delivery of heat to the ice sheet margins, in particular to ice shelf cavities and calving fronts (e.g., Jacobs et al., 2011). This delivery of heat is in turn the result of the temperature and salinity of ocean waters, but also ocean circulation controlled by winds, and the details of the bathymetry on the continental shelves, near glacier fronts and beneath ice shelves (Pritchard et al., in submission). Changes in any of these parameters around the edges of major ice sheets will have a direct and rapid impact on ice loss.

Ice grounded on a reverse bed-slope, deepening towards the ice sheet interior, is potentially subject to the marine ice sheet instability (Schoof, 2007; Weertman, 1974; see Chapter 13). Much of the bed of the West Antarctic Ice Sheet (WAIS) lies below sea level and on a reverse bed-slope, with basins extending to depths greater than 2 km (Figure 4.6). The marine parts of the WAIS contain at least ~3.3 m of sea level rise (Bamber et al., 2009) and a variety of evidence strongly suggests that the ice sheet has been much smaller than present in the last 1 million years, during periods with temperatures similar to those predicted in the next century (Kopp et al., 2009). Potentially unstable marine ice sheets also exist in East Antarctica, e.g., in Wilkes Land (Pritchard et al., 2009; Young et al., 2011), and these contain more ice than WAIS (9 m sea level equivalent for Wilkes Land). The Totten, Cook Ice Shelf and Denman glaciers, East Antarctica, are showing signs of dynamic thinning at present. In northern Greenland, ice is also grounded below sea level, with reverse slopes (Figure 4.18) (Thomas et al., 2011). In north Greenland, marine sectors have not yet shown significant thinning.

Observations since AR4 confirm that rapid changes are occurring at the marine margins of ice sheets, and that these changes can penetrate hundreds of kilometers inland quickly (Joughin et al., 2008; Pritchard et al., 2009). Collapse of floating ice shelves on the Antarctic Peninsula has resulted in speeding up of tributary glaciers of 300–800%. This speed-up in turn has drawn down ice in the interior, accelerating the loss of grounded ice previously buttressed by the ice shelves. The glaciers on this peninsula contain only a few cm of sea level, however, similar processes acting on the larger ice shelves further south could lead to rapid loss of ice from the West Antarctic Ice Sheet. The Amundsen Sea sector of West Antarctica is grounded significantly below sea level and is the region presently changing most rapidly. As a result of grounding line retreat very likely caused by the intrusion of warm ocean water into the sub-ice shelf cavity (Jenkins et al., 2010), Pine Island Glacier has sped up 73% since 1974 (Rignot, 2008) and the glacier floating ice tongue thinned throughout 1995–2008 at increasing rates (Wingham et al., 2009). Neighboring Thwaites, Smith and Kohler glaciers are also speeding-up and thinning (Figure 4.14).

Similarly, in Greenland, the recent rapid retreat of Jakobshavns Isbrae was very likely caused by the intrusion of warm ocean water beneath the floating ice tongue (Holland et al., 2008a) combined with other factors. It is likely that recent variations in South-East Greenland's glaciers have been caused by the intrusion of warm waters of sub-tropical origin. Since AR4 it has become clear that the mid-2000s speed up of South-East Greenland glaciers, which caused a doubling of ice loss from the Greenland ice sheet (Howat et al., 2008; Luthcke et al., 2006; Rignot and Kanagaratnam, 2006; Wouters et al., 2008), was a pulse which was followed by a partial slow down (Howat et al., 2008; Murray et al., 2010).

In contrast to the rapidly changing marine margins of the ice sheets, the land-terminating regions of the Greenland Ice Sheet are changing more slowly, and those changes are largely explained by changes in the input of snow and loss of meltwater (Sole et al., 2011). Surface meltwater, while abundant on the Greenland Ice Sheet, does not seem to be driving significant changes in basal lubrication that impact on the ice sheet flow (Joughin et al., 2010b; Selmes et al., 2011; Sundal et al., 2011).

The Antarctic Peninsula has continued to experience irreversible changes, coincident with air temperatures at some stations rising at four to six times the global average (Vaughan et al., 2003) and with warm Circumpolar Deep Water becoming widespread on the western continental shelf (Martinson et al., 2008). The 2002 collapse of the Larsen B Ice Shelf has been unprecedented in the last 10,000 years (Domack et al., 2005) and is irreversible: even if iceberg calving were to cease entirely, regrowth of the Larsen B ice shelf to its pre-collapse state would take centuries.

In contrast, in Greenland changes do not yet appear irreversible. For example, the breakup of the floating tongue of Jakobshavn Isbrae and consequent loss of buttressing has increased ice flow speeds and discharge from the ice sheet, but Jakobshavn has undergone significant margin changes over the last ~8,000 years which have been both more and less extensive than the recent ones (Young et al., 2011).

Despite many new observations that demonstrate changes can happen more rapidly than previously thought together with strong evidence that ice-ocean interactions are the likely key to future decadal changes, there is still an incomplete basis for future projection. At least another decade of monitoring forcing and response, together with major progress in numerical modelling, will be required before robust projections are possible. However, it is very likely to certain that rapid changes in the marine margins of both Antarctica and Greenland will be observed in coming decades.

4.5 Seasonal Snow and Freshwater Ice Cover

4.5.1 Background

Snow is measured using a variety of instruments and techniques, and reported as one of several quantitative metrics including snow cover extent (SCE), the seasonal sum of daily snowfall, snow depth, number of days with snow above a threshold depth, or snow water equivalent (SWE). Long-duration, consistent records of snow are rare owing to many challenges of measuring it. While weather stations in inhabited snowy areas often report snow depth, records of snowfall are often patchy or use techniques that change over time (e.g., Kunkel et al., 2007), except in certain parts of the European Alps. The density of stations and the choice of snow metric also varies considerably from country to country. The longest satellite-based record of SCE is the visible-wavelength weekly product of the National Oceanic and Atmospheric Administration (NOAA) dating to 1966 (Robinson et al., 1993) but this only covers the Northern Hemisphere (NH). Measurement challenges are particularly acute in the Southern Hemisphere (SH): in contrast to the geostationary NOAA satellites, which see only the NH, satellite-based mapping of SCE, snow depth, and SWE in the SH began only in 1978; but for the data to be useful for trends, differences between passive microwave instruments used before and after 1987 must be resolved (e.g., Jezek et al., 1993). With hardly any inhabited snowy areas in the SH, only 10 long-duration records continue to recent times: six in the central Andes and four in southeast Australia.

4.5.2 Hemispheric View

By blending *in situ* and satellite records, Brown and Robinson (2011) have updated a key indicator of climate change, namely the time series of NH SCE (Figure 4.19), which shows significant reductions over the past 90 years and a higher rate of decrease during the last 40 years. Decreases were larger in spring than in other seasons (Dery and Brown, 2007). Averaged March and April NH SCE was around 8% lower (7 Million km^2) over the period 1970–2010 than over the period 1922–1970. Viewed another way, the NOAA SCE data indicate that the duration of the snow season averaged over NH grid points declined by 5.3 days per decade since 1972–1973 owing to earlier spring snowmelt (Choi et al., 2010). In North America, Dyer and Mote (2006) used a gridded dataset of snow depth derived from observations for 1960–2000, finding minimal change in early winter and regional decreases beginning in late January. Over Eurasia, in situ data show significant increases in winter snow accumulation but a shorter snowmelt season (Bulygina et al., 2009). From analysis of passive microwave satellite data since 1979, significant trends toward a shortening of the snowmelt season have been identified over much of Eurasia (Takala et al., 2009) and the pan-Arctic region (Tedesco et al., 2009), with a trend toward earlier melt of about –0.5 days yr^{-1} for the beginning of the melt season, and about +1 day yr^{-1} for the end of the melt season.

[INSERT FIGURE 4.19 HERE]
Figure 4.19: Variability April NH SCE over the period of available data with13-term filtered values of the mean and 95% confidence interval. The width of the smoothed confidence interval is also influenced by the interannual variability in SCE. From Brown and Robinson (2011), updated.

The correlation between spring temperature and SCE (Figure 4.20) demonstrates that trends in spring SCE are linked to rising temperature, and for a well-understood reason. The spring snow cover-albedo feedback contributes substantially to the hemispheric response to rising greenhouse gases and provides a useful test of GCMs (Fernandes et al., 2009) (see also Chapter 9). Indeed, the observed declines in land snow cover and sea ice have contributed roughly the same amount to reductions in the surface energy balance, and the albedo feedback of the NH cryosphere is likely in the range 0.3 – 1.1 W m^{-2} K^{-1} (Flanner et al., 2011). Brown et al. (2010) used satellite, reanalyses and in situ observations to document variability and trend in Arctic spring (May-June) SCE over the 1967–2008 period. In June, with Arctic albedo feedback at a maximum, SCE decreased 46% and air temperature explains 56% of the variability; SCE and sea ice extent in June are both significantly correlated to air temperature and decreased by similar amounts.

[INSERT FIGURE 4.20 HERE]

Figure 4.20: Relationship between NH April SCE and corresponding land area air temperature anomalies over 40°N–60°N from the CRU dataset. Air temperature explains 48.7% of the variance. From Brown and Robinson (2011).

For the SH, as noted above, there are no corresponding visible-wavelength satellite records, but microwave data date from 1979. Foster et al. (2009) presented the first satellite study of variability and trends in any measure of snow for South America, in this case SWE from microwave data. They focused on the May-September period and noted large year-to-year and lower frequency variability – the July with most extensive snow cover had almost 6 times as much as the July with the least extensive snow cover – but no trends.

4.5.3 Trends from In Situ Measurements

AR4 stimulated a review paper (Brown and Mote, 2009) that synthesized modelling results as well as observations from 14 countries, noting that decreases in various metrics of snow are most likely to be observed in spring and at locations near the freezing point, where changes in temperature are most effective at reducing snow accumulation, increasing snowmelt, or both. Unravelling the competing effects of rising temperatures and changing precipitation remains an important challenge in understanding and interpreting observed changes. Figure 4.21 is a compilation of many published studies of trends at individual locations; where results were not tabulated in the source paper, the data presented in the paper were obtained from the author for plotting. Some studies did not include relative changes. Ke et al. (2009) looked at snowfall trends by month at 25 stations in Qinghai province, China over 1957–2007; for annual mean snowfall, 5 stations showed significant decreases, 2 showed significant increases, and 18 had insignificant changes. The most significant trends were in May, with 11 decreases and no increases. Visual observations of snow cover duration on a mountain in Scotland showed no trend over the 1954–2003 period but downward trends at all altitudes (130 – 1,200 m) for 1979–2003 (Trivedi et al., 2007).

[INSERT FIGURE 4.21 HERE]

Figure 4.21: Summary of station trends in metrics of snow that, based on the work of Brown and Mote (2009), are (top half) more reflective of mid-winter conditions and (bottom half) more reflective of spring conditions. Where symbols are circles, the quantity plotted is the percentage change of a linear fit divided by the number of years of the fit. For the Bulygina study, the quantity plotted is the trend in cm yr^{-1} (top) and # days yr^{-1} (bottom). Solid circles in the Skaugen study were statistically significant. Christy (In submission) combined records from over 500 stations into 18 regions (hence the asterisk); none of the trends was statistically significant. He judged time series from some regions unsuitable for statistical analysis and these are indicated here by an 'x'. For studies with more than 50 sites, the median, 25th and 75th percentiles are shown with vertical lines. In a few cases, some plotted trends lie beyond the edges of the graph; these are indicated by a numeral at the corresponding edge of the graph, e.g., 2 sites >2% yr^{-1} for the Ishizaka study. Colours indicate temperature or, where indicated, elevation using the lowest and highest site to set the colour scale. Note the prevalence of negative trends at lower/warmer sites, especially in spring.

4.5.4 Changes in Snow Albedo

In addition to reductions in snow cover, the reflectivity (albedo) of snow may also be changing in response to human activities. There are two related causes of albedo change (Flanner et al., 2007): 1) darker snow grains as a result of increased combustion of both fossil fuels and northern forests, and 2) accelerated snow metamorphosis as a result of warming. Unfortunately, there are extremely limited data on the changes of albedo over time, and we must rely instead on analyses from ice cores, direct recent observations, and modeling. Flanner et al. (2007), using a detailed snow radiative model coupled to a GCM and estimates of biomass burning in years with low (2001) and high (1998) amounts of Arctic wildfire, estimated that the human-induced radiative forcing by black carbon is roughly 0.05 W m^{-2}, of which 80% is from fossil fuels. However, spatially comprehensive surveys of impurities in Arctic snow in the late-2000s and mid-1980s indicate that impurities decreased between those two periods (Doherty et al., 2010) and hence albedo changes have not been responsible for reductions in Arctic ice and snow.

4.5.5 River and Lake Ice

The number of observations of freshwater-ice has declined sharply in recent decades (Prowse et al., in press). In the case of long-term lake and river sites in the Northern Hemisphere with ice-phenology records longer than 100 years, Magnuson et al. (2000) reported that 38 of the 39 time series (1846–1995) showed either later freeze-up (15 sites averaging +6.3 d/100 y) or earlier break-up (24 sites averaging –5.8 d/100 y), thus resulting in an average reduction in ice duration of 12.1 d/100 y. A subsequent analysis (by B.J. Benson and J.J. Magnuson, reported by Koc et al. (2009)) of a smaller set of 9 lakes for freeze-up and 17 for break-up for the winters 1855/1856 to 2004/2005 indicates larger changes: +10.7 d/100 y for freeze-up and –8.8 d/100 y for break-up, reducing average ice duration by 19.5 d/100 y. The larger changes could stem from a combination of smaller sample size or the addition of data from 1995 to 2005, which exhibited large changes in timing.

Changes in timing of both ice break-up and freeze-up tends to be more sensitive to variations in air temperature at lower latitudes than at higher latitudes (Livingstone et al., 2010), but data obtained by remote-sensing of Canadian lakes (Latifovic and Pouliot, 2007) indicates that very high-latitude lakes appear to be experiencing more rapid reductions in ice cover than those at lower latitudes. Specifically, while the majority of all sites showed earlier break-up and delayed freeze-up (averaging –0.18 and +0.12 d/y, respectively) for the period 1950s to 2004, as well as increases (to averages of –0.23 d/y and +0.16 d/y) for the 1970–2004 period, the most rapid rates of change (–0.99 d/y and +0.76 d/y) occurred in six high-latitude lakes (primarily on the Canadian Archipelago) for the even more recent period of 1985 to 2004. This translates into an ice-cover reduction rate of 1.75 d/y, or about 4.5 times that found for the more southern parts of Canada for the most rapid depletion period of 1970 to 2004. The degree to which this reflects the more recent or higher-latitude warming, or potential differences in observational techniques, is unclear (Prowse and Brown, 2010).

Studies of changes in river ice have used disparate data and time intervals, ranging in duration from multi-decade to over two centuries. Beltaos and Prowse (2009), summarizing most available information for northern rivers, noted an almost universal trend towards earlier breakup dates but considerable spatial variability in those for freeze-up, and noted too that changes were often more pronounced during the last few decades of the twentieth century. They note that 20th Century mean air temperature increase of 2–3°C in spring and autumn has produced in many areas an approximate 10- to 15-day advance in break-up and delay in freeze-up, respectively, although the relationship with air temperatures is complicated by the roles of snow accumulation and spring runoff.

4.6 Frozen Ground

4.6.1 Background

Frozen ground is a product of cold weather and climate and can be diurnal, seasonal, or perennial, but where the ground is perennially frozen, and remains or below 0^{o}C for at least two consecutive years, it is called permafrost (van Everdingen, 1998). Changes in permafrost temperature and extent are sensitive indicators of climate change (Osterkamp, 2007). The seasonal freezing and thawing of frozen ground, is directly coupled to the land-surface energy and moisture balances, hence to the atmospheric system, and thus climate. When ice-rich permafrost degrades, dramatic changes in ecosystem and hydrological processes can occur (White et al., 2007). Furthermore, permafrost contains considerable quantities of carbon, roughly twice the amount of carbon currently in the atmosphere (Tarnocai et al., 2009). Therefore, permafrost thawing, which increases organic matter in the active layer and newly-developed taliks, exposes frozen carbon to microbial degradation, releasing CO2 and CH4 into the atmosphere (Schaefer et al., 2011; Schuur et al., 2009; Zimov et al., 2006). Permafrost degradation would also affect the lives of northern inhabitants through dramatic changes in landscape, vegetation and impacts on infrastructure.

4.6.2 Changes in Permafrost

4.6.2.1 Permafrost Temperature

Temperature is the key parameter that determines the state of permafrost. In the Antarctic, permafrost temperature has been observed as low as –23.6°C (Vieira et al., 2010), but in the northern hemisphere, it ranges from –15°C to within a few tenths of a degree from the freezing point (Figure 4.22) (Romanovsky et al., 2010a). In the NH permafrost temperatures are usually lowest in high Arctic regions and gradually increase southwards, but substantial difference does occur at the same latitude. For example, due to the effect of warm ocean currents, the southern boundary of permafrost is farther north (Brown et al., 1998), and permafrost temperature is higher in Scandinavia, and north-west Russia, than it is in Arctic regions of Siberia and North America (McBean et al., 2005).

Elevation is another major factor controlling permafrost temperature and distribution (Cheng and Wu, 2007; Zhou et al., 2000). Indeed, permafrost can occur at high altitude as far south as 26°N in the Himalayas (Brown et al., 1998). Site-specific factors, such as slope aspect, snow cover, vegetation cover, soil type and moisture content control permafrost distribution and temperature.

In Russia, permafrost temperature measurements reach back to the early-1930s (Romanovsky et al., 2010b), in North America to the late-1940s (Brewer, 1958), and in China to the early-1960s (Zhou et al., 2000). Systematic measurements, however, mostly began in the late-1970s and early-1980s (Osterkamp, 2007; Smith et al., 2010; Zhou et al., 2000).

[INSERT FIGURE 4.22 HERE]

Figure 4.22: Time series of mean annual ground temperatures at depths between 10 and 20 m for boreholes throughout the circumpolar northern permafrost regions (Romanovsky et al., 2010b). Data sources for North American, Russian and Nordic sites are Smith et al. (2010), Romanovsky et al. (2010a) and Christiansen et al. (2010), respectively. **C** Canadian site; **A** Alaskan site; **R** Russian site. The Svalbard site is Janssonhaugen (PACE-10) (Isaksen et al., 2007). Measurement depth for Russian boreholes and 85–8A is 10 m, Gulkana, Oldman and Alert are 15 m, and 20m for all other boreholes. Borehole locations are: ZS-124 – 67.48°N 063.48°E; 85-8A – 61.68°N 121.18°W; Gulkana – 62.28°N 145.58°W; YA-1 – 67.58°N 648°E; Oldman – 66.48°N 150.68°W; Happy Valley – 69.18°N 148.88°W; Svalbard – 78.28°N 016.58°E; Deadhorse –70.28°N 148.58°W; West Dock – 70.48°N 148.58°W; Alert – 82.58°N 062.48°W.

Permafrost temperatures have generally increased during the past three decades, although at some sites, they show little change, or slight decrease (Figure 4.21; Table 4.6). In this regard, it is important to discriminate *cold permafrost*, with mean annual ground temperature below –2°C at depths from 10 to 15 m (Cheng and Wu, 2007; Smith et al., 2010; Wu and Zhang, 2010) from *warm permafrost* or those with mean temperature of –2°C or higher. Overall, warming is faster in cold permafrost than in warm permafrost, especially where the permafrost is ice-rich. Cold permafrost accounts for the majority of continuous and discontinuous permafrost zones, where permafrost temperatures have increased by 2.0 – 3.0°C during the last three decades (Table 4.5). The majority of warming occurred between the early-1980s and the late-1990s, with small changes during the 2000s. Temperatures of warm permafrost also increased, but generally by less than 1.0°C. Near-isothermal conditions of warm permafrost are also often observed in mountain permafrost regions such as the European Alps (Noetzli and Vonder Muehll, 2010), Scandinavia (Christiansen et al., 2010), the Western Cordillera of North America (Smith et al., 2010), the Qinghai-Tibetan Plateau (Cheng and Wu, 2007; Wu and Zhang, 2008; Zhao et al., 2010) and in the southern margins of discontinuous permafrost regions at high latitudes (Romanovsky et al., 2010b; Smith et al., 2010). In these areas, permafrost temperatures have shown little or no change, indicating that permafrost is thawing internally (Riseborough, 1990). Episodic cooling as part of temperature fluctuations has been observed but is usually been short-lived and controlled by site-specific conditions (Marchenko et al., 2007; Noetzli and Vonder Muehll, 2010; Wu and Zhang, 2008; Zhao et al., 2010).

Table 4.6: Permafrost temperatures during the International Polar Year (2007–2009) and their recent trends.

Region	Permafrost Temperature during IPYa (°C)	Permafrost Temperature Change (°C)	Depth (m)	Period of Record	Reference
North America					
Northern Alaska,	–5.0 to –14.0	1.9 – 3.1	10 – 20	Late-1960s–	Burn and Kokelj, 2009;

Mackenzie Delta, and Ellesmere Island				2009	Osterkamp, 2007; Smith et al., 2010
Interior of Alaska, Mackenzie Valley, and Northern Quebec	0.0 to –5.0	0.3 – 2.0	15 – 20	1985–2009	Allard et al., 1995; Burn and Kokelj, 2009; Smith et al., 2010
Europe					
Russian European North	–0.1 to –4.1	0.3 – 2.0	8 – 22	1971–2009	Malkova, 2008; Oberman, 2008; Romanovsky et al., 2010b
Nordic Countries	–0.1 to –5.6	0.0 – 1.0	2 – 15	1999–2009	Christiansen et al., 2010; Isaksen et al., 2011
Central Asia					
Qinghai-Xizang Plateau	–0.2 to –3.4	0.2 – 0.7	6	1996–2010	Cheng and Wu, 2007, Li et al., 2008; Wu and Zhang, 2008; Zhao et al., 2010
Tian Shan	–0.4 to –1.1	0.3 – 0.9	10 – 25	1974–2009	Marchenko et al., 2007; Zhao et al., 2010
Mongolia	0.0 to –0.5	0.2 – 1.0	10 – 15	1970–2009	Sharkhuu et al., 2007; Zhao et al., 2010
Others					
Antarctic	–8.3 to –23.6	–	2 – 15	2007–2009	Vieira et al., 2010
East Greenland	–8.1	–	3.25	2008–2009	Christiansen et al., 2010
East Siberia	–4.3 to –10.8	0.5 – 1.5	3.2 – 20	Early-1950s–2009	Romanovsky et al., 2010b

Permafrost warming is mainly caused by increased air temperature and changing snow cover (see Box 4.1). In cold permafrost regions, where permafrost warming rates have been fastest, changes in snow cover conditions may play an important role (Smith et al., 2010; Zhang, 2005). Over relatively warm permafrost, especially ice-rich warm permafrost, changes in permafrost temperature are relatively small due to the effect of latent heat (Isaksen et al., 2011; Riseborough, 1990; Smith et al., 2010).

4.6.2.2 Permafrost Degradation

Permafrost degradation refers to any decrease in thickness and/or areal extent. In particular, the degradation may be manifested by the thickening of the active layer, or top-down or bottom-up thawing, talik development (areas of unfrozen ground within permafrost), or the poleward migration of permafrost boundaries. Permafrost degradation can be identified through geomorphologic indicators including thermokarst terrain (Jorgenson et al., 2006), expansion of thaw lakes (Sannel and Kuhry, 2011), active-layer detachment slides along slopes, and rock falls (Ravanel et al., 2010), destabilized rock glaciers (Delaloye et al., 2011). Although, most permafrost has been degrading since the Little Ice Age (Halsey et al., 1995), the trend has been relatively modest until the past two decades when acceleration of degradation has been observed (Romanovsky et al., 2010b).

Significant permafrost degradation has been reported in the Russian European North. Permafrost with thickness of 10 to 15 m completely thawed in the period 1975–2005 in the Vorkuta area (Oberman, 2008), while the southern permafrost boundary moved north by about 80 km and the boundary of continuous permafrost has moved north by 15 – 50 km (Oberman, 2008). Taliks have also developed in relatively thick permafrost during the past several decades. In the Vorkuta region, the thickness of existing closed taliks increased by 0.6 to 6.7 m over the past 30 years (Romanovsky et al., 2010b). Permafrost thawing and talik formation is occurring in the Nadym and Urengoy regions in north western Russian (Drozdov et al., 2010). Long-term permafrost thawing has been reported around the city of Yakutsk, but this was due mainly to forest fires or human disturbance (Fedorov and Konstantinov, 2008). Permafrost degradation has also been reported on the Qinghai-Xizang (Tibet) Plateau (Cheng and Wu, 2007; Li et al., 2008).

Permafrost degradation has caused erosion and an accelerated retreat of many Arctic coasts in recent years (Jones et al., 2009). This implies a transformation of some cold terrestrial permafrost that is immersed in seawater. Such cold permafrost immediately degrades under the influence of both thermal and chemical impact of overlying sea water (Rachold et al., 2007) and geothermal heat flux (Romanovskii et al., 2004). Subsea permafrost degradation rates (from above) have been estimated to be 1 – 20 cm a^{-1} on the East Siberian Shelf (Overduin et al., 2007) and 1 – 4 cm a^{-1} in the Alaskan Chukchi Sea (Overduin et al., submitted). Similar impacts arise for permafrost beneath new thaw lakes, the number and area of which is increasing (Sannel and Kuhry, 2011; van Huissteden et al., 2011). In northern Alaska, permafrost thawing under thaw lakes ranges from 0.9 – 1.7 cm a^{-1} (Ling, 2003).

During recent years, destabilized rock glaciers have received increased attention by researchers. Timeseries acquired during recent decades by terrestrial surveys indicate dramatic speed-up of some rock glaciers as well as seasonal velocity changes related with ground temperatures (Bodin et al., 2009; Delaloye et al., 2011; Noetzli and Vonder Muehll, 2010; Schoeneich et al., 2010). Photo comparison and photogrammetry indicates an increased activity and collapse-like features on some rock glaciers (Roer et al.). The clear relationship between mean annual air temperature at the rock glacier front and rock glacier velocity points to a temperature dependence and thus, a plausible causal connection to climate (Kaab et al., 2007). Strong surface lowering of rock glaciers has been reported in the Andes (Bodin et al., 2010), indicating melting of ground ice in rock glaciers and permafrost degrading.

Many rock fall events have originated from permafrost slopes during recent years (Ravanel and Deline, 2011; Ravanel et al., 2010). Increasing evidence based on exposed ice and on event statistics supports the hypothesis that this is in part due to thaw of permafrost on steep slopes (Gruber and Haeberli, 2007).

4.6.3 Subsea Permafrost

Subsea permafrost is similar to its terrestrial counterpart, but lies beneath the coastal seas and the ocean. Subsea permafrost in the Arctic is generally relict terrestrial permafrost (Vigdorchik, 1980), inundated after the last glaciation and now degrading under the overlying shelf sea. Permafrost may, however, also form when the sea is shallow, permitting sediment freezing through bottom-fast ice in the winter (Solomon et al., 2008). One 76-year timeseries of bottom water temperature in the Laptev Sea (Dmitrenko et al., 2011) showed warming of 2.1°C since 1985 in the near-shore zone (<10 m water depth), as lengthening summers reduced sea ice extent and increased solar heating. Increasing permafrost degradation rates due to warming Arctic shelf bottom water have not been directly observed.

Circum-arctic subsea permafrost is regarded as a substantial reservoir and/or a confining layer for gas hydrates (O'Connor et al., 2010), roughly estimated as containing 2 – 65 Pg of CH_4 hydrate (McGuire et al., 2009). The gas hydrate stability zone (GSHZ) relies on subsea permafrost, so degradation of subsea permafrost could destabilize the GSHZ (Romanovskii et al., 2005) and potentially release CH_4 into the atmosphere. Observations of gas trapped in subsea permafrost on the East Siberian Shelf (Shakhova et al., 2010b) and high methane concentrations in water-column and air above (Shakhova et al., 2010a; Shakhova et al., 2010b) have led to the suggestion that thawed zones act as pathways through permafrost for gas release. Much current debate focusses on whether or not measured methane emission rates from arctic shelf seas represent an increase (Petrenko et al., 2010), thus a link between changes in subsea permafrost and climate change remains speculative.

4.6.4 Changes in Seasonally-Frozen Ground

Seasonally-frozen ground is a soil layer that freezes and thaws annually, which may, or may not, overlie terrestrial permafrost, and also includes portions of the Arctic seabed thaw freeze in winter.

4.6.4.1 Changes in Active-Layer Thickness

The active layer is that portion of the soil above permafrost that thaws in summer and re-freezes in winter. Observations have revealed a strong positive trend in the active-layer thickness (ALT) of discontinuous permafrost regions at high latitudes (Figure 4.23). Active-layer thickening has been observed since the 1970s and has accelerated since 1995 in northern Europe (Akerman and Johansson, 2008; Callaghan et al., 2010), and on Svalbard and Greenland since the late-1990s (Christiansen et al., 2010). ALT has increased significantly in the Russian European North (Mazhitova, 2008), East Siberia (Fyodorov-Davydov et al., 2008), and Chukotka (Zamolodchikov, 2008) since the mid-1990s (Figure 1). ALT increase has been observed over discontinuous permafrost regions in the interior of Alaska during the past two decades (Viereck et al., 2008). Increase of 8 cm in ALT between 1983 and 2008 has been observed in the northern portion of the Mackenzie River Valley (Burn and Kokelj, 2009). ALT has increased since the mid-1990s in the eastern portion of the Canadian Arctic with the largest increase occurring in the bedrock of the discontinuous permafrost zone (Smith et al., 2010).

[INSERT FIGURE 4.23 HERE]
Figure 4.23: Locations for the Circumpolar Active Layer Monitoring (CALM) sites (top) and changes in active layer thickness (bottom) from Shiklomanov et al. (2010).

Over mountain permafrost regions, ALT has increased of about 7.8 cm yr^{-1} over a period from 1995 through 2010 on the Qinghai-Tibetan Plateau (Wu and Zhang, 2010; Zhao et al., 2010). Rates of up to 40 cm yr^{-1} were observed in Mongolian sites characterized by warm permafrost during the past decade (Sharkhuu et al., 2007). A clear trend of increasing ALT was also detected in Tian Shan (Marchenko et al., 2007; Zhao et al., 2010), and in the European Alps, changes in ALT were largest in response to years with hot summers, although a strong dependence on surface and subsurface characteristics was noted (Noetzli and Vonder Muehll, 2010).

Changes in ALT on the Alaskan North Slope, displayed no trend from 1993–2010 (Shiklomanov et al., 2010; Streletskiy et al., 2008), with similar results noted in the Mackenzie Valley (Smith et al., 2009) and in the West Siberia (Vasiliev et al., 2008) since the mid-1990s. Low rates or no change in ALT increase occurred in shallow active-layer areas over ice-rich and cold permafrost on the Qinghai-Tibetan Plateau (Zhao et al., 2010). Little or no observed trend in ALT change may be in part explained by observed surface subsidence. Thaw penetration into ice-rich permafrost at the base of the active layer is often accompanied by loss of volume due to thaw consolidation manifested as a ground surface subsidence. Results from ground-based measurements at selected sites on the North Slope of Alaska indicate 11 – 13 cm in surface subsidence over the period 2001–2006 (Streletskiy et al., 2008), 6 – 15 cm from 2003 to 2005 in the Brooks Range (Overduin and Kane, 2006), and up to 20 cm in the Russian European North (Mazhitova and Kaverin, 2007).

Subsidence has also been identified using space-borne interferometric synthetic aperture radar (InSAR) data. Liu et al. (2010) detected surface deformation over permafrost on the North Slope of Alaska during the 1992–2000 thaw seasons and a long-term surface subsidence of 1 – 4 cm per decade. These results could explain why in situ measurements at some locations reveal negligible trends in ALT changes during the past two decades, despite the fact that atmospheric and permafrost temperatures increased during that time.

4.6.4.2 Changes in Seasonally Frozen Ground in Areas not Underlain by Permafrost

An estimate based on monthly mean soil temperatures from 387 stations across Russia, suggested that the thickness of seasonally frozen ground decreased by about 0.32 m in the period 1930–2000 (Figure 3, Frauenfeld and Zhang, submitted). Inter-decadal variability was such that no trend could be identified late-1960s, after which seasonal freeze depths decreased significantly until the early-1990s. From then, until about 2008, no further change was evident. Such changes are closely linked with the freezing index, but also mean annual air temperatures, and snow depth (Frauenfeld and Zhang, submitted).

Thickness of seasonally frozen ground in western China decreased by 20 – 40 cm since the early-1960s (Li et al., 2008). Evidence from the satellite record indicates that the onset dates of spring thaw advanced by 14 days, while the autumn freeze date was delayed by 10 days on the Qinghai-Xizang (Tibetan) Plateau from 1988 through 2007 (Li et al., submitted).

[INSERT FIGURE 4.24 HERE]
Figure 4.24: Top: distribution of hydrometeorological stations across Russia; bottom: changes in thickness of seasonally frozen ground (From Frauenfeld and Zhang, 2011).

[START FAQ 4.1 HERE]

FAQ 4.1: Are Glaciers in Mountain Regions Disappearing?

In many mountain ranges around the world, individual glaciers are disappearing in response to atmospheric temperature increases of past decades. For example, in the Swiss Alps, more than one hundred glaciers disappeared from 1850 to the 1970s. Similar losses have been reported in the Austrian Alps, Pyrenees on the Spanish/French border, Jotunheimen in Norway, North Cascades in the USA, on the Tibetan Plateau, in Irian Jaya in Indonesia, and in Bolivia. If warming continues through the 21st century it will be inevitable that many more individual glaciers will disappear. It is also likely that some entire mountain ranges that currently contain glaciers will become largely, or possibly entirely, glacier free.

In all mountain regions where glaciers exist today, the glacier mass has decreased considerably since the end of the Little Ice Age in the middle of the 19th century. Since that time many small glaciers disappeared altogether. Although there were some local exceptions, on a global scale, after phases of little change during the 1920s and the 1970s, glacier retreat was widespread and strong during the 1940s and has been since the 1980s. There is robust evidence from conventional ground measurements, and increasingly also from airborne and satellite measurements, showing that the rate of glacier shrinkage was higher during the past two decades than during the previous periods in most mountain regions, and that glacier shrinkage is ongoing. Apart from a few exceptional regions that are subject to special local conditions (e.g., west coast of New Zealand), this picture is similar in all glacierised mountain regions world-wide.

Presently, most glaciers are larger than they would be if they had adjusted their extent to current climate. In most cases, the areas where snow accumulates on a glacier are currently too small to sustain their current size, a direct result of the fact that the response of the glacier terminus to a change in climate is considerably delayed. This delay generally increases with increasing glacier size. For these reasons, mass loss and retreat of most glaciers will continue for years to decades before they have fully adjusted their extent to the present climate.

The question of whether a particular glacier will eventually disappear entirely depends on several factors which vary substantially from region to region, and can even vary between neighbouring glaciers. These include size, slope, elevation range, the distribution of area with elevation, and the particular characteristics of the glacier surface (e.g., whether or not the glacier is debris-covered). External factors, like the surrounding topography (that might shade portions of a glacier from direct solar radiation) or the climatic regime (e.g., polar, maritime, tropical, continental) are also important for future glacier evolution.

While on a short time scale (i.e., a few decades), each glacier may respond differently to climate change, and exceptions from a general trend can have multiple causes, there are, however, robust modelling approaches that can be used to understand and predict long-term trends (i.e., >50 years) in glacier volume. Such models are built on an understanding of the basic physical principles, illustrated in FAQ 4.1, Figure 1. For example, an increase in local mean air temperature, with no change in precipitation, will cause an upward shift of the equilibrium line altitude (ELA) by about 150 m per degree of warming. This shift will reduce the accumulation area of the glacier (FAQ 4.1, Figure 1a) and, at the same time, increase the ablation area, where ice is lost through melt (FAQ 4.1, Figure 1b). This implies an imbalance between accumulation and ablation that will result in an overall loss of ice from the glacier. As this loss continues, the glacier front retreats and the ablation area decreases in size until the glacier has adjusted its extent to the new climatic conditions (FAQ 4.1, Figure 1c). Where climate change is sufficiently strong to raise the ELA persistently above the highest point of a glacier (FAQ 4.1, Figure 1b, right), the glacier will disappear entirely (FAQ 4.1, Figure 1c, right). Higher glaciers that still have an accumulation area under these conditions will shrink but not disappear (FAQ 4.1, Figure 1c, left and middle). A large valley glacier might lose much of its tongue, probably leaving a lake in its place (FAQ 4.1, Figure 1c, left). Although temperature is the dominant factor, others could also drive changes in the ELA; for example, a change in the quantity and seasonality of precipitation.

A large number of observations have confirmed that different glacier types indeed have show notable differences in their response to recent climate change. For example, the flat and low-lying tongues of large valley glaciers currently show the strongest mass losses (e.g., in Alaska, Canada, the Alps or Svalbard) largely independent of aspect, shading or debris cover. This type of glacier adjusts to new climatic conditions only slowly and initially shows strong thinning without substantial terminus retreat (down-wasting). In contrast, smaller mountain glaciers, with more or less constant slopes, adjust to a new climate more quickly, and show mass loss mainly close to the terminus (FAQ 4.1, Figure 1c, middle).

Whereas the long-term response of most glacier types can be determined very well with the approach illustrated in FAQ 4.1, Figure 1, modelling of the short-term response and more complex glacier types (e.g., heavily debris covered or calving) is more difficult and requires detailed knowledge of glacier characteristics. For the majority of glaciers world-wide, these characteristics (e.g., elevation range, slope) and their response to climate change is not properly known. One region with a wide variety of glacier types and climatic conditions and particularly poorly known glacier characteristics, is the Hindukush – Karakoram – Himalaya mountain range. The future evolution of glaciers in this range is thus particularly uncertain. However, increased use of satellite data (e.g., to compile glacier inventories) and extension of the ground-based measurement network, will allow the gaps in knowledge about this region to be substantially reduced in coming years.

In summary, the fate of glaciers in the various mountain regions around the world will be highly variable and dependent on their specific characteristics. Some individual glaciers will disappear; others will lose most of their low-lying ice mass located in the flat and thick tongues that still occupy valley floors, without changing too much in their upper parts. Currently, glaciers are disappearing where the ELA is already above the highest glacier elevation. In the future, glaciers will also disappear in regions where the ELA will rise above that elevation.

[INSERT FAQ 4.1, FIGURE 1 HERE]

FAQ 4.1, Figure 1: Schematic of three types of glaciers located at different elevations and their response to an upward shift of the equilibrium line altitude ELA. (a) For a given climate, the EL has a specific altitude (ELA1) and all glaciers have a specific size. (b) Due to a temperature increase the ELA shifts upwards to a new altitude ELA2, initially resulting in reduced accumulation and larger ablation areas for all glaciers. (c) After glacier size has adjusted to the new ELA, the valley glacier (left) has lost its tongue and the small cirque glacier (right) has disappeared entirely.

[END FAQ 4.1 HERE]

[START FAQ 4.2 HERE]

FAQ 4.2: How is Sea Ice Changing in the Arctic and Antarctic?

The sea ice that covers the Arctic Ocean and the Southern Ocean around Antarctica have quite different characteristics, and are showing different changes with time. Over the last 32 years, there has been a significant trend of –4 %/decade in the annual average extent of sea ice in the Arctic. The average winter thickness of Arctic Ocean sea ice has thinned by 1.8 m between 1978 and 2008, and the total volume (mass) of Arctic sea ice has decreased significantly at all times of year. The more rapid decrease in the extent of sea ice at the summer minimum is a consequence of these trends. In contrast, over the same 32-year period, the total extent of Antarctic sea ice has increased slightly (1.3 % per decade), but there are strong regional differences in the changes around the Antarctic. Measurements of Antarctic sea ice thickness are too few to be able to judge whether it total volume (mass) is decreasing, steady, or increasing.

A large part of the total Arctic sea ice cover lies above 60°N (FAQ 4.2, Figure 1) and is surrounded by land to the south with openings to the Canadian Arctic Archipelago, and the Bering, the Barents, and Greenland seas. A fraction of the ice within the Arctic basin survives for several seasons, growing in thickness by basal freezing and by deformation (ridging and rafting). Seasonal sea ice grows to only ~2 m but multiyear sea ice can be several metres thicker. Sea ice drifts within the basin, driven by wind and ocean currents: the mean drift pattern is dominated by a clockwise circulation pattern in the western Arctic and a Transpolar Drift Stream that transports Siberian sea ice across the Arctic and exports it from the basin through the Fram Strait.

Satellites with the capability to distinguish ice and open water have provided a picture of the changes of the sea ice cover. Since 1979, the annual average extent of ice in the Arctic has decreased by 4% per decade.

The decline in extent at the end of summer (in late-September) has been even greater at 12% per decade, reaching a record minimum in 2007. The decadal average extent of the September minimum Arctic ice cover has decreased for each decade since satellite records began. Submarine and satellite records show that the thickness of Arctic ice, and hence the total volume, is also decreasing. This is occurring because of loss of the thicker multiyear ice: approximately 17% of this type of sea ice per decade has been lost to melt and export out of the basin since 1979 and 40% since 1999. While the areal coverage of Arctic sea ice can fluctuate from year to year because of variable seasonal production, the proportion of thick multiyear ice, and the total sea ice volume, can only recover slowly.

Unlike the Arctic, the sea ice cover around Antarctica is constrained to latitudes below 78°S because of the presence of the continental land mass. The sea ice cover is primarily seasonal with very little ice more than two years old. The ice edge is exposed to the open ocean and the snowfall rate over Antarctic sea ice is higher than in the Arctic. Consequently, snow-to-ice conversion rather than predominantly basal freezing (as in the Arctic) contributes to the seasonal growth in ice thickness and total ice volume in the Antarctic. When the snow load from snowfall is sufficient to depress the ice surface below sea level, seawater infiltrates the base of the snow pack and snow-ice is formed when the resultant slush freezes. Snow-ice formation is sensitive to changes in precipitation and thus changes in regional climate. The consequence of changes in precipitation on Antarctic sea ice thickness and volume remains a focus for research. Unconstrained by land boundaries, the latitudinal extent of the Antarctic sea ice cover is highly variable. Close to the Antarctic continent, sea ice drift is predominantly from east to west, but further north, it is from west to east and highly divergent. Distinct clockwise circulation patterns that transport ice northward can be found in the Weddell and Ross Seas, while the circulation is more variable around East Antarctica. The northward extent of the sea ice cover is controlled in part by the divergent drift that is conducive in winter months to new ice formation in persistent open water areas (polynyas) along the coastlines. These zones of ice formation result in densification of ocean water and become one of the primary sources of the deepest water found in the global oceans.

The Antarctic sea ice cover is largely seasonal, with an average thickness of only ~1 m at the time of maximum extent in September. Only a small fraction of the ice cover survives the summer and the ice retreats to a minimum in February.

Over the 32-year satellite record, there has been a small increase in total extent of Antarctic sea ice of 1.3% per decade. However, there are large regional differences in trends with decreases seen in the Bellingshausen and Amundsen seas, but a significant increase in sea ice extent in the Ross Sea that dominates the overall trend. Whether the small overall increase in Antarctic sea ice extent is meaningful as an indicator of climate is uncertain because the extent varies so much from year to year and from place to place around the continent. Without better ice thickness and ice volume estimates, it is difficult to characterize how Antarctic sea ice cover is responding to changing climate, or which climate parameters are most influential.

There are large differences in the physical environment and processes that affect the state of Arctic and Antarctic sea ice cover and contribute to their dissimilar responses to climate change. The long, and unbroken, record of satellite observations have provided a clear picture of the decline of the Arctic sea ice cover, but available evidence precludes us from making strong statements about overall changes in Antarctic sea ice and their causes.

[INSERT FAQ 4.2, FIGURE 1 HERE]

FAQ 4.2, Figure 1: The mean circulation pattern of sea ice and the decadal trends (%) in annual average ice extent in different sectors of the Arctic and Antarctic. The average sea ice cover for the period 1979–2010, from satellite observations, at maximum (minimum) extent is shown as light (dark) grey shading.

[END FAQ 4.2 HERE]

4.7 Synthesis

There is overwhelming evidence that the cryosphere has been undergoing significant transformations over the last few decades. During the relatively short time period of satellite observation, the extent of the Arctic summer sea ice cover has declined by about 40% compared to the 1980s. Unless an extended period of cooling occurs, ice albedo feedback effects will likely accelerate the decline and seasonal sea ice will become the dominant sea ice cover in the Arctic basin. Likewise, the volume of a large fraction of mountain glaciers has also been reduced substantially over the last five decades. Although the uncertainties are still large, estimates of mass loss in the large ice sheets of Greenland and Antarctica have been considerable. Confidence in the observation of these changes has been enhanced by the consistency of results derived from independent techniques including those from new and relatively reliable sensors (e.g., GRACE; AMSR-E, ICESat) that have been introduced in recent years. The extent of snow cover and its thickness have been decreasing while a large fraction of the permafrost has been thawing on account of increases in subsurface temperature.

The physically intuitive coherence of the results from different aspects of the cryosphere is intriguing and is likely a manifestation that the elements of the cryosphere are acting in concert to global warming signals. Moreover, as more years accumulate (i.e., since AR4), these signals appear even stronger than what models have previously projected. Yet there are aspects of the changes in the cryosphere that we do not completely understand. For example, unlike the Arctic, the sea ice cover in the Antarctic is increasing in extent while a significant fraction of Antarctica and surrounding oceans is showing some cooling. Recent studies show some insights into this phenomenon but additional research in this direction is required for more accurate interpretation. Our knowledge about changes in mountain glaciers is also relatively incomplete since changes in a large fraction of the world's glaciers have not been previously reported or adequately quantified. Much of the glacier change data are available only in local and non-English publications. Fortunately, through the availability of high-resolution satellite data and the introduction of new technologies, the gaps in knowledge are slowly being filled. There are also challenges in the observation of snow thickness and density, especially since the material is ephemeral and data from the most accurate satellite observational tools are often compromised by cloud cover. Regional changes in snow cover can be difficult to interpret since regionally-specific factors can dominate. An important issue is how to address the areas of cryospheric research where the mainstream peer-reviewed science literature is not the only medium in which important and significant scientific information can be obtained. Such issue is most relevant in areas like permafrost research (in both land and sea) where a large fraction of the information appear only in non-peer reviewed reports and/or commercial publications. Sometimes, such information is regarded as un-reliable, however, they may provide the only means to accurately interpret ongoing field measurements.

References

Abdalati, W., et al., 2004: Elevation changes of ice caps in the Canadian Arctic Archipelago. *J. Geophys. Res.-Earth Surf.*, **109**, 11.

Abdalati, W., et al., 2010: The ICESat-2 Laser Altimetry Mission. *Proceedings of the Ieee*, **98**, 735-751.

Abermann, J., A. Lambrecht, A. Fischer, and M. Kuhn, 2009: Quantifying changes and trends in glacier area and volume in the Austrian Otztal Alps (1969-1997-2006). *Cryosphere*, **3**, 205-215.

Aizen, V. B., V. A. Kuzmichenok, A. B. Surazakov, and E. M. Aizen, 2007: Glacier changes in the Tien Shan as determined from topographic and remotely sensed data. *Glob. Planet. Change*, **56**, 328-340.

Akerman, H. J., and M. Johansson, 2008: Thawing permafrost and thicker active layers in sub-arctic Sweden. *Permafrost Periglacial Process.*, **19**, 279-292.

Allard, M., B. L. Wang, and J. A. Pilon, 1995: RECENT COOLING ALONG THE SOUTHERN SHORE OF HUDSON STRAIT, QUEBEC, CANADA, DOCUMENTED FROM PERMAFROST TEMPERATURE-MEASUREMENTS. *Arctic and Alpine Research*, **27**, 157-166.

Alley, R. B., et al., 2008: A Simple Law for Ice shelf Calving. *Science*, **322**, 1344-1344.

Amundson, J. M., M. Fahnestock, M. Truffer, J. Brown, M. P. Luthi, and R. J. Motyka, 2010: Ice melange dynamics and implications for terminus stability, Jakobshavn Isbrae Greenland. *J. Geophys. Res.-Earth Surf.*, **115**, 12.

Andreassen, L. M., F. Paul, A. Kaab, and J. E. Hausberg, 2008: Landsat-derived glacier inventory for Jotunheimen, Norway, and deduced glacier changes since the 1930s. *Cryosphere*, **2**, 131-145.

Arendt, A., et al., 2006: Updated estimates of glacier volume changes in the western Chugach Mountains, Alaska, and a comparison of regional extrapolation methods. *J. Geophys. Res.-Earth Surf.*, **111**, 12.

Arendt, A. A., and E. Al, cited 2011: Summary of global glacier complex inventory

Arendt, A. A., K. A. Echelmeyer, W. D. Harrison, C. S. Lingle, and V. B. Valentine, 2002: Rapid wastage of Alaska glaciers and their contribution to rising sea level. *Science*, **297**, 382-386.

Arthern, R. J., D. P. Winebrenner, and D. G. Vaughan, 2006: Antarctic snow accumulation mapped using polarization of 4.3-cm wavelength microwave emission. *J. Geophys. Res.-Atmos.*, **111**.

Azam, M. F., et al., submitted: Imbalance between climate and glacier: a comparison of ice fluxes and mass balance measurements on Chhota Shigri Glacier, Western Himalaya, India. *Journal of Glaciology*.

Bahr, D. B., M. F. Meier, and S. D. Peckham, 1997: The physical basis of glacier volume-area scaling. *Journal of Geophysical Research-Solid Earth*, **102**, 20355-20362.

Bahr, D. B., M. Dyurgerov, and M. F. Meier, 2009: Sea level rise from glaciers and ice caps: A lower bound. *Geophysical Research Letters*, **36**.

Bamber, J. L., R. E. M. Riva, B. L. A. Vermeersen, and A. M. LeBrocq, 2009: Reassessment of the Potential Sea level Rise from a Collapse of the West Antarctic Ice Sheet. *Science*, **324**, 901-903.

Bartholomew, I., P. Nienow, A. Sole, D. Mair, T. Cowton, S. Palmer, and J. Wadham, 2011a: Supraglacial forcing of subglacial drainage in the ablation zone of the Greenland ice sheet. *Geophysical Research Letters*, **38**, 5.

Bartholomew, I. D., P. Nienow, A. Sole, D. Mair, T. Cowton, M. A. King, and S. Palmer, 2011b: Seasonal variations in Greenland Ice Sheet motion: Inland extent and behaviour at higher elevations. *Earth Planet. Sci. Lett.*, **307**, 271-278.

Baur, O., M. Kuhn, and W. E. Featherstone, 2009: GRACE-derived ice-mass variations over Greenland by accounting for leakage effects. *Journal of Geophysical Research-Solid Earth*, **114**, 13.

Belchansky, G. I., D. C. Douglas, and N. G. Platonov, 2004: Duration of the Arctic Sea ice melt season: Regional and interannual variability, 1979-2001. *Journal of Climate*, **17**, 67-80.

Beltaos, S., and T. Prowse, 2009: River-ice hydrology in a shrinking cryosphere. *Hydrol. Process.*, **23**, 122-144.

Benn, D. I., and F. Lehmkuhl, 2000: Mass balance and equilibrium-line altitudes of glaciers in high-mountain environments. *Quat. Int.*, **65-6**, 15-29.

Benn, D. I., C. R. Warren, and R. H. Mottram, 2007: Calving processes and the dynamics of calving glaciers. *Earth-Sci. Rev.*, **82**, 143-179.

Berthier, E., R. Le Bris, L. Mabileau, L. Testut, and F. Remy, 2009: Ice wastage on the Kerguelen Islands (49 degrees S, 69 degrees E) between 1963 and 2006. *J. Geophys. Res.-Earth Surf.*, **114**, 11.

Berthier, E., E. Schiefer, G. K. C. Clarke, B. Menounos, and F. Remy, 2010: Contribution of Alaskan glaciers to sea level rise derived from satellite imagery. *Nat. Geosci.*, **3**, 92-95.

Bindschadler, R., 2006: Climate change - Hitting the ice sheets where it hurts. *Science*, **311**, 1720-1721.

Bindschadler, R., and and 17 others, 2011: Getting around Antarctica: new high-resolution mappings of the grounded and freely-floating boundaries of the Antarctic ice sheet created for the International Polar Year. *The Cryosphere*, **5**, 569-588.

Blaszczyk, M., J. A. Jania, and J. O. Hagen, 2009: Tidewater glaciers of Svalbard: Recent changes and estimates of calving fluxes. *Pol. Polar. Res.*, **30**, 85-142.

Bodin, X., F. Rojas, and A. Brenning, 2010: Status and evolution of the cryosphere in the Andes of Santiago (Chile, 33.5 degrees S.). *Geomorphology*, **118**, 453-464.

Bodin, X., et al., 2009: Two Decades of Responses (1986-2006) to Climate by the Laurichard Rock Glacier, French Alps. *Permafrost Periglacial Process.*, **20**, 331-344.

Bolch, T., 2007: Climate change and glacier retreat in northern Tien Shan (Kazakhstan/Kyrgyzstan) using remote sensing data. *Glob. Planet. Change*, **56**, 1-12.
Bolch, T., B. Menounos, and R. Wheate, 2010a: Landsat-based inventory of glaciers in western Canada, 1985-2005. *Remote Sens. Environ.*, **114**, 127-137.
Bolch, T., M. Buchroithner, T. Pieczonka, and A. Kunert, 2008: Planimetric and volumetric glacier changes in the Khumbu Himal, Nepal, since 1962 using Corona, Landsat TM and ASTER data. *Journal of Glaciology*, **54**, 592-600.
Bolch, T., et al., 2010b: A glacier inventory for the western Nyainqentanglha Range and the Nam Co Basin, Tibet, and glacier changes 1976-2009. *Cryosphere*, **4**, 419-433.
Boning, C. W., A. Dispert, M. Visbeck, S. R. Rintoul, and F. U. Schwarzkopf, 2008: The response of the Antarctic Circumpolar Current to recent climate change. *Nat. Geosci.*, **1**, 864-869.
Box, J. E., L. Yang, D. H. Bromwich, and L. S. Bai, 2009: Greenland Ice Sheet Surface Air Temperature Variability: 1840-2007. *Journal of Climate*, **22**, 4029-4049.
Box, J. E., et al., 2006: Greenland ice sheet surface mass balance variability (1988-2004) from calibrated polar MM5 output. *Journal of Climate*, **19**, 2783-2800.
Brewer, M. C., 1958: Some results of geothermal investigations of permafrost. 19-26.
Bromwich, D. H., J. P. Nicolas, and A. J. Monaghan, 2011: An Assessment of Precipitation Changes over Antarctica and the Southern Ocean since 1989 in Contemporary Global Reanalyses. *Journal of Climate*, **24**, 4189-4209.
Brown, J., O. J. Ferrians Jr., J. A. Heginbottom, and E. S. Melnikov, 1998: *Circum-Arctic Map of Permafrost and Land Ice Conditions (revised February 2001)*. National Snow and Ice Data Center / World Data Center for Glaciology.
Brown, R., C. Derksen, and L. B. Wang, 2010: A multi-data set analysis of variability and change in Arctic spring snow cover extent, 1967-2008. *J. Geophys. Res.-Atmos.*, **115**.
Brown, R. D., and P. W. Mote, 2009: The Response of Northern Hemisphere Snow Cover to a Changing Climate. *Journal of Climate*, **22**, 2124-2145.
Brown, R. D., and D. A. Robinson, 2011: Northern Hemisphere spring snow cover variability and change over 1922–2010 including an assessment of uncertainty. *The Cryosphere*, **5**, 219-229.
Bulygina, O. N., V. N. Razuvaev, and N. N. Korshunova, 2009: Changes in snow cover over Northern Eurasia in the last few decades. *Environ. Res. Lett.*, **4**.
Burn, C. R., and S. V. Kokelj, 2009: The Environment and Permafrost of the Mackenzie Delta Area. *Permafrost Periglacial Process.*, **20**, 83-105.
Callaghan, T. V., F. Bergholm, T. R. Christensen, C. Jonasson, U. Kokfelt, and M. Johansson, 2010: A new climate era in the sub-Arctic: Accelerating climate changes and multiple impacts. *Geophysical Research Letters*, **37**.
Cazenave, A., et al., 2009: Sea level budget over 2003-2008: A reevaluation from GRACE space gravimetry, satellite altimetry and Argo. *Glob. Planet. Change*, **65**, 83-88.
Chapman, W. L., and J. E. Walsh, 2007: A synthesis of Antarctic temperatures. *Journal of Climate*, **20**, 4096-4117.
Charrassin, J. B., et al., 2008: Southern Ocean frontal structure and sea ice formation rates revealed by elephant seals. *Proceedings of the National Academy of Sciences of the United States of America*, **105**, 11634-11639.
Chen, J. L., C. R. Wilson, and B. D. Tapley, 2006: Satellite gravity measurements confirm accelerated melting of Greenland ice sheet. *Science*, **313**, 1958-1960.
——, 2011: Interannual variability of Greenland ice losses from satellite gravimetry. *Journal of Geophysical Research-Solid Earth*, **116**, 11.
Chen, J. L., C. R. Wilson, D. Blankenship, and B. D. Tapley, 2009: Accelerated Antarctic ice loss from satellite gravity measurements. *Nat. Geosci.*, **2**, 859-862.
Chen, J. L., C. R. Wilson, B. D. Tapley, D. D. Blankenship, and E. R. Ivins, 2007: Patagonia icefield melting observed by gravity recovery and climate experiment (GRACE). *Geophysical Research Letters*, **34**, 6.
Cheng, G. D., and T. H. Wu, 2007: Responses of permafrost to climate change and their environmental significance, Qinghai-Tibet Plateau. *J. Geophys. Res.-Earth Surf.*, **112**.
Choi, G., D. A. Robinson, and S. Kang, 2010: Changing Northern Hemisphere Snow Seasons. *Journal of Climate*, **23**, 5305-5310.
Christiansen, H. H., et al., 2010: The Thermal State of Permafrost in the Nordic Area during the International Polar Year 2007-2009. *Permafrost Periglacial Process.*, **21**, 156-181.
Christoffersen, P., et al., 2011: Warming of waters in an East Greenland fjord prior to glacier retreat: mechanisms and connection to large-scale atmospheric conditions. *Cryosphere*, **5**, 701-714.
Christy, J. R., In submission: Searching for information in 133 years of California snowfall observations.
Cia, J. C., A. J. Andres, M. A. S. Sanchez, J. C. Novau, and J. I. L. Moreno, 2005: Responses to climatic changes since the little ice age on maladeta glacier (Central pyrenees). *Geomorphology*, **68**, 167-182.
Cogley, J. G., 2009a: Geodetic and direct mass-balance measurements: comparison and joint analysis. *Annals of Glaciology*, **50**, 96-100.
Cogley, J. G., 2009b: A more complete version of the World Glacier Inventory. *Ann. Glaciol.*, **50**, 32-38.
——, 2009c: Geodetic and direct mass-balance measurements: comparison and joint analysis. *Ann. Glaciol.*, **50**, 96-100.
Cogley, J. G., et al., 2011: *Glossary of Glacier Mass Balance and Related Terms.* UNESCO-IHP.

Comiso, J. C., 2002: A rapidly declining perennial sea ice cover in the Arctic. *Geophysical Research Letters*, **29**, art. no.-1956.
——, 2010: *Polar Oceans from Space.* Springer, 507 pp.
——, 2011: Large decadal decline in the Arctic multiyear ice cover. *Journal of Climate*, doi:10.1175/JCLI-D-11-00113.1.
Comiso, J. C., and F. Nishio, 2008: Trends in the sea ice cover using enhanced and compatible AMSR-E, SSM/I, and SMMR data. *Journal of Geophysical Research-Oceans*, **113**.
Comiso, J. C., C. L. Parkinson, R. Gersten, and L. Stock, 2008: Accelerated decline in the Arctic Sea ice cover. *Geophysical Research Letters*, **35**.
Comiso, J. C., R. Kwok, S. Martin, and A. L. Gordon, 2011: Variability and trends in sea ice extent and ice production in the Ross Sea. *Journal of Geophysical Research-Oceans*, **116**.
Cook, A. J., and D. G. Vaughan, 2010: Overview of areal changes of the ice shelves on the Antarctic Peninsula over the past 50 years. *The Cryosphere*, **4**, 77-98.
Costa, D. P., J. M. Klinck, E. E. Hofmann, M. S. Dinniman, and J. M. Burns, 2008: Upper ocean variability in west Antarctic Peninsula continental shelf waters as measured using instrumented seals. *Deep-Sea Res. Part II-Top. Stud. Oceanogr.*, **55**, 323-337.
Cullen, N. J., T. Molg, G. Kaser, K. Hussein, K. Steffen, and D. R. Hardy, 2006: Kilimanjaro Glaciers: Recent areal extent from satellite data and new interpretation of observed 20th century retreat rates. *Geophysical Research Letters*, **33**, 6.
Daniault, N., H. Mercier, and P. Lherminier, 2011: The 1992-2009 transport variability of the East Greenland-Irminger Current at 60 degrees N. *Geophysical Research Letters*, **38**, 4.
Das, S. B., I. Joughin, M. D. Behn, I. M. Howat, M. A. King, D. Lizarralde, and M. P. Bhatia, 2008: Fracture propagation to the base of the Greenland Ice Sheet during supraglacial lake drainage. *Science*, **320**, 778-781.
Davis, C. H., Y. H. Li, J. R. McConnell, M. M. Frey, and E. Hanna, 2005: Snowfall-driven growth in East Antarctic ice sheet mitigates recent sea level rise. *Science*, **308**, 1898-1901.
Debeer, C. M., and M. J. Sharp, 2007: Recent changes in glacier area and volume within the southern Canadian Cordillera. *Annals of Glaciology, Vol 46, 2007*, **46**, 215-221.
DeConto, R. M., and D. Pollard, 2003: Rapid Cenozoic glaciation of Antarctica induced by declining atmospheric CO2. *Nature*, **421**, 245-249.
Delaloye, R., et al., cited 2011: Recent interannual variations of rock glacier creep in the European Alps. [Available online at http://www.zora.uzh.ch/7031/.]
DeLiberty, T. L., C. A. Geiger, S. F. Ackley, A. P. Worby, and M. L. Van Woert, 2011: Estimating the annual cycle of sea ice thickness and volume in the Ross Sea. *Deep-Sea Res. Part II-Top. Stud. Oceanogr.*, **58**, 1250-1260.
Dery, S. J., and R. D. Brown, 2007: Recent Northern Hemisphere snow cover extent trends and implications for the snow-albedo feedback. *Geophysical Research Letters*, **34**, 6.
Ding, Q. H., E. J. Steig, D. S. Battisti, and M. Kuttel, 2011: Winter warming in West Antarctica caused by central tropical Pacific warming. *Nat. Geosci.*, **4**, 398-403.
Dmitrenko, I. A., et al., 2011: Recent changes in shelf hydrography in the Siberian Arctic: Potential for subsea permafrost instability. *Journal of Geophysical Research-Oceans*, **116**, 10.
Doake, C. S. M., and D. G. Vaughan, 1991: RAPID DISINTEGRATION OF THE WORDIE ICE SHELF IN RESPONSE TO ATMOSPHERIC WARMING. *Nature*, **350**, 328-330.
Doherty, S. J., S. G. Warren, T. C. Grenfell, A. D. Clarke, and R. E. Brandt, 2010: Light-absorbing impurities in Arctic snow. *Atmospheric Chemistry and Physics*, **10**, 11647-11680.
Domack, E., et al., 2005: Stability of the Larsen B ice shelf on the Antarctic Peninsula during the Holocene epoch. *Nature*, **436**, 681-685.
Dong-Chen, E., Y.-D. Yang, and D.-B. Chao, 2009: The sea level change from the Antarctic ice sheet based on GRACE. *Chinese J. Geophys.-Chinese Ed.*, **52**, 2222-2228.
Drobot, S. D., and M. R. Anderson, 2001: An improved method for determining snowmelt onset dates over Arctic sea ice using scanning multichannel microwave radiometer and Special Sensor Microwave/Imager data. *J. Geophys. Res.-Atmos.*, **106**, 24033-24049.
Drozdov, D. S., N. G. Ukraintseva, A. M. Tsarev, and S. N. Chekrygina, 2010: Changes in the temperature field and in the state of the geosystems within the territory of the Urengoy field during the last 35 years (1974-2008). *Earth's Cryosphere*, **14**, 22-31.
Drucker, R., S. Martin, and R. Kwok, 2011: Sea ice production and export from coastal polynyas in the Weddell and Ross Seas. *Geophysical Research Letters*, **38**, 4.
Dyer, J. L., and T. L. Mote, 2006: Spatial variability and trends in observed snow depth over North America. *Geophysical Research Letters*, **33**.
Dyuergerov, M., and M. F. Meier, 2005: Glaciers and the Changing Earth System: A 2004 Snapshot. Institute of Arctic and Alpine Research, 118 pp.
Ettema, J., M. R. van den Broeke, E. van Meijgaard, W. J. van de Berg, J. L. Bamber, J. E. Box, and R. C. Bales, 2009: Higher surface mass balance of the Greenland ice sheet revealed by high-resolution climate modeling. *Geophysical Research Letters*, **36**.

Farinotti, D., M. Huss, A. Bauder, M. Funk, and M. Truffer, 2009: A method to estimate the ice volume and ice-thickness distribution of alpine glaciers. *Journal of Glaciology*, **55**, 422-430.
Fedorov, A. N., and P. Y. Konstantinov, 2008: Recent changes in ground temperature and the effect on permafrost landscapes in Central Yakutia. *9th International Conference on Permafrost*, Institute of Northern Engineering, University of Alaska, Fairbanks, 433-438.
Fernandes, R., H. X. Zhao, X. J. Wang, J. Key, X. Qu, and A. Hall, 2009: Controls on Northern Hemisphere snow albedo feedback quantified using satellite Earth observations. *Geophysical Research Letters*, **36**.
Fettweis, X., M. Tedesco, M. van den Broeke, and J. Ettema, 2011: Melting trends over the Greenland ice sheet (1958-2009) from spaceborne microwave data and regional climate models. *Cryosphere*, **5**, 359-375.
Flanner, M. G., C. S. Zender, J. T. Randerson, and P. J. Rasch, 2007: Present-day climate forcing and response from black carbon in snow. *J. Geophys. Res.-Atmos.*, **112**.
Flanner, M. G., K. M. Shell, M. Barlage, D. K. Perovich, and M. A. Tschudi, 2011: Radiative forcing and albedo feedback from the Northern Hemisphere cryosphere between 1979 and 2008. *Nat. Geosci.*, **4**, 151-155.
Foster, J. L., D. K. Hall, R. E. J. Kelly, and L. Chiu, 2009: Seasonal snow extent and snow mass in South America using SMMR and SSM/I passive microwave data (1979-2006). *Remote Sens. Environ.*, **113**, 291-305.
Fraser, A. D., R. A. Massom, K. J. Michael, B. K. Galton-Fenzi, and J. L. Lieser, in press: East Antarctic landfast sea ice distribution and variability, 2000-2008. *Journal of Climate*, doi: 10.1175/JCLI-D-10-05032.1.
Frauenfeld, O., and T. Zhang, submitted: An observational 71-year history of seasonally frozen ground change in the Eurasian high latitudes. *Environ. Res. Lett.*
Fyodorov-Davydov, D. G., A. L. Kholodov, V. E. Ostroumov, G. N. Kraev, V. A. Sorokovikov, S. P. Davudov, and A. A. Merekalova, 2008: Seasonal Thaw of Soils in the North Yakutian Ecosystems. *9th International Conference on Permafrost*, Institute of Northern Engineering, University of Alaska, Fairbanks, 481-486.
Gardner, A. S., et al., 2011: Sharply increased mass loss from glaciers and ice caps in the Canadian Arctic Archipelago. *Nature*, **473**, 357-360.
Giles, A. B., R. A. Massom, and V. I. Lytle, 2008a: Fast-ice distribution in East Antarctica during 1997 and 1999 determined using RADARSAT data. *Journal of Geophysical Research-Oceans*, **113**, 15.
Giles, K. A., S. W. Laxon, and A. L. Ridout, 2008b: Circumpolar thinning of Arctic sea ice following the 2007 record ice extent minimum. *Geophysical Research Letters*, **35**.
Gille, S. T., 2002: Warming of the Southern Ocean since the 1950s. *Science*, **295**, 1275-1277.
Gille, S. T., 2008: Decadal-scale temperature trends in the Southern Hemisphere ocean. *Journal of Climate*, **21**, 4749-4765.
Glazovsky, A., and Y. Macheret, 2006: Eurasian Arctic. *Glaciation in north and central Eurasia in present time*, V. M. Kotlyakov, Ed., Nauka.
Gloersen, P., W. Campbell, D. Cavalieri, J. Comiso, C. Parkinson, and H. J. Zwally, 1992: Arctic and Antarctic sea ice: satellite passive microwave observations and analysis.
Gordon, A. L., M. Visbeck, and J. C. Comiso, 2007: A possible link between the Weddell Polynya and the Southern Annular Mode. *Journal of Climate*, **20**, 2558-2571.
Griggs, J. A., and J. L. Bamber, 2009: A new 1 km digital elevation model of Antarctica derived from combined radar and laser data - Part 2: Validation and error estimates. *Cryosphere*, **3**, 113-123.
——, 2011a: Updated bedrock elevation model for Greenland. European Union Framework 7 Programme ice2sea.
——, 2011b: Antarctic ice shelf thickness from satellite radar altimetry. *Journal of Glaciology*, **57**, 485-498.
Gruber, S., and W. Haeberli, 2007: Permafrost in steep bedrock slopes and its temperature-related destabilization following climate change. *J. Geophys. Res.-Earth Surf.*, **112**, 10.
Gunter, B., et al., 2009: A comparison of coincident GRACE and ICESat data over Antarctica. *Journal of Geodesy*, **83**, 1051-1060.
Haas, C., A. Pfaffling, S. Hendricks, L. Rabenstein, J. L. Etienne, and I. Rigor, 2008: Reduced ice thickness in Arctic Transpolar Drift favors rapid ice retreat. *Geophysical Research Letters*, **35**.
Halsey, L. A., D. H. Vitt, and S. C. Zoltai, 1995: DISEQUILIBRIUM RESPONSE OF PERMAFROST IN BOREAL CONTINENTAL WESTERN CANADA TO CLIMATE-CHANGE. *Clim. Change*, **30**, 57-73.
Hanna, E., et al., 2008: Increased runoff from melt from the Greenland Ice Sheet: A response to global warming. *Journal of Climate*, **21**, 331-341.
Heid, T., and A. Kääb, 2011: Worldwide widespread decadal-scale decrease of glacier speed revealed using repeat optical satellite images. *The Cryosphere Discussion*, **5**, 3025–3051.
Hirabayashi, Y., P. Doll, and S. Kanae, 2010: Global-scale modeling of glacier mass balances for water resources assessments: Glacier mass changes between 1948 and 2006. *J. Hydrol.*, **390**, 245-256.
Hock, R., M. de Woul, V. Radic, and M. Dyurgerov, 2009: Mountain glaciers and ice caps around Antarctica make a large sea level rise contribution. *Geophysical Research Letters*, **36**.
Hoelzle, M., W. Haeberli, M. Dischl, and W. Peschke, 2003: Secular glacier mass balances derived from cumulative glacier length changes. *Glob. Planet. Change*, **36**, 295-306.
Holland, D. M., and A. Jenkins, 1999: Modeling thermodynamic ice-ocean interactions at the base of an ice shelf. *J. Phys. Oceanogr.*, **29**, 1787-1800.
Holland, D. M., R. H. Thomas, B. De Young, M. H. Ribergaard, and B. Lyberth, 2008a: Acceleration of Jakobshavn Isbrae triggered by warm subsurface ocean waters. *Nat. Geosci.*, **1**, 659-664.

Holland, P. R., A. Jenkins, and D. M. Holland, 2008b: The response of ice shelf basal melting to variations in ocean temperature. *Journal of Climate*, **21**, 2558-2572.
Horwath, M., and R. Dietrich, 2009: Signal and error in mass change inferences from GRACE: the case of Antarctica. *Geophysical Journal International*, **177**, 849-864.
Howat, I. M., I. Joughin, and T. A. Scambos, 2007: Rapid changes in ice discharge from Greenland outlet glaciers. *Science*, **315**, 1559-1561.
Howat, I. M., I. Joughin, M. Fahnestock, B. E. Smith, and T. A. Scambos, 2008: Synchronous retreat and acceleration of southeast Greenland outlet glaciers 2000-06: ice dynamics and coupling to climate. *Journal of Glaciology*, **54**, 646-660.
Hughes, T. J., 1973: Is the West Antarctic ice sheet disintegrating? *J.Geophys.Res.*
Huilin, L., L. Zhongqin, Z. Mingjun, and L. Wenfeng, 2011: An improved method based on shallow ice approximation to calculate ice thickness along flow-line and volume of mountain glaciers. *Journal of Earth Science*, **22**.
Hulbe, C. L., T. A. Scambos, T. Youngberg, and A. K. Lamb, 2008: Patterns of glacier response to disintegration of the Larsen B ice shelf, Antarctic Peninsula. *Glob. Planet. Change*, **63**, 1-8.
Humbert, A., et al., 2010: Deformation and failure of the ice bridge on the Wilkins Ice Shelf, Antarctica. *Ann. Glaciol.*, **51**, 49-55.
Hurrell, J. W., 1995: DECADAL TRENDS IN THE NORTH-ATLANTIC OSCILLATION - REGIONAL TEMPERATURES AND PRECIPITATION. *Science*, **269**, 676-679.
Huss, M., 2011: Present and future contribution of glacier storage change to runoff from macroscale drainage basins in Europe. *Water Resour. Res.*, **47**, 14.
Huss, M., R. Stockil, G. Kappenberger, and H. Blatter, 2008: Temporal and spatial changes of Laika Glacier, Canadian Arctic, since 1959, inferred from satellite remote sensing and mass-balance modelling. *Journal of Glaciology*, **54**, 857-866.
IPCC, 2007: Summary for Policymakers. *Climate Change 2007: The Physical Science Basis. Contribution of Working Group I to the Fourth Assessment Report of the Intergovernmental Panel on Climate Change*, S. Solomon, et al., Eds., CUP.
Isaksen, K., J. L. Sollid, P. Holmlund, and C. Harris, 2007: Recent warming of mountain permafrost in Svalbard and Scandinavia. *J. Geophys. Res.-Earth Surf.*, **112**, 11.
Isaksen, K., et al., 2011: Degrading mountain permafrost in southern Norway: spatial and temporal variability of mean ground temperatures, 1999-2009. *Permafrost Periglacial Process.*, doi:10.1002/ppp.1728.
Ivins, E. R., and T. S. James, 2005: Antarctic glacial isostatic adjustment: a new assessment. *Antarct Sci*, **17**, 541-553.
Ivins, E. R., E. Rignot, X. P. Wu, T. S. James, and G. Casassa, 2005: *Ice mass balance and Antarctic gravity change: Satellite and terrestrial perspectives.* 3-12 pp.
Ivins, E. R., M. M. Watkins, D. N. Yuan, R. Dietrich, G. Casassa, and A. Rulke, 2011: On-land ice loss and glacial isostatic adjustment at the Drake Passage: 2003-2009. *Journal of Geophysical Research-Solid Earth*, **116**, 24.
Jacobs, S. S., H. H. Hellmer, and A. Jenkins, 1996: Antarctic ice sheet melting in the Southeast Pacific. *Geophysical Research Letters*, **23**, 957-960.
Jacobs, S. S., A. Jenkins, C. F. Giulivi, and P. Dutrieux, 2011: Stronger ocean circulation and increased melting under Pine Island Glacier ice shelf. *Nat. Geosci.*, **4**, 519-523.
Jacobs, S. S., H. H. Helmer, C. S. M. Doake, A. Jenkins, and R. M. Frolich, 1992: Melting of ice shelves and the mass balance of Antarctica. *Journal of Glaciology*, **38**, 375-387.
Jenkins, A., 2011: Convection-driven melting near the grounding lines of ice shelves and tidewater glaciers. *Journal of Climate*. doi: 10.1175/JPO-D-1111-1103.1171.
Jenkins, A., P. Dutrieux, S. S. Jacobs, S. D. McPhail, J. R. Perrett, A. T. Webb, and D. White, 2010: Observations beneath Pine Island Glacier in West Antarctica and implications for its retreat. *Nat. Geosci.*, **3**, 468-472.
Jezek, K. C., C. J. Merry, and D. J. Cavalieri, 1993: COMPARISON OF SMMR AND SSM/I PASSIVE MICROWAVE DATA COLLECTED OVER ANTARCTICA. *Annals of Glaciology, Vol 17*. 131-136.
Jia, L. L., H. S. Wang, and L. W. Xiang, 2009: Effect of glacio-static adjustment on the estiamte of ice mass balance over Antarctic and uncertainties. *Chinese Journal of Geophysics*, **54**, 1466-1477.
Jiskoot, H., C. J. Curran, D. L. Tessler, and L. R. Shenton, 2009: Changes in Clemenceau Icefield and Chaba Group glaciers, Canada, related to hypsometry, tributary detachment, length-slope and area-aspect relations. *Ann. Glaciol.*, **50**, 133-143.
Johannessen, O., E. Shalina, and M. Miles, 1999: Satellite Evidence for an Arctic Sea Ice Cover in Transformation. *Science*, **286**, 1937-1939.
Jones, B. M., C. D. Arp, M. T. Jorgenson, K. M. Hinkel, J. A. Schmutz, and P. L. Flint, 2009: Increase in the rate and uniformity of coastline erosion in Arctic Alaska. *Geophysical Research Letters*, **36**, 5.
Jorgenson, M. T., Y. L. Shur, and E. R. Pullman, 2006: Abrupt increase in permafrost degradation in Arctic Alaska. *Geophysical Research Letters*, **33**, 4.
Joughin, I., W. Abdalati, and M. Fahnestock, 2004: Large fluctuations in speed on Greenland's Jakobshavn Isbrae glacier. *Nature*, **432**, 608-610.
Joughin, I., B. E. Smith, and D. M. Holland, 2010a: Sensitivity of 21st century sea level to ocean-induced thinning of Pine Island Glacier, Antarctica. *Geophysical Research Letters*, **37**, L20502.

Joughin, I., B. E. Smith, I. M. Howat, T. Scambos, and T. Moon, 2010b: Greenland flow variability from ice sheet-wide velocity mapping. *Journal of Glaciology*, **56**, 415-430.
Joughin, I., et al., 2008: Ice-front variation and tidewater behavior on Helheim and Kangerdlugssuaq Glaciers, Greenland. *J. Geophys. Res.-Earth Surf.*, **113**, 11.
Kaab, A., 2008: Glacier Volume Changes Using ASTER Satellite Stereo and ICESat GLAS Laser Altimetry. A Test Study on Edgeoya, Eastern Svalbard. *IEEE Trans. Geosci. Remote Sensing*, **46**, 2823-2830.
Kaab, A., R. Frauenfelder, and I. Roer, 2007: On the response of rockglacier creep to surface temperature increase. *Glob. Planet. Change*, **56**, 172-187.
Kaser, G., J. G. Cogley, M. B. Dyurgerov, M. F. Meier, and A. Ohmura, 2006a: Mass balance of glaciers and ice caps: Consensus estimates for 1961-2004. *Geophysical Research Letters*, **33**.
Kaser, G., J. G. Cogley, M. B. Dyurgerov, M. M. Meier, and A. Ohmura, 2006b: Mass balance of glaciers and ice caps: Consensus estimates for 1961–2004. *Geophysical Research Letters*, **33**.
Ke, C. Q., T. Yu, K. Yu, G. D. Tang, and L. King, 2009: Snowfall trends and variability in Qinghai, China. *Theor. Appl. Climatol.*, **98**, 251-258.
Khan, S. A., J. Wahr, M. Bevis, I. Velicogna, and E. Kendrick, 2010: Spread of ice mass loss into northwest Greenland observed by GRACE and GPS. *Geophysical Research Letters*, **37**.
Khromova, T. E., G. B. Osipova, D. G. Tsvetkov, M. B. Dyurgerov, and R. G. Barry, 2006: Changes in glacier extent in the eastern Pamir, Central Asia, determined from historical data and ASTER imagery. *Remote Sens. Environ.*, **102**, 24-32.
Klein, A. G., and J. L. Kincaid, 2006: Retreat of glaciers on Puncak Jaya, Irian Jaya, determined from 2000 and 2002 IKONOS satellite images. *Journal of Glaciology*, **52**, 65-79.
Koc, N., et al., 2009: *Melting snow and ice: a call for action.* Centre for Ice, Climate and Ecosystems, Norwegian Polar Institute.
Kopp, R. E., F. J. Simons, J. X. Mitrovica, A. C. Maloof, and M. Oppenheimer, 2009: Probabilistic assessment of sea level during the last interglacial stage. *Nature*, **462**, 863-U851.
Kozlovsky, A. M., Y. L. Nazintsev, V. I. Fedotov, and N. V. Cherepanov, 1977: Fast ice of the Eastern Antarctic (in Russian). *Proceedings of the Soviet Antarctic Expedition*, **63**, 1-129.
Krabill, W., et al., 1999: Rapid thinning of parts of the southern Greenland ice sheet. *Science*, **283**, 1522-1524.
Krabill, W. B., et al., 2002: Aircraft laser altimetry measurement of elevation changes of the greenland ice sheet: technique and accuracy assessment. *J Geodyn*, **34**, 357-376.
Kulkarni, A. V., I. M. Bahuguna, B. P. Rathore, S. K. Singh, S. S. Randhawa, R. K. Sood, and S. Dhar, 2007: Glacial retreat in Himalaya using Indian Remote Sensing satellite data. *Curr. Sci.*, **92**, 69-74.
Kunkel, K. E., M. A. Palecki, K. G. Hubbard, D. A. Robinson, K. T. Redmond, and D. R. Easterling, 2007: Trend identification in twentieth-century US snowfall: The challenges. *J. Atmos. Ocean. Technol.*, **24**, 64-73.
Kutuzov, S., and M. Shahgedanova, 2009: Glacier retreat and climatic variability in the eastern Terskey-Alatoo, inner Tien Shan between the middle of the 19th century and beginning of the 21st century. *Glob. Planet. Change*, **69**, 59-70.
Kwok, R., 2004: Annual cycles of multiyear sea ice coverage of the Arctic Ocean: 1999-2003. *Journal of Geophysical Research-Oceans*, **109**.
——, 2005: Variability of Nares Strait ice flux. *Geophysical Research Letters*, **32**.
——, 2007: Near zero replenishment of the Arctic multiyear sea ice cover at the end of 2005 summer. *Geophysical Research Letters*, **34**.
——, 2009: Outflow of Arctic Ocean Sea Ice into the Greenland and Barents Seas: 1979-2007. *Journal of Climate*, **22**, 2438-2457.
Kwok, R., and D. A. Rothrock, 1999: Variability of Fram Strait ice flux and North Atlantic Oscillation. *Journal of Geophysical Research-Oceans*, **104**, 5177-5189.
——, 2009: Decline in Arctic sea ice thickness from submarine and ICESat records: 1958-2008. *Geophysical Research Letters*, **36**.
Kwok, R., and G. F. Cunningham, 2010: Contribution of melt in the Beaufort Sea to the decline in Arctic multiyear sea ice coverage: 1993-2009. *Geophysical Research Letters*, **37**.
Kwok, R., G. F. Cunningham, M. Wensnahan, I. Rigor, H. J. Zwally, and D. Yi, 2009: Thinning and volume loss of the Arctic Ocean sea ice cover: 2003-2008. *Journal of Geophysical Research-Oceans*, **114**.
Lambrecht, A., and M. Kuhn, 2007: Glacier changes in the Austrian Alps during the last three decades, derived from the new Austrian glacier inventory. *Annals of Glaciology, Vol 46, 2007*, **46**, 177-184.
Larsen, C. F., R. J. Motyka, A. A. Arendt, K. A. Echelmeyer, and P. E. Geissler, 2007: Glacier changes in southeast Alaska and northwest British Columbia and contribution to sea level rise. *J. Geophys. Res.-Earth Surf.*, **112**, 11.
Latifovic, R., and D. Pouliot, 2007: Analysis of climate change impacts on lake ice phenology in Canada using the historical satellite data record. *Remote Sens. Environ.*, **106**, 492-507.
Laxon, S., N. Peacock, and D. Smith, 2003: High interannual variability of sea ice thickness in the Arctic region. *Nature*, **425**, 947-950.
Le Bris, R., F. Paul, H. Frey, and T. Bolch, 2011: A new satellite-derived glacier inventory for western Alaska. *Ann. Glaciol.*, **52**, 135-143.

Leclercq, P. W., J. Oerlemans, and J. G. Cogley, 2011: Estimating the Glacier Contribution to Sea level Rise for the Period 1800-2005. *Surv. Geophys.*, **32**, 519-535.
Lemke, P., et al., 2007: Observations: Changes in Snow, Ice and Frozen Ground. *Climate Change 2007: The Physical Science Basis. Contribution of Working Group I to the Fourth Assessment Report of the Intergovernmental Panel on Climate Change*, Cambridge University Press.
Lenaerts, J. T. M., M. R. van den Broeke, W. J. van de Berg, E. van Meijgaard, and P. Kuipers Munneke, In press: A new, high-resolution surface mass balance map of Antarctica (1989-2009) based on regional atmospheric climate modeling. *Geophysical Research Letters*.
Leysinger Vieli, G., and G. H. Gudmundsson, 2004: On estimating length fluctuations of glaciers caused by changes in climatic forcing. *J.Geophys.Res.*, **109**, doi 10.1029/2003JF000027.
Li, B. L., A. X. Zhu, Y. C. Zhang, T. Pei, C. Z. Qin, and C. H. Zhou, 2006: Glacier change over the past four decades in the middle Chinese Tien Shan. *Journal of Glaciology*, **52**, 425-432.
Li, X., R. Jin, X. Pan, T. Zhang, and J. Guo, submitted: Changes in the surface soil freeze-thaw cycle on the Qinghai-Tibetan Plateau.
Li, X., et al., 2008: Cryospheric change in China. *Glob. Planet. Change*, **62**, 210-218.
Ling, F., 2003: Numerical simulation of permafrost thermal regime and talik development under shallow thaw lakes on the Alaskan Arctic Coastal Plain. *J. Geophys. Res.-Atmos.*, **108**, 11.
Liu, L., T. J. Zhang, and J. Wahr, 2010: InSAR measurements of surface deformation over permafrost on the North Slope of Alaska. *J. Geophys. Res.-Earth Surf.*, **115**.
Livingstone, D. M., R. Adrian, T. Blencker, G. George, and G. A. Weyhenmeyer, 2010: Chapter 4: Lake Ice Phenology. *The Impact of Climate Change on European Lakes*, D. G. George, Ed., 51-61, doi:10.1007.1978-1090-1481-2945-1004_1004.
Luckman, A., and T. Murray, 2005: Seasonal variation in velocity before retreat of Jakobshavn Isbrae, Greenland. *Geophysical Research Letters*, **32**, 4.
Luethi, M. P., A. Bauder, and M. Funk, 2010: Volume change reconstruction of Swiss glaciers from length change data. *J. Geophys. Res.-Earth Surf.*, **115**.
Luthcke, S. B., A. A. Arendt, D. D. Rowlands, J. J. McCarthy, and C. F. Larsen, 2008: Recent glacier mass changes in the Gulf of Alaska region from GRACE mascon solutions. *Journal of Glaciology*, **54**, 767-777.
Luthcke, S. B., et al., 2006: Recent Greenland ice mass loss by drainage system from satellite gravity observations. *Science*, **314**, 1286-1289.
Lythe, M., D. G. Vaughan, and The BEDMAP Consortium, 2001: BEDMAP: a new ice thickness and subglacial topographic model of Antarctica. *J.Geophys.Res.*, **106**, 11335-11352.
MacAyeal, D. R., et al., 2006: Transoceanic wave propagation links iceberg calving margins of Antarctica with storms in tropics and Northern Hemisphere. *Geophysical Research Letters*, **33**, 4.
Magnuson, J. J., et al., 2000: Historical trends in lake and river ice cover in the Northern Hemisphere. *Science*, **289**, 1743-1746.
Magnusson, E., H. Bjornsson, J. Dall, and F. Palsson, 2005: Volume changes of Vatnajokull ice cap, Iceland, due to surface mass balance, ice flow, and subglacial melting at geothermal areas. *Geophysical Research Letters*, **32**, 4.
Mahoney, A., H. Eicken, and L. Shapiro, 2007: How fast is landfast sea ice? A study of the attachment and detachment of nearshore ice at Barrow, Alaska. *Cold Reg. Sci. Tech.*, **47**, 233-255.
Maisch, M., 2000: *Die Gletscher der Schwiezen Alpen: Gletscherhochstand 1850, aktuelle Vergletscherung, Gletscherschwund-Szenarien.* Hochschulverlag AG an der ETH.
Malkova, G. V., 2008: The last twenty-five years of changes in permafrost temperature of the European Russian Arctic. *Ninth International Conference on Permafrost*, Institute of Northern Engineering, University of Alaska Fairbanks, 1119-1124.
Marchenko, S. S., A. P. Gorbunov, and V. E. Romanovsky, 2007: Permafrost warming in the Tien Shan Mountains, Central Asia. *Glob. Planet. Change*, **56**, 311-327.
Markus, T., and D. J. Cavalieri, 2000: An enhancement of the NASA Team sea ice algorithm. *IEEE Trans. Geosci. Remote Sensing*, **38**, 1387-1398.
Markus, T., J. C. Stroeve, and J. Miller, 2009: Recent changes in Arctic sea ice melt onset, freezeup, and melt season length. *Journal of Geophysical Research-Oceans*, **114**.
Marshall, G. J., A. Orr, N. P. M. van Lipzig, and J. C. King, 2006: The Impact of a Changing Southern Hemisphere Annular Mode on Antarctic Peninsula Summer Temperatures. *Journal of Climate*, **19**, 5388--5404.
Martinson, D. G., S. E. Stammerjohn, R. A. Iannuzzi, R. C. Smith, and M. Vernet, 2008: Western Antarctic Peninsula physical oceanography and spatio-temporal variability. *Deep-Sea Res. Part II-Top. Stud. Oceanogr.*, **55**, 1964-1987.
Marzeion, B., M. Hofer, A. Jarosch, G. Kaser, and T. Molg, 2011: A minimal model for reconstructing interannual mass balance variability of glaciers in the European Alps. *The Cryosphere Discussions*, **5**, 2799-2839.
Maslanik, J. A., C. Fowler, J. Stroeve, S. Drobot, J. Zwally, D. Yi, and W. Emery, 2007: A younger, thinner Arctic ice cover: Increased potential for rapid, extensive sea ice loss. *Geophysical Research Letters*, **34**.
Massom, R. A., et al., 2008: West Antarctic Peninsula sea ice in 2005: Extreme ice compaction and ice edge retreat due to strong anomaly with respect to climate. *Journal of Geophysical Research-Oceans*, **113**, 23.

Matsuo, K., and K. Heki, 2010: Time-variable ice loss in Asian high mountains from satellite gravimetry. *Earth Planet. Sci. Lett.*, **290**, 30-36.
Mazhitova, G. G., 2008: Soil temperature regimes in the discontinuous permafrost zone in the east European Russian Arctic. *Eurasian Soil Science*, **41**, 48-62.
Mazhitova, G. G., and D. A. Kaverin, 2007: Thaw depth dynamics and soil surface subsidence at a Circumpolar Active Layer Monitoring (CALM) site in the East European Russian Arctic. *Kriosfera Zemli*, **vol. XI, N**, 20-30.
McBean, G., et al., 2005: Arctic Climate: Past and Present. *Arctic Climate Impact Assessment*, Cambridge University Press, 21-60.
McGuire, A. D., et al., 2009: Sensitivity of the carbon cycle in the Arctic to climate change. *Ecol. Monogr.*, **79**, 523-555.
Mercer, J. H., 1978: WEST ANTARCTIC ICE SHEET AND CO2 GREENHOUSE EFFECT - THREAT OF DISASTER. *Nature*, **271**, 321-325.
Moholdt, G., B. Wouters, and A. Gardner, submitted: Recent contribution to sea level from glaciers and ice caps in the Russian High Arctic.
Moholdt, G., C. Nuth, J. O. Hagen, and J. Kohler, 2010: Recent elevation changes of Svalbard glaciers derived from ICESat laser altimetry. *Remote Sens. Environ.*, **114**, 2756-2767.
Monaghan, A. J., D. H. Bromwich, and S. H. Wang, 2006: Recent trends in Antarctic snow accumulation from Polar MM5 simulations. *Philos T R Soc A*, **364**, 1683-1708.
Moore, P., and M. A. King, 2008: Antarctic ice mass balance estimates from GRACE: Tidal aliasing effects. *J. Geophys. Res.-Earth Surf.*, **113**.
Motyka, R. J., L. Hunter, K. A. Echelmeyer, and C. Connor, 2003: Submarine melting at the terminus of a temperate tidewater glacier, LeConte Glacier, Alaska, USA. *Annals of Glaciology, Vol 36*, **36**, 57-65.
Murray, T., et al., 2010: Ocean regulation hypothesis for glacier dynamics in southeast Greenland and implications for ice sheet mass changes. *J. Geophys. Res.-Earth Surf.*, **115**.
Myers, P. G., N. Kulan, and M. H. Ribergaard, 2007: Irminger Water variability in the West Greenland Current. *Geophysical Research Letters*, **34**.
Myers, P. G., C. Donnelly, and M. H. Ribergaard, 2009: Structure and variability of the West Greenland Current in Summer derived from 6 repeat standard sections. *Progress in Oceanography*, **80**, 93-112.
Narama, C., Y. Shimamura, D. Nakayama, and K. Abdrakhmatov, 2006: Recent changes of glacier coverage in the western Terskey-Alatoo range, Kyrgyz Republic, using Corona and Landsat. *Annals of Glaciology, Vol 43, 2006*, **43**, 223-229.
Nerem, R. S., and J. Wahr, 2011: Recent changes in the Earth's oblateness driven by Greenland and Antarctic ice mass loss. *Geophysical Research Letters*, **38**, 6.
Nghiem, S. V., I. G. Rigor, D. K. Perovich, P. Clemente-Colon, J. W. Weatherly, and G. Neumann, 2007: Rapid reduction of Arctic perennial sea ice. *Geophysical Research Letters*, **34**, 6.
Nick, F. M., A. Vieli, I. M. Howat, and I. Joughin, 2009: Large-scale changes in Greenland outlet glacier dynamics triggered at the terminus. *Nat. Geosci.*, **2**, 110-114.
Nick, F. M., C. J. van der Veen, A. Vieli, and D. I. Benn, 2010: A physically based calving model applied to marine outlet glaciers and implications for the glacier dynamics. *Journal of Glaciology*, **56**, 781-794.
Nie, Y., Y. L. Zhang, L. S. Liu, and J. P. Zhang, 2010: Glacial change in the vicinity of Mt. Qomolangma (Everest), central high Himalayas since 1976. *J. Geogr. Sci.*, **20**, 667-686.
Noetzli, J., and D. Vonder Muehll, 2010: Permafrost in Switzerland 2006/2007 and 2007/2008. Cryospheric Commission of the Swiss Academy of Sciences.
Nuth, C., G. Moholdt, J. Kohler, J. O. Hagen, and A. Kaab, 2010: Svalbard glacier elevation changes and contribution to sea level rise. *J. Geophys. Res.-Earth Surf.*, **115**, 16.
O'Connor, F. M., et al., 2010: POSSIBLE ROLE OF WETLANDS, PERMAFROST, AND METHANE HYDRATES IN THE METHANE CYCLE UNDER FUTURE CLIMATE CHANGE: A REVIEW. *Reviews of Geophysics*, **48**, 33.
Oberman, N. G., 2008: Contemporary Permafrost Degradation of Northern European Russia. *Ninth International Conference on Permafrost*, Institute of Northern Engineering, University of Alaska, Fairbanks, 1305-1310.
Ohmura, A., 2009: Completing the World Glacier Inventory. *Ann. Glaciol.*, **50**, 144-148.
Osterkamp, T. E., 2007: Characteristics of the recent warming of permafrost in Alaska. *J. Geophys. Res.-Earth Surf.*, **112**, 10.
Overduin, P. P., and D. L. Kane, 2006: Frost boils and soil ice content: Field observations. *Permafrost Periglacial Process.*, **17**, 291-307.
Overduin, P. P., H.-W. Hubberten, V. Rachold, N. Romanovskii, M. N. Grigoriev, and M. Kasymskaya, 2007: Evolution and degradation of coastal and offshore permafrost in the Laptev and East Siberian Seas during the last climatic cycle. *GSA Special Papers*, 97-111.
Overduin, P. P., S. Westermann, K. Yoshikawa, T. Haberlau, V. Romanovsky, and S. Wetterich, submitted: Geoelectric observations of the degradation of near-shore submarine permafrost at Barrow (Alaskan Beaufort Sea). *J.Geophys.Res.*
Palmer, S., A. Shepherd, P. Nienow, and I. Joughin, 2011: Seasonal speedup of the Greenland Ice Sheet linked to routing of surface water. *Earth Planet. Sci. Lett.*, **302**, 423-428.

Parizek, B. R., and R. B. Alley, 2004: Implications of increased Greenland surface melt under global-warming scenarios: ice sheet simulations. *Quat. Sci. Rev.*, **23**, 1013-1027.
Parkinson, C. L., 2002: Trends in the length of the Southern Ocean sea ice season, 1979-99. *Annals of Glaciology, Vol 34, 2002*, **34**, 435-440.
Parkinson, C. L., and J. C. Comiso, 2008: Antarctic sea ice parameters from AMSR-E data using two techniques and comparisons with sea ice from SSM/I. *Journal of Geophysical Research-Oceans*, **113**.
Paul, F., and A. Kaab, 2005: Perspectives on the production of a glacier inventory from multispectral satellite data in Arctic Canada: Cumberland Peninsula, Baffin Island. *Annals of Glaciology, Vol 42, 2005*, **42**, 59-66.
Paul, F., and W. Haeberli, 2008: Spatial variability of glacier elevation changes in the Swiss Alps obtained from two digital elevation models. *Geophysical Research Letters*, **35**, 5.
Paul, F., and L. M. Andreassen, 2009: A new glacier inventory for the Svartisen region, Norway, from Landsat ETM plus data: challenges and change assessment. *Journal of Glaciology*, **55**, 607-618.
Paul, F., and A. Linsbauer, in press: Modeling of glacier bed topography using glacier outlines and a DEM. *International Journal of Geographic Information Science*.
Paul, F., A. Kaab, and W. Haeberli, 2007: Recent glacier changes in the Alps observed by satellite: Consequences for future monitoring strategies. *Glob. Planet. Change*, **56**, 111-122.
Paul, F., A. Kaab, M. Maisch, T. Kellenberger, and W. Haeberli, 2004: Rapid disintegration of Alpine glaciers observed with satellite data. *Geophysical Research Letters*, **31**, 4.
Paulson, A., S. J. Zhong, and J. Wahr, 2007: Inference of mantle viscosity from GRACE and relative sea level data. *Geophys. J. Int.*, **171**, 497-508.
Payne, A. J., A. Vieli, A. Shepherd, D. J. Wingham, and E. Rignot, 2004: Recent dramatic thinning of largest West Antarctic ice stream triggered by oceans. *Geophysical Research Letters*, **31**, doi:10.1029/1204GL021284.
Peduzzi, P., C. Herold, and W. Silverio, 2010: Assessing high altitude glacier thickness, volume and area changes using field, GIS and remote sensing techniques: the case of Nevado Coropuna (Peru). *Cryosphere*, **4**, 313-323.
Peltier, W. R., 2009: Closure of the budget of global sea level rise over the GRACE era: the importance and magnitudes of the required corrections for global glacial isostatic adjustment. *Quat. Sci. Rev.*, **28**, 1658-1674.
Pelto, M. S., 2010: Forecasting temperate alpine glacier survival from accumulation zone observations. *Cryosphere*, **4**, 67-75.
Perovich, D. K., J. A. Richter-Menge, K. F. Jones, and B. Light, 2008: Sunlight, water, and ice: Extreme Arctic sea ice melt during the summer of 2007. *Geophysical Research Letters*, **35**, doi: 10.1029/2008GL034007.
Petrenko, V. V., et al., 2010: Methane from the East Siberian Arctic Shelf. *Science*, **329**, 1146-1147.
Pfeffer, W. T., 2011: Land Ice and Sea Level Rise A Thirty-Year Perspective. *Oceanography*, **24**, 94-111.
Phillips, T., H. Rajaram, and K. Steffen, 2010: Cryo-hydrologic warming: A potential mechanism for rapid thermal response of ice sheets. *Geophysical Research Letters*, **37**.
Pollard, D., and R. M. DeConto, 2009: Modelling West Antarctic ice sheet growth and collapse through the past five million years. *Nature*, **458**, 329-U389.
Pritchard, H. D., and D. G. Vaughan, 2007: Widespread acceleration of tidewater glaciers on the Antarctic Peninsula. *J. Geophys. Res.-Earth Surf.*, **112**.
Pritchard, H. D., S. B. Luthcke, and A. H. Fleming, 2010: Understanding ice sheet mass balance: progress in satellite altimetry and gravimetry. *Journal of Glaciology*, **56**, 1151-1161.
Pritchard, H. D., R. J. Arthern, D. G. Vaughan, and L. A. Edwards, 2009: Extensive dynamic thinning on the margins of the Greenland and Antarctic ice sheets. *Nature*, **461**, 971-975.
Pritchard, H. D., S. R. M. Ligtenberg, H. A. Fricker, D. G. Vaughan, M. van den Broeke, and L. Padman, In submission: Antarctic ice loss driven by ice shelf melt. *Nature*.
Pritchard, H. P., P. Fertwell, and D. G. Vaughan, 2011: Bedmap-2 - a benchmark new dataset for Antarctic Earth Science. *American Geophysical Union, Fall Meeting*, AGU.
Prowse, T., et al., in press: Changing lake and river ice regimes: trends, effects, and implications. *SWIPA, Snow, Water, Ice Permafrost in the Arctic*, Scientific Assessment of the Arctic Monitoring and Assessment Program.
Prowse, T. D., and K. Brown, 2010: Hydro-ecological effects of changing Arctic river and lake ice covers: a review. *Hydrol. Res.*, **41**, 454-461.
Rachold, V., et al., 2007: Near-shore Arctic Subsea Permafrost in Transition. *EOS Transactions of the American Geophysical Union*, **88**, 149-156.
Racoviteanu, A. E., Y. Arnaud, M. W. Williams, and J. Ordonez, 2008: Decadal changes in glacier parameters in the Cordillera Blanca, Peru, derived from remote sensing. *Journal of Glaciology*, **54**, 499-510.
Radic, V., and R. Hock, 2010: Regional and global volumes of glaciers derived from statistical upscaling of glacier inventory data. *J. Geophys. Res.-Earth Surf.*, **115**.
Ramillien, G., A. Lombard, A. Cazenave, E. R. Ivins, M. Llubes, F. Remy, and R. Biancale, 2006: Interannual variations of the mass balance of the Antarctica and Greenland ice sheets from GRACE. *Glob. Planetary Change*, **53**, 198-208.
Rampal, P., J. Weiss, and D. Marsan, 2009: Positive trend in the mean speed and deformation rate of Arctic sea ice, 1979-2007. *Journal of Geophysical Research-Oceans*, **114**.
Ravanel, L., and P. Deline, 2011: Climate influence on rockfalls in high-Alpine steep rockwalls: The north side of the Aiguilles de Chamonix (Mont Blanc massif) since the end of the 'Little Ice Age'. *Holocene*, **21**, 357-365.

Ravanel, L., F. Allignol, P. Deline, S. Gruber, and M. Ravello, 2010: Rock falls in the Mont Blanc Massif in 2007 and 2008. *Landslides*, **7**, 493-501.
Ridley, J., J. M. Gregory, P. Huybrechts, and J. Lowe, 2010: Thresholds for irreversible decline of the Greenland ice sheet. *Clim. Dyn.*, **35**, 1065-1073.
Rignot, E., 2006: Changes in ice dynamics and mass balance of the Antarctic ice sheet. *Phillosphical Transactions of the Royal Society of London, Series A*, **364**, 1637-1655.
——, 2008: Changes in West Antarctic ice stream dynamics observed with ALOS PALSAR data. *Geophysical Research Letters*.
Rignot, E., and S. S. Jacobs, 2002: Rapid bottom melting widespread near Antarctic Ice Sheet Grounding lines. *Science*, **296**, 2020-2023.
Rignot, E., and R. H. Thomas, 2002: Mass balance of polar ice sheets. *Science*, **297**, 1502-1506.
Rignot, E., and P. Kanagaratnam, 2006: Changes in the velocity structure of the Greenland ice sheet. *Science*, **311**, 986-990.
Rignot, E., A. Rivera, and G. Casassa, 2003: Contribution of the Patagonia Icefields of South America to sea level rise. *Science*, **302**, 434-437.
Rignot, E., M. Koppes, and I. Velicogna, 2010: Rapid submarine melting of the calving faces of West Greenland glaciers. *Nat. Geosci.*, **3**, 187-191.
Rignot, E., J. Mouginot, and B. Scheuchl, 2011a: Antarctic grounding line mapping from differential satellite radar interferometry. *Geophysical Research Letters*, **38**.
Rignot, E., J. E. Box, E. Burgess, and E. Hanna, 2008a: Mass balance of the Greenland ice sheet from 1958 to 2007. *Geophys. Res. Let.*, **35**, 5.
Rignot, E., I. Velicogna, M. R. van den Broeke, A. Monaghan, and J. Lenaerts, 2011b: Acceleration of the contribution of the Greenland and Antarctic ice sheets to sea level rise. *Geophys. Res. Let.*, **38**, 5.
Rignot, E., G. Casassa, P. Gogineni, W. Krabill, A. Rivera, and R. Thomas, 2004: Accelerated ice discharge from the Antarctic Peninsula following the collapse of Larsen B ice shelf. *Geophysical Research Letters*, **31**, doi:10.1029/2004GL020679.
Rignot, E., J. L. Bamber, M. R. van den Broeke, C. Davis, Y. Li, W. J. van de Berg, and E. Van Meijgaard, 2008b: Recent Antarctic ice mass loss from radar interferometry and regional climate modelling. *Nat. Geosci.*, **1**, 106-110.
Riseborough, D. W., 1990: Soil latent heat as a filter of the climate signal in permafrost. *Proceedings of the Fifth Canadian Permafrost Conference, Collection Nordicana*, Universite Laval, Quebec, 199-205.
Riva, R. E. M., et al., 2009: Glacial Isostatic Adjustment over Antarctica from combined ICESat and GRACE satellite data. *Earth Planet. Sci. Lett.*, **288**, 516-523.
Rivera, A., G. Casassa, J. Bamber, and A. Kaab, 2005: Ice-elevation changes of Glaciar Chico, southern Patagonia, using ASTER DEMs, aerial photographs and GPS data. *Journal of Glaciology*, **51**, 105-112.
Rivera, A., T. Benham, G. Casassa, J. Bamber, and J. A. Dowdeswell, 2007: Ice elevation and areal changes of glaciers from the Northern Patagonia Icefield, Chile. *Glob. Planet. Change*, **59**, 126-137.
Robinson, D. A., K. F. Dewey, and R. R. Heim, 1993: GLOBAL SNOW COVER MONITORING - AN UPDATE. *Bull. Amer. Meteorol. Soc.*, **74**, 1689-1696.
Roer, I., W. Haeberli, M. Avian, V. Kaufmann, R. Delaloye, C. Lambiel, and A. Kääb, Observations and considerations on destabilizing active rock glaciers in the European Alps. *Ninth International Conference on Permafrost*, Institute of Northern Engineering, University of Alaska, Fairbanks, 1505–1510.
Rogers, J. C., and M. P. Hung, 2008: The Odden ice feature of the Greenland Sea and its association with atmospheric pressure, wind, and surface flux variability from reanalyses. *Geophysical Research Letters*, **35**, 5.
Romanovskii, N. N., H. W. Hubberten, A. Gavrilov, V. E. Tumskoy, and A. L. Kholodov, 2004: Permafrost of the east Siberian Arctic shelf and coastal lowlands. *Quat. Sci. Rev.*, **23**, 1359-1369.
Romanovskii, N. N., H. W. Hubberten, A. V. Gavrilov, A. A. Eliseeva, and G. S. Tipenko, 2005: Offshore permafrost and gas hydrate stability zone on the shelf of East Siberian Seas. *Geo-Mar. Lett.*, **25**, 167-182.
Romanovsky, V. E., S. L. Smith, and H. H. Christiansen, 2010a: Permafrost Thermal State in the Polar Northern Hemisphere during the International Polar Year 2007-2009: a Synthesis. *Permafrost Periglacial Process.*, **21**, 106-116.
Romanovsky, V. E., et al., 2010b: Thermal State of Permafrost in Russia. *Permafrost Periglacial Process.*, **21**, 136-155.
Rothrock, D. A., Y. Yu, and G. A. Maykut, 1999: Thinning of the Arctic sea ice cover. *Geophysical Research Letters*, **26**, 3469-3472.
Rothrock, D. A., D. B. Percival, and M. Wensnahan, 2008: The decline in arctic sea ice thickness: Separating the spatial, annual, and interannual variability in a quarter century of submarine data. *Journal of Geophysical Research-Oceans*, **113**.
Rott, H., F. Muller, T. Nagler, and D. Floricioiu, 2011: The imbalance of glaciers after disintegration of Larsen-B ice shelf, Antarctic Peninsula. *Cryosphere*, **5**, 125-134.
Sannel, A. B. K., and P. Kuhry, 2011: Warming-induced destabilization of peat plateau/thermokarst lake complexes. *Journal of Geophysical Research-Biogeosciences*, **116**, 16.
Sasgen, I., and others, In review: Timing and origin of recent regional ice-mass loss in Greenland, Earth. *Earth and Planetary Science Letters*.

Scambos, T. A., C. Hulbe, M. Fahnestock, and J. Bohlander, 2000: The link between climate warming and break-up of ice shelves in the Antarctic Peninsula. *Journal of Glaciology*, **46**, 516-530.
Scambos, T. A., J. A. Bohlander, C. A. Shuman, and P. Skvarca, 2004: Glacier acceleration and thinning after ice shelf collapse in the Larsen B embayment, Antarctica. *Geophysical Research Letters*, **31**, 4.
Schaefer, K., T. J. Zhang, L. Bruhwiler, and A. P. Barrett, 2011: Amount and timing of permafrost carbon release in response to climate warming. *Tellus Ser. B-Chem. Phys. Meteorol.*, **63**, 165-180.
Schiefer, E., B. Menounos, and R. Wheate, 2007: Recent volume loss of British Columbian glaciers, Canada. *Geophysical Research Letters*, **34**, 6.
Schneider, C., M. Schnirch, C. Acuna, G. Casassa, and R. Kilian, 2007: Glacier inventory of the Gran Campo Nevado Ice Cap in the Southern Andes and glacier changes observed during recent decades. *Glob. Planet. Change*, **59**, 87-100.
Schoeneich, P., X. Bodin, J. Krysiecki, P. Deline, and L. Ravanel, 2010: Permafrost in France, 1st report. Grenoble: Institut de Géographie Alpine, Université Joseph Fourier, 68 pp.
Schoof, C., 2007: Ice sheet grounding line dynamics: Steady states, stability, and hysteresis. *J. Geophys. Res.-Earth Surf.*, **112**.
——, 2010: Ice sheet acceleration driven by melt supply variability. *Nature*, **468**, 803-806.
Schrama, E. J. O., and B. Wouters, 2011: Revisiting Greenland ice sheet mass loss observed by GRACE. *J. Geophys. Res.-Solid Earth*, **116**, 10.
Schuur, E. A. G., J. G. Vogel, K. G. Crummer, H. Lee, J. O. Sickman, and T. E. Osterkamp, 2009: The effect of permafrost thaw on old carbon release and net carbon exchange from tundra. *Nature*, **459**, 556-559.
Selmes, N., T. Murray, and T. D. James, 2011: Fast draining lakes on the Greenland Ice Sheet. *Geophysical Research Letters*, **38**, 5.
Shahgedanova, M., G. Nosenko, T. Khromova, and A. Muraveyev, 2010: Glacier shrinkage and climatic change in the Russian Altai from the mid-20th century: An assessment using remote sensing and PRECIS regional climate model. *J. Geophys. Res.-Atmos.*, **115**, 12.
Shakhova, N., I. Semiletov, A. Salyuk, V. Yusupov, D. Kosmach, and O. Gustafsson, 2010a: Extensive Methane Venting to the Atmosphere from Sediments of the East Siberian Arctic Shelf. *Science*, **327**, 1246-1250.
Shakhova, N., I. Semiletov, I. Leifer, A. Salyuk, P. Rekant, and D. Kosmach, 2010b: Geochemical and geophysical evidence of methane release over the East Siberian Arctic Shelf. *Journal of Geophysical Research-Oceans*, **115**, 14.
Sharkhuu, A., et al., 2007: Permafrost monitoring in the Hovsgol mountain region, Mongolia. *J. Geophys. Res.-Earth Surf.*, **112**, 11.
Shepherd, A., D. Wingham, T. Payne, and P. Skvarca, 2003: Larsen ice shelf has progressively thinned. *Science*, **302**, 856-859.
Shepherd, A., A. Hubbard, P. Nienow, M. King, M. McMillan, and I. Joughin, 2009: Greenland ice sheet motion coupled with daily melting in late summer. *Geophysical Research Letters*, **36**.
Shepherd, A., D. Wingham, D. Wallis, K. Giles, S. Laxon, and A. V. Sundal, 2010: Recent loss of floating ice and the consequent sea level contribution. *Geophysical Research Letters*, **37**, 5.
Shi, H. L., Y. Lu, Z. L. Du, L. L. Jia, Z. Z. Zhang, and C. X. Zhou, 2011: Mass change detection in Antarctic ice sheet using ICESat block analysis techniques from 2003 similar to 2008. *Chinese J. Geophys.-Chinese Ed.*, **54**, 958-965.
Shiklomanov, N. I., et al., 2010: Decadal variations of active-layer thickness in moisture-controlled landscapes, Barrow, Alaska. *Journal of Geophysical Research-Biogeosciences*, **115**.
Siegfried, M. R., R. L. Hawley, and J. F. Burkhart, 2011: High-Resolution Ground-Based GPS Measurements Show Intercampaign Bias in ICESat Elevation Data Near Summit, Greenland. *IEEE Trans. Geosci. Remote Sensing*, **49**, 3393-3400.
Silverio, W., and J. M. Jaquet, 2005: Glacial cover mapping (1987-1996) of the Cordillera Blanca (Peru) using satellite imagery. *Remote Sens. Environ.*, **95**, 342-350.
Simmonds, I., C. Burke, and K. Keay, 2008: Arctic Climate Change as Manifest in Cyclone Behavior. *Journal of Climate*, **21**, 5777-5796.
Slobbe, D. C., P. Ditmar, and R. C. Lindenbergh, 2009: Estimating the rates of mass change, ice volume change and snow volume change in Greenland from ICESat and GRACE data. *Geophys. J. Int.*, **176**, 95-106.
Smith, D. M., 1998: Recent increase in the length of the melt season of perennial Arctic sea ice. *Geophysical Research Letters*, **25**, 655-658.
Smith, S. L., S. A. Wolfe, D. W. Riseborough, and F. M. Nixon, 2009: Active-Layer Characteristics and Summer Climatic Indices, Mackenzie Valley, Northwest Territories, Canada. *Permafrost Periglacial Process.*, **20**, 201-220.
Smith, S. L., et al., 2010: Thermal State of Permafrost in North America: A Contribution to the International Polar Year. *Permafrost Periglacial Process.*, **21**, 117-135.
Sole, A. J., D. W. F. Mair, P. W. Nienow, I. D. Bartholomew, M. A. King, M. J. Burke, and I. Joughin, 2011: Seasonal speedup of a Greenland marine-terminating outlet glacier forced by surface melt-induced changes in subglacial hydrology. *J. Geophys. Res.-Earth Surf.*, **116**, 11.

Solomon, S. M., A. E. Taylor, and C. W. Stevens, 2008: Nearshore Ground Temperatures, Seasonal Ice Bonding and Permafrost Formation Within the Bottom-Fast Ice Zone, Mackenzie Delta, NWT. *Proceedings of the Ninth International Conference of Permafrost*, D. L. Kane, and K. M. Hinkel, Eds., Institute of Northern Engineering, University of Alaska, Fairbanks, 1675-1680.
Sorensen, L. S., et al., 2011: Mass balance of the Greenland ice sheet (2003-2008) from ICESat data - the impact of interpolation, sampling and firn density. *Cryosphere*, **5**, 173-186.
Spreen, G., R. Kwok, and D. Menemenlis, 2011: Trends in Arctic sea ice drift and role of wind forcing: 1992-2009. *Geophysical Research Letters*, **38**, 6.
Spreen, G., S. Kern, D. Stammer, and E. Hansen, 2009: Fram Strait sea ice volume export estimated between 2003 and 2008 from satellite data. *Geophysical Research Letters*, **36**.
Stammerjohn, S., R. Massom, D. Rind, and D. Martinson, in submission: Regions of rapid sea ice decline: north-south seasonal differences and implications.
Stammerjohn, S. E., D. G. Martinson, R. C. Smith, X. Yuan, and D. Rind, 2008: Trends in Antarctic annual sea ice retreat and advance and their relation to El Nino-Southern Oscillation and Southern Annular Mode variability. *Journal of Geophysical Research-Oceans*, **113**.
Steele, M., W. Ermold, and J. Zhang, 2008: Arctic Ocean surface warming trends over the past 100 years. *Geophysical Research Letters*, **35**, doi: 10.1029/2007GL031651.
Straneo, F., R. G. Curry, D. A. Sutherland, G. S. Hamilton, C. Cenedese, K. Vage, and L. A. Stearns, 2011: Impact of fjord dynamics and glacial runoff on the circulation near Helheim Glacier. *Nat. Geosci.*, **4**, 322-327.
Straneo, F., et al., 2010: Rapid circulation of warm subtropical waters in a major glacial fjord in East Greenland. *Nat. Geosci.*, **3**, 182-186.
Streletskiy, D. A., N. I. Shiklomanov, F. E. Nelson, and A. E. Klene, 2008: 13 Years of Observations at Alaskan CALM Sites: Long-term Active Layer and Ground Surface Temperature Trends. *9th International Conference on Permafrost*, Institute of Northern Engineering, University of Alaska, Fairbanks, 1727-1732.
Stroeve, J., M. M. Holland, W. Meier, T. Scambos, and M. Serreze, 2007: Arctic sea ice decline: Faster than forecast. *Geophysical Research Letters*, **34**.
Sundal, A. V., A. Shepherd, P. Nienow, E. Hanna, S. Palmer, and P. Huybrechts, 2011: Melt-induced speed-up of Greenland ice sheet offset by efficient subglacial drainage. *Nature*, **469**, 522-U583.
Surazakov, A. B., V. B. Aizen, E. M. Aizen, and S. A. Nikitin, 2007: Glacier changes in the Siberian Altai Mountains, Ob river basin, (1952-2006) estimated with high resolution imagery. *Environ. Res. Lett.*, **2**, 7.
Takala, M., J. Pulliainen, S. J. Metsamaki, and J. T. Koskinen, 2009: Detection of Snowmelt Using Spaceborne Microwave Radiometer Data in Eurasia From 1979 to 2007. *IEEE Trans. Geosci. Remote Sensing*, **47**, 2996-3007.
Tamura, T., and K. I. Ohshima, 2011: Mapping of sea ice production in the Arctic coastal polynyas. *Journal of Geophysical Research-Oceans*, **116**, 20.
Tarnocai, C., J. G. Canadell, E. A. G. Schuur, P. Kuhry, G. Mazhitova, and S. Zimov, 2009: Soil organic carbon pools in the northern circumpolar permafrost region. *Glob. Biogeochem. Cycle*, **23**, 11.
Tedesco, M., M. Brodzik, R. Armstrong, M. Savoie, and J. Ramage, 2009: Pan arctic terrestrial snowmelt trends (1979-2008) from spaceborne passive microwave data and correlation with the Arctic Oscillation. *Geophysical Research Letters*, **36**.
Tedesco, M., et al., 2011: The role of albedo and accumulation in the 2010 melting record in Greenland. *Environ. Res. Lett.*, **6**, 6.
Thomas, E. R., G. J. Marshall, and J. R. McConnell, 2008a: A doubling in snow accumulation in the western Antarctic Peninsula since 1850. *Geophysical Research Letters*, **35**, 5.
Thomas, R., E. Frederick, W. Krabill, S. Manizade, and C. Martin, 2006: Progressive increase in ice loss from Greenland. *Geophysical Research Letters*, **33**, 4.
——, 2009: Recent changes on Greenland outlet glaciers. *Journal of Glaciology*, **55**, 147-162.
Thomas, R., C. Davis, E. Frederick, W. Krabill, Y. H. Li, S. Manizade, and C. Martin, 2008b: A comparison of Greenland ice sheet volume changes derived from altimetry measurements. *Journal of Glaciology*, **54**, 203-212.
Thomas, R., et al., 2011: Accelerating ice loss from the fastest Greenland and Antarctic glaciers. *Geophysical Research Letters*, **38**.
Thomas, R. H., 2004: Force-perturbation analysis of recent thinning and acceleration of Jakobshavn Isbr ae, Greenland. *Journal of Glaciology*, **50**, 57-66.
Thomas, R. H., and C. R. Bentley, 1978: A model for Holocene retreat of the West Antarctic Ice Sheet, **10**, 150-170.
Thompson, D. W. J., and J. M. Wallace, 2000: Annular modes in the extratropical circulation. Part I: Month-to-month variability. *Journal of Climate*, **13**, 1000-1016.
Thompson, D. W. J., Solomon, S., P. J. Kushner, M. H. England, K. M. Grise, and D. J. Karoly, 2011: Signatures of he Antarctic ozone hole in Southern Hemisohere climate change. *Nat. Geosci.*, doi: 10.1038/NGEO1296.
Thost, D. E., and M. Truffer, 2008: Glacier recession on Heard Island, southern Indian Ocean. *Arct. Antarct. Alp. Res.*, **40**, 199-214.
Trivedi, M. R., M. K. Browne, P. M. Berry, T. P. Dawson, and M. D. Morecroft, 2007: Projecting climate change impacts on mountain snow cover in central Scotland from historical patterns. *Arct. Antarct. Alp. Res.*, **39**, 488-499.

Turner, J., et al., 2005: Antarctic climate change during the last 50 years. *Int. J. Climatol.*, **25**, 279-294.
UNEP, 2007: *Global outlook for snow and ice.* UNEP/GRID.
van de Wal, R. S. W., W. Boot, M. R. van den Broeke, C. Smeets, C. H. Reijmer, J. J. A. Donker, and J. Oerlemans, 2008: Large and rapid melt-induced velocity changes in the ablation zone of the Greenland Ice Sheet. *Science*, **321**, 111-113.
van den Broeke, M., W. J. van de Berg, and E. van Meijgaard, 2006: Snowfall in coastal West Antarctica much greater than previously assumed. *Geophysical Research Letters*, **33**.
van den Broeke, M., et al., 2009: Partitioning Recent Greenland Mass Loss. *Science*, **326**, 984-986.
van den Broeke, M. R., J. Ettema, E. van Meijgaard, and W. J. van de Berg, 2010: Climate of the Greenland ice sheet using a high-resolution climate model - Part 2: Near-surface climate and energy balance. *Cryosphere*, **4**, 529-544.
van Everdingen, R., Ed., 1998: *Multi-language glossary of permafrost and related ground-ice terms*. National Snow and Ice Data Center / World Data Center for Glaciology.
van Huissteden, J., C. Berrittella, F. J. W. Parmentier, Y. Mi, T. C. Maximov, and A. J. Dolman, 2011: Methane emissions from permafrost thaw lakes limited by lake drainage. *Nat. Clim. Chang.*, **1**, 119-123.
Vasiliev, A. A., M. O. Leibman, and N. G. Moskalenko, 2008: Active Layer Monitoring in West Siberia under the CALM II Program. *9th International Conference on Permafrost*, Institute of Northern Engineering, University of Alaska, Fairbanks, 1815-1821.
Vaughan, D. G., et al., 2003: Recent rapid regional climate warming on the Antarctic Peninsula. *Clim. Change*, **60**, 243-274.
Velicogna, I., 2009: Increasing rates of ice mass loss from the Greenland and Antarctic ice sheets revealed by GRACE. *Geophysical Research Letters*, **36**, 4.
Velicogna, I., and J. Wahr, 2006a: Measurements of time-variable gravity show mass loss in Antarctica. *Science*, **311**, 1754-1756.
——, 2006b: Acceleration of Greenland ice mass loss in spring 2004. *Nature*, **443**, 329-331.
Vieira, G., et al., 2010: Thermal State of Permafrost and Active-layer Monitoring in the Antarctic: Advances During the International Polar Year 2007-2009. *Permafrost Periglacial Process.*, **21**, 182-197.
Viereck, L. A., N. R. Werdin-Pfistere, C. A. Phyllis, and K. Yoshikawa, 2008: Effect of Wildfire and Fireline Construction on the Annual Depth of Thaw in a Black Spruce Permafrost Forest in Interior Alaska: A 360Year Record of Recovery. *9th International Conference on Permafrost*, Institute of Northern Engineering, University of Alaska, Fairbanks, 1845-1850.
Vigdorchik, M. E., 1980: *Arctic Pleistocene history and the development of submarine permafrost.* Westview Press.
Vinje, T., 2001: Fram strait ice fluxes and atmospheric circulation: 1950-2000. *Journal of Climate*, **14**, 3508-3517.
Walsh, J. E., and W. L. Chapman, 2001: 20th-century sea ice variations from observational data. *Annals of Glaciology, Vol 33*, **33**, 444-448.
Wang, Y. T., S. G. Hou, and Y. P. Liu, 2009: Glacier changes in the Karlik Shan, eastern Tien Shan, during 1971/72-2001/02. *Ann. Glaciol.*, **50**, 39-45.
Weertman, J., 1974: Stability of the junction of an ice sheet and an ice shelf. *Journal of Glaciology*, **13**, 3-11.
Weidick, A., C. E. Boggild, and N. T. Knudsen, 1992: Glacier inventory of west Greenland - Digital media. National Snow and Ice Data Center.
Wendt, J., A. Rivera, A. Wendt, F. Bown, R. Zamora, G. Casassa, and C. Bravo, 2010: Recent ice-surface-elevation changes of Fleming Glacier in response to the removal of the Wordie Ice Shelf, Antarctic Peninsula. *Ann. Glaciol.*, **51**, 97-102.
WGMS, 2008: *Global Glacier Changes: facts and figures.* UNEP.
WGMS(ICSI-IAHS), variousyears: *Fluctuations of Glaciers.*
White, D., et al., 2007: The arctic freshwater system: Changes and impacts. *Journal of Geophysical Research-Biogeosciences*, **112**.
White, W. B., and R. G. Peterson, 1996: An Antarctic circumpolar wave in surface pressure, wind, temperature and sea ice extent, **380**, 699-702.
Wingham, D. J., D. W. Wallis, and A. Shepherd, 2009: Spatial and temporal evolution of Pine Island Glacier thinning, 1995-2006. *Geophysical Research Letters*, **36**, L17501.
Wingham, D. J., A. Shepherd, A. Muir, and G. J. Marshall, 2006a: Mass balance of the Antarctic ice sheet. *Philos T R Soc A*, **364**, 1627-1635.
Wingham, D. J., A. J. Ridout, R. Scharroo, R. J. Arthern, and C. K. Schum, 1998: Antarctic elevation change from 1992 to 1996. *Science*, **282**, 456-458.
Wingham, D. J., et al., 2006b: CryoSat: A mission to determine the fluctuations in Earth's land and marine ice fields. *Adv Space Res*, **37**, 841-871.
Worby, A. P., C. A. Geiger, M. J. Paget, M. L. Van Woert, S. F. Ackley, and T. L. DeLiberty, 2008: Thickness distribution of Antarctic sea ice. *Journal of Geophysical Research-Oceans*, **113**.
Wouters, B., D. Chambers, and E. J. O. Schrama, 2008: GRACE observes small-scale mass loss in Greenland. *Geophysical Research Letters*, **35**, 5.
Wu, Q. B., and T. J. Zhang, 2008: Recent permafrost warming on the Qinghai-Tibetan plateau. *J. Geophys. Res.-Atmos.*, **113**.

——, 2010: Changes in active layer thickness over the Qinghai-Tibetan Plateau from 1995 to 2007. *J. Geophys. Res.-Atmos.*, **115**.

Wu, X. P., et al., 2010: Simultaneous estimation of global present-day water transport and glacial isostatic adjustment. *Nat. Geosci.*, **3**, 642-646.

Xie, H., et al., 2011: Sea ice thickness distribution of the Bellingshausen Sea from surface measurements and ICESat altimetry. *Deep-Sea Res. Part II-Top. Stud. Oceanogr.*, **58**, 1039-1051.

Ye, Q. H., S. C. Kang, F. Chen, and J. H. Wang, 2006a: Monitoring glacier variations on Geladandong mountain, central Tibetan Plateau, from 1969 to 2002 using remote-sensing and GIS technologies. *Journal of Glaciology*, **52**, 537-545.

Ye, Q. H., T. D. Yao, S. C. Kang, F. Chen, and J. H. Wang, 2006b: Glacier variations in the Naimona'nyi region, western Himalaya, in the last three decades. *Annals of Glaciology, Vol 43, 2006*, **43**, 385-389.

Young, D. A., et al., 2011: A dynamic early East Antarctic Ice Sheet suggested by ice-covered fjord landscapes. *Nature*, **474**, 72-75.

Zamolodchikov, D., 2008: Recent climate and active layer changes in Northeast Russia: regional output of Circumpolar Active Layer Monitoring (CALM). *9th International Conference on Permafrost*, Institute of Northern Engineering, University of Alaska, Fairbanks, 2021-2027.

Zemp, M., M. Hoelzle, and W. Haeberli, 2009: Six decades of glacier mass-balance observations: a review of the worldwide monitoring network. *Ann. Glaciol.*, **50**, 101-111.

Zemp, M., H. J. Zumbhul, S. U. Nussbaumer, M. H. Masiokas, L. E. Espizua, and P. Pitte, 2011: Extending glacier monitoring into the Little Ice Age and beyond. 67-69.

Zhang, T., and e. al., 1999: Statistics and characteristics of permafrost and ground-ice distribution in the Northern Hemisphere. *Polar Geogr.*, **23**, 132-154.

Zhang, T., and e. al., 2003: Distribution of seasonally and perennially frozen ground in the Northern Hemisphere. *Proceedings of the 8th International Conference on Permafrost, 21-25 July 2003*, Zurich, Switerland, A.A. Balkema, Lisse, the Netherlands, 1289–1294.

Zhang, T. J., 2005: Influence of the seasonal snow cover on the ground thermal regime: An overview. *Reviews of Geophysics*, **43**.

Zhao, L., Q. B. Wu, S. S. Marchenko, and N. Sharkhuu, 2010: Thermal State of Permafrost and Active Layer in Central Asia during the International Polar Year. *Permafrost Periglacial Process.*, **21**, 198-207.

Zheltyhina, N., 2005: GLIMS Glacier Database - Digital Media. National Snow and Ice Data Center/World Data Center for Glaciology.

Zhou, C. P., W. B. Yang, L. A. Wu, and S. Y. Liu, 2009: Glacier changes from a new inventory, Nianchu river basin, Tibetan Plateau. *Ann. Glaciol.*, **50**, 87-92.

Zhou, Y., D. Guo, G. Qiu, G. Cheng, and S. Li, 2000: *Geocryology in China.* Science Press, 450 pp.

Zimov, S. A., E. A. G. Schuur, and F. S. Chapin, 2006: Permafrost and the global carbon budget. *Science*, **312**, 1612-1613.

Zwally, H. J., and P. Gloersen, 2008: Arctic sea ice surviving the summer melt: interannual variability and decreasing trend. *Journal of Glaciology*, **54**, 279-296.

Zwally, H. J., D. H. Yi, R. Kwok, and Y. H. Zhao, 2008: ICESat measurements of sea ice freeboard and estimates of sea ice thickness in the Weddell Sea. *Journal of Geophysical Research-Oceans*, **113**.

Zwally, H. J., J. C. Comiso, C. L. Parkinson, D. J. Cavalieri, and P. Gloersen, 2002: Variability of Antarctic sea ice 1979-1998. *Journal of Geophysical Research-Oceans*, **107**, 21.

Zwally, H. J., et al., 2005: Mass changes of the Greenland and Antarctic ice sheets and shelves and contributions to sea level rise: 1992-2002. *Journal of Glaciology*, **51**, 509-527.

Zwally, H. J., et al., 2011: Greenland ice sheet mass balance: distribution of increased mass loss with climate warming; 2003-07 versus 1992-2002. *Journal of Glaciology*, **57**, 88-102.

Appendix 4.A: Assessing the Loss of Ice from Polar Ice Sheets 1992 to 2009

Figure 4.15, 4.16 and 4.17 and Table 4.5 give the cumulative sea level contribution from the Greenland and Antarctic ice sheets over the period 1992–2009 derived from a number of recent studies. All studies available for Greenland, and the sub-set of those selected for this assessment are listed in Appendix 4.A, Tables 1 and 2. Those available for Antarctica are shown in Appendix 4.A, Tables 3 and 4. These studies include estimates made from satellite gravimetry, satellite altimetry and the mass balance method. The studies selected are the latest made by 12 different research groups, for each of Greenland and Antarctica, and do not include earlier estimates from the same researchers when those have been updated by more recent analyses using extended data.

Figures 4.15 and 4.16 (main text) show the average cumulative mass loss estimated as a weighted average of the selected estimates for any particular year. The number of estimates available varies with time, with as few as two estimates per year in the 1990s and up to 12 per year after 2002. In calculating the average, each estimate has been weighted based on an assessment of its reliability: High reliability = weighting of 1.0, Medium = 0.5, Low = 0.2. The reliability weightings used, and the reason for the assessment, are shown in Appendix 4.A, Tables 1 and 3. No weighting has been applied to uncertainty estimates cited in the original studies.

The cumulative uncertainties shown in Figures 4.15 and 4.16 are based on the uncertainty cited in the original studies. However, since the yearly estimates from different studies often do not overlap within the quoted uncertainties, the error limits used in this assessment are based on the absolute maximum and minimum mass balance estimate for each year within uncertainty ranges cited in the original studies. The cumulative error is weighted by $1/\sqrt{n}$, where n is the number of years accumulated.

Despite year-to-year differences between the various original analyses, there is broad agreement in the overall magnitude and temporal change in mass loss from both Greenland and Antarctica. It is virtually certain from this multi-study assessment that both the Greenland and Antarctica have lost mass over the last 18 years, and very likely that there has been a considerable increase in the rate of mass loss from both ice sheets over the period. The average rate of sea level increase from this mass loss is shown in Table 4.5 (main text). The total sea level contribution from both ice sheets has been 9.4 mm (±2.7 mm) over the period 1992–2009, with 7.4 mm (±2.2 mm) contributed from 2002 to 2009.

Appendix 4.A, Table 1: Sources used for calculation of ice loss from Greenland.

Source	Method	Start	End	Gt/yr	Cited uncert-ainty	Relia-bility	Comment
Wu et al., 2010	GRACE+GPS	2002.375	2008.958	–104	23	L	Global inversion technique affected due to paucity of GPS data around Greenland
Sorensen et al., 2011	ICESAT	2003.875	2008.292	–210	21	M	Density assumption for snow vs ice is listed
Sasgen and others, in review	GRACE	2002	2009	–236.4	3.7	H	
Schrama and Wouters, 2011	GRACE	2003.3	2010.2	–201	18	H	
Cazenave et al., 2009	GRACE	2003	2008	–136	18	M	CNES fields are truncated to lower harmonics than other fields
Zwally et al., 2011	ERS1,2/ICESAT	1992	2002	–7	3	L	SRALT not effective in SE Greenland where most losses are located
Zwally et al., 2011	ERS1,2/ICESAT	2003	2007	–171	4	M	Density assumption for snow vs ice is not clear
Velicogna, 2009	GRACE	2002	2009	–223.7	33	H	Yearly estimates given and

							used in compilation
Pritchard et al., 2010	GRACE	2003.9	2009.875	–195.0	22	H	
Baur et al., 2009	GRACE	2002.9	2008.583	–177.0	12	H	
Slobbe et al., 2009	GRACE	2002.5	2007.5	–214	78	M	
Slobbe et al., 2009	ICESAT	2003.2	2007.417	–139.0	68	M	Density assumption for snow vs ice
Rignot et al., 2011b	Flux	1992.00	2009.92	–154.4	51	H	Yearly estimates given and used in compilation
Chen et al., 2011	GRACE	2002.3	2005.25	–157.3	38	H	
Chen et al., 2011	GRACE	2005.3	2009.917	–247.9	38	H	

Appendix 4.A, Table 2: Sources NOT used for calculation of ice loss from Greenland.

Source	Method	Start	End	Gt/yr	Cited uncert-ainty	Relia-bility	Comment
Krabill et al., 1999	Airborne	1993	1999	–47			Includes only half the ice sheet and fills in the rest with melt model
Rignot and Kanagaratnam, 2006	Flux	1996	1996	–83	28		Superseded (Rignot et al., 2011b)
Rignot and Kanagaratnam, 2006	Flux	2000	2000	–127	28		Superseded (Rignot et al., 2011b)
Rignot and Kanagaratnam, 2006	Flux	2002	2005	–75	38		Superseded (Rignot et al., 2011b)
Rignot et al., 2008a	Flux	1996	1996	–97	47		Superseded (Rignot et al., 2011b)
Rignot et al., 2008a	Flux	2000	2000	–156	44		Superseded (Rignot et al., 2011b)
Rignot et al., 2008a	Flux	2004	2007	–264	39		Superseded (Rignot et al., 2011b)1
Thomas et al., 2006	Altimetry	1994	1999	–27	23		Includes only half the ice sheet and fills in the rest with melt model
Zwally et al., 2005	ERS1,2	1992.375	2002.875	–11.7	2.5		Superseded (Zwally et al., 2011)
Thomas et al., 2006	Altimetry	1999	2004	–81	24		Includes only half the ice sheet and fills in the rest with melt model
Velicogna and Wahr, 2006b	GRACE	2002	2004	–75	21		Superseded (Velicogna, 2009)
Ramillien et al., 2006	GRACE	2002	2005	–169	66		Superseded (Cazenave et al., 2009)
Chen et al., 2006	GRACE	2002.375	2005	–219	21		Superseded (Chen et al., 2011)
Luthcke et al., 2006	GRACE	2003	2005	–101	16		Superseded (Pritchard et al., 2010)
Wouters et al., 2008	GRACE	2003.2	2008.1	–179	25		Superseded (Schrama and Wouters, 2011)
van den Broeke et	Flux	2003	2008	–237	20		Superseded (Rignot et al.,

al., 2009	2011b)

Appendix 4.A, Table 3: Sources used for calculation of ice loss from Antarctica.

Source	Method	Start	End	Gt/yr	Cited uncert-ainty	Relia-bility	Comment
Wu et al., 2010	GRACE+GPS	2002.375	2008.958	–87	43	L	Paucity of GPS data around Antarctica to constrain the inversion
Wingham et al., 2006a	ERS-1/2	1992.83	2003.17	27	69	L	No data in Peninsula (uncertainty increased to compensate); series truncated within 100 km of coast
Velicogna, 2009	GRACE	2002	2009	–144.2	73	H	Yearly estimates given and used in compilation
Chen et al., 2009	GRACE	2002.33	2006	–144.0	58	H	
Chen et al., 2009	GRACE	2006	2009	–220.0	89	H	
Rignot et al., 2011b	Flux	1992.00	2009.92	–82.9	91	H	Yearly estimates given and used in compilation
Horwath and Dietrich, 2009	GRACE	2002.33	2008	–109.0	48	L	Not clear why value is so much lower than other estimates with same data
Moore and King, 2008	GRACE	2002.33	2006	–164.0	80	H	
Cazenave et al., 2009	GRACE	2003	2008	–198.0	22	M	Fields truncated to lower number of harmonics than other estimates
Dong-Chen et al., 2009	GRACE	2002.583	2007.75	–78.0	37	L	Methodology unclear and incompletely described; quantification of errors not explained
Shi et al., 2011	ICESAT	2003.167	2008.25	–77.5	4.5	L	Methodology unclear and incompletely described; quantification of errors not explained
Zwally et al., 2005	Altimetry	1992.29	2001.29	–30.3	52	L	No data in Peninsula (uncertainty increased to compensate); firn compaction not validated, unclear performance at coast
Ivins et al., 2005	GRACE+GPS	2003	2009.25	–41.5	9	H	Uses Antarctic Peninsula from GRACE, INSAR, GPS to correct altimetry estimates; GPS network and data quality insures a higher quality of this local solution versus global solutions of Wu et al., 2010

Appendix 4.A, Table 4: Sources NOT used for calculation of ice loss from Antarctica.

Source	Method	Start	End	Gt/yr	Cited uncert-ainty	Relia-bility	Comment
Rignot et al.,	Flux	1996	1996	–112	91		Superseded (Rignot et al.,

2008b						2011b)
Rignot et al., 2008b	Flux	2006	2006	–196	92	Superseded (Rignot et al., 2011b)
Wingham et al., 1998	Altimetry	1992.29	1997	–60	76	Superseded (Wingham et al., 2006a)
Rignot and Thomas, 2002	Flux	1995	2000	–26	37	Not an ice sheet wide estimate
Davis et al., 2005	Altimetry	1992	2002	43	23	Superseded by Helsen et al 2009
Velicogna and Wahr, 2006b	GRACE	2002	2005	–139	73	Superseded (Velicogna, 2009)
Ramillien et al., 2006	GRACE	2002	2005	–39.6	32	Superseded (Cazenave et al., 2009)
Jia et al., 2009	GRACE	?	?	–82.0	29	Methodology to obtain this number is unclear
Gunter et al., 2009	Altimetry	2003.17	2007.17	–100.0	?	No error bar and no final estimate

Chapter 4: Observations: Cryosphere

Coordinating Lead Authors: Josefino C. Comiso (USA), David G. Vaughan (UK)

Lead Authors: Ian Allison (Australia), Jorge Carrasco (Chile), Georg Kaser (Austria), Ronald Kwok (USA), Philip Mote (USA), Tavi Murray (UK), Frank Paul (Switzerland), Jiawen Ren (China), Eric Rignot (USA), Olga Solomina (Russia), Koni Steffen (USA), Tingjun Zhang (USA)

Contributing Authors: Anthony A. Arendt (USA), David B. Bahr (USA), Michiel van den Broeke, (Netherlands), Ross Brown (Canada), J. Graham Cogley (Canada), Alex S. Gardner (USA), Stephan Gruber (Switzerland), Christian Haas (Canada), Jon Ove Hagen (Norway), Regine Hock (USA), David Holland, (USA), Thorsten Markus (USA), Rob Massom (Australia), Pier Paul Overduin (Germany), W. Tad Pfeffer (USA), Terry Prowse (Canada), Valentina Radic (Canada), David Robinson (USA), Martin Sharp (Canada), K. Shikomanov (USA), Sharon Stammerjohn (USA), Isabella Velicogna, (USA), Anthony Worby (Australia), L. Zhao (China)

Review Editors: Jonathan Bamber (UK), Philippe Huybrechts (Belgium), Peter Lemke (Germany)

Date of Draft: 16 December 2011

Notes: TSU Compiled Version

Figures

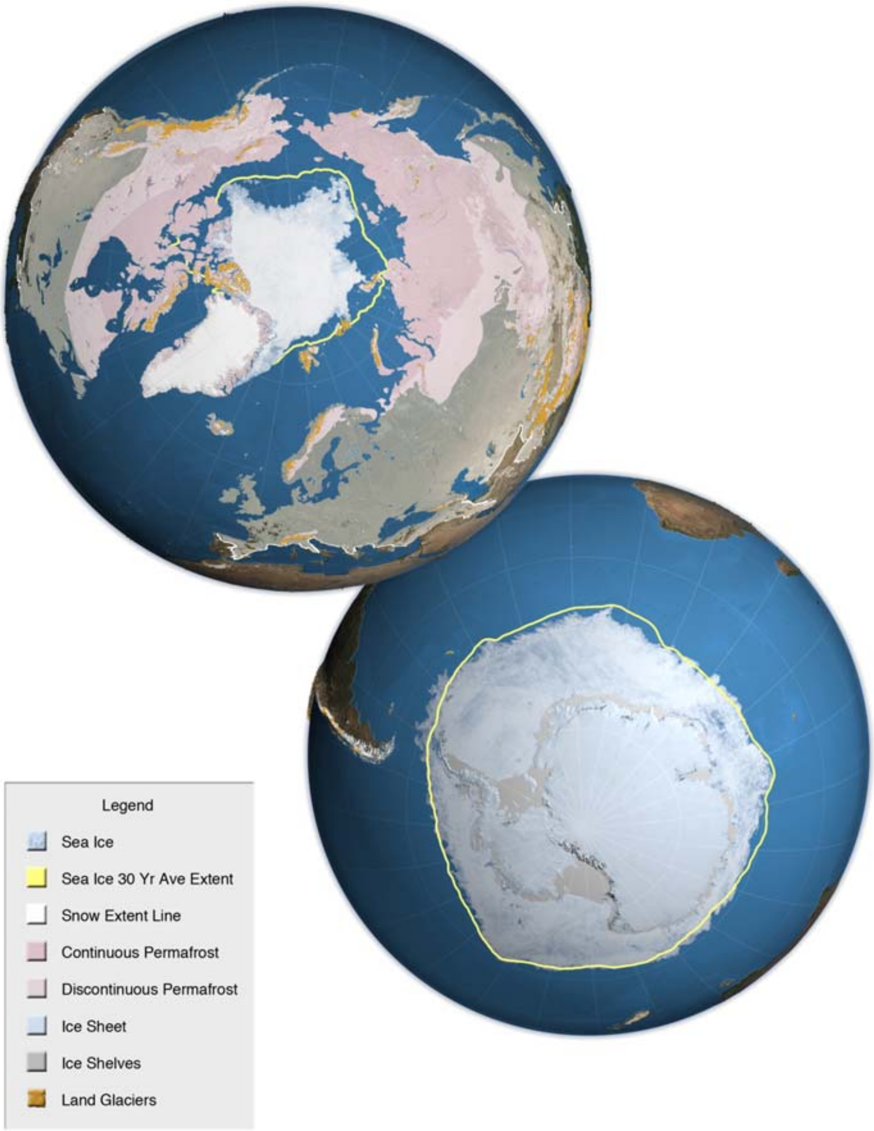

Figure 4.1: The cryosphere in the Northern and Southern Hemispheres in polar projection. The map of the Northern Hemisphere shows the sea ice cover during minimum extent (9th September 2011). The yellow line is the average location of the ice edge (15% ice concentration) for the yearly minima for 1979 to 2011. Areas of continuous permafrost are shown in darker pink, discontinuous permafrost in lighter pink. The shaded area over land and permafrost shows snow cover as derived from MODIS data (July 2009 to March 2010) with the greatest extent during that period represented by the white line. The Greenland ice sheet (white) and locations of glaciers (yellow) are also shown, but the glaciers within the ice sheet are shown as part of the ice sheet. The map of the Southern Hemisphere shows approximately the maximum sea ice cover during an austral winter (9th September 2011). The yellow line shows the average ice edge (15% ice concentration) during maximum extents of the sea ice cover for 1979 to 2011. Some of the elements (e.g., some glaciers and snow) located at low latitudes are not visible in this projection (see Figure 4.8). The source of the data for sea ice, permafrost, snow and ice sheet are datasets held at the National Snow and Ice Data Center (NSIDC), University of Colorado, on behalf of the North American Atlas, Instituto Nacional de Estadstica Geografa e Informatica, Natural Resources Canada, U.S. Geological Survey, Government of Canada, Canada Centre for Remote Sensing and The Atlas of Canada. Sources of glacier outlines: Weidick et al. (1992); Zheltyhina (2005). Figure courtesy of the NASA Visualization Group.

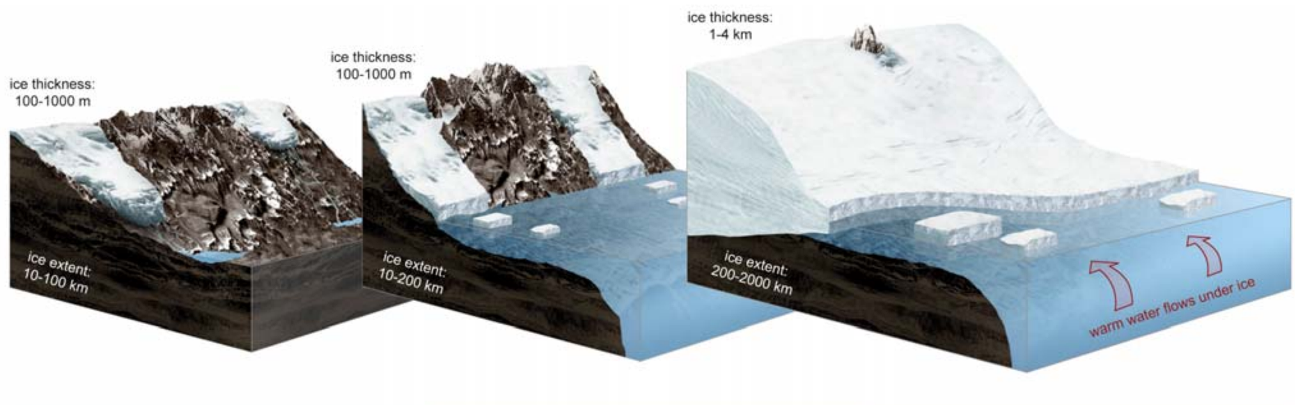

Type: Land-terminating glaciers in mountainous areas	**Type:** Tidewater and marine-terminating glaciers	**Type:** Ice sheets terminating in ice shelves
Location of examples: European Alps, Andes, Himalayas, Africa	**Location of examples:** Alaska, Patagonia, Svalbard, Greenland, Antarctica	**Location of examples:** Greenland and Antarctica
Primary external forcing: Atmospheric temperature, precipitation	**Primary external forcing:** Atmospheric temperature, precipitation, ocean	**Primary external forcing:** Atmospheric temperature, precipitation, ocean
Climatic regime: Temperate, high mountain	**Climatic regime:** Cool temperate to polar	**Climatic regime:** Polar

Figure 4.2: Block diagram showing the progression of characteristics from glaciers in mountainous regions, which exist across a wide range of latitudes, through tidewater and marine glaciers, to polar ice sheets which occur exclusively in polar regions. (Drafted by J. Oliver, BAS)

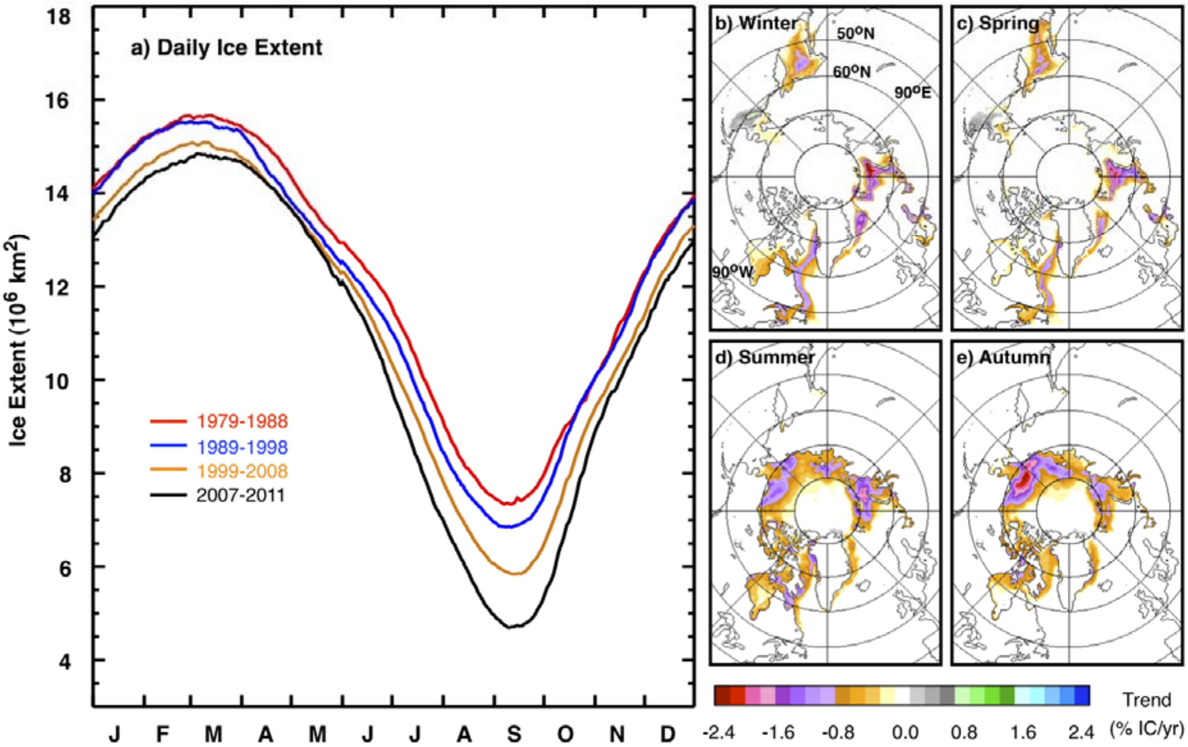

Figure 4.3: (a) Plots of decadal averages of daily sea ice extent in the Arctic (1979 to 1988 in red, 1989 to 1998 in blue, 1999 to 2008 in gold) and a five-year average daily ice extent from 2007 to 2011; ice concentration trends (1979–2010) in (b) winter, (c) spring, (d) summer and (e) autumn (Comiso and Nishio, 2008).

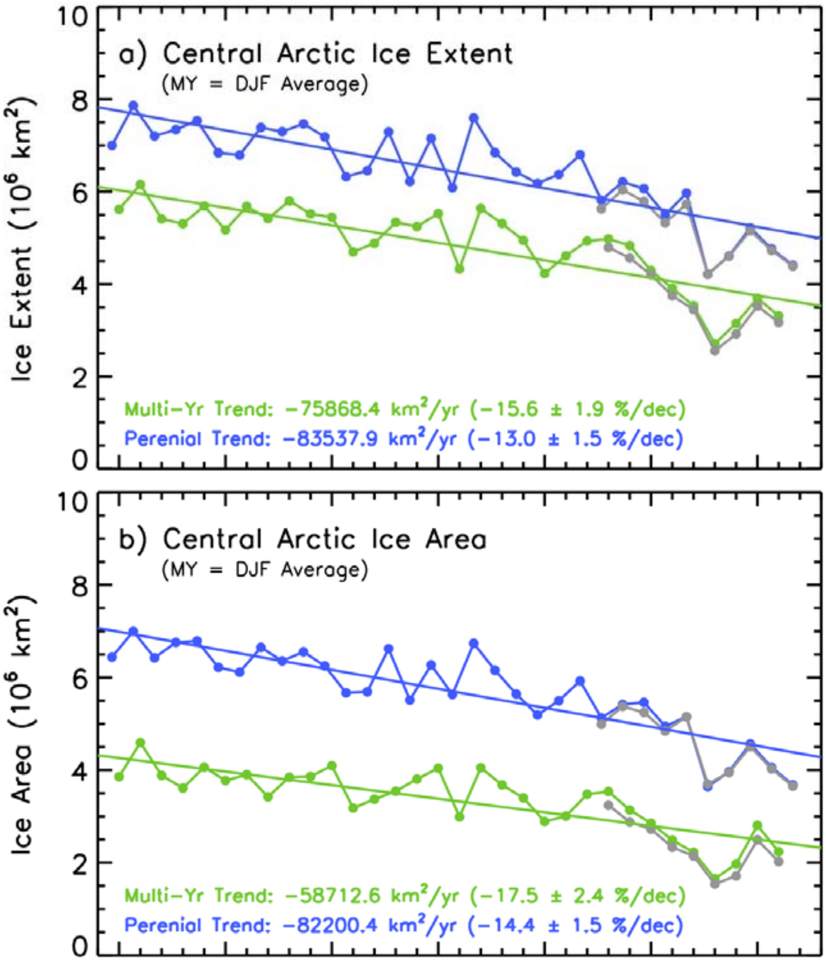

Figure 4.4: Yearly perennial (blue) and multiyear (green) ice extent (a) and ice area (b) in the Central Arctic for each year from 1979 to 2011 as derived from satellite passive microwave data. Perennial ice values are derived from summer ice minimum values, while the multiyear ice values are averages of December, January and February data. The gray lines (after 2002) are derived from AMSR-E data (Comiso, 2011).

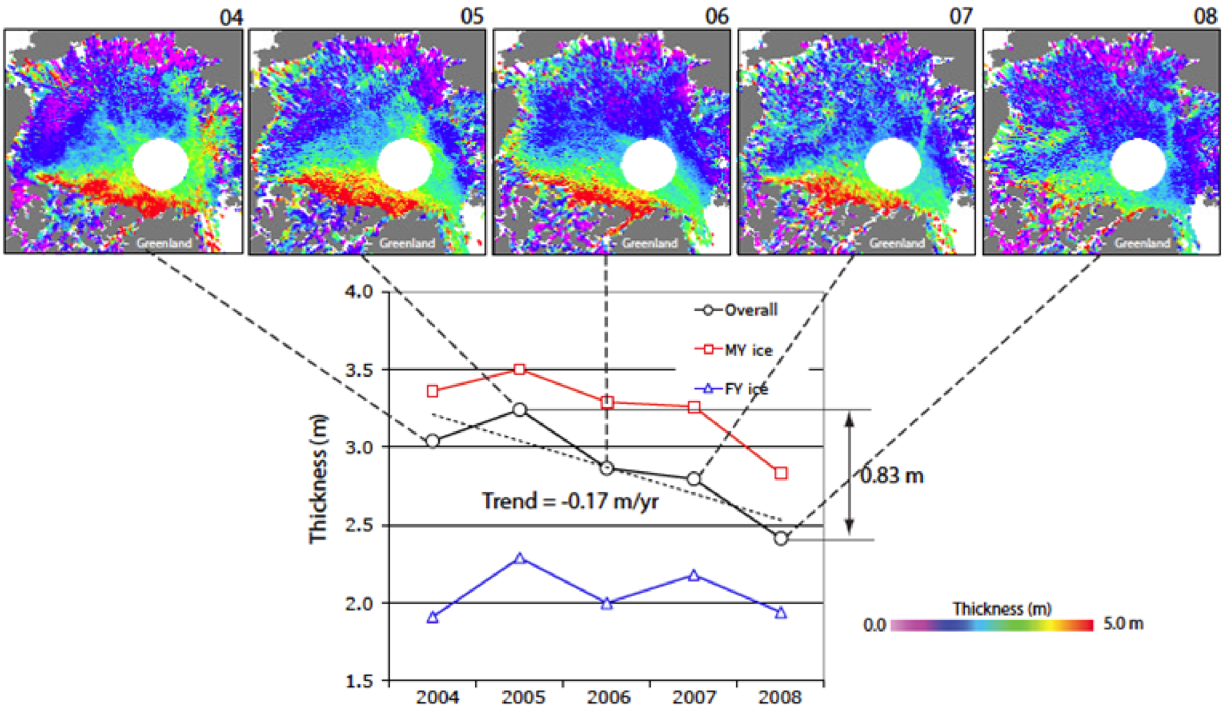

Figure 4.5: The distribution of winter sea ice thickness in the Arctic and the trends in average, first-year (FY) ice, and multiyear (MY) ice thickness derived from ICESat records, 2004–2008 (Kwok, 2009).

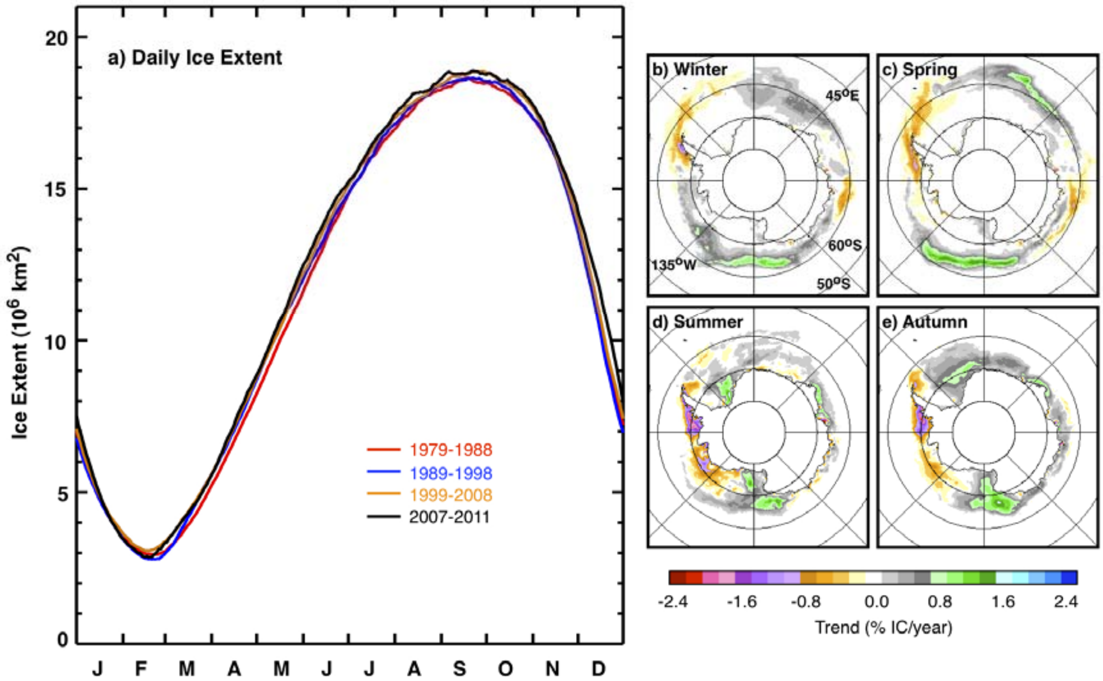

Figure 4.6: (a) Plots of decadal averages of daily sea ice extent in the Antarctic (1979 to 1988 in red, 1989 to 1998 in blue, 1999 to 2008 in gold) and yearly values of daily ice extents in 2007, 2010 and 2011; ice concentration trends (1979–2010) in (b) winter, (c) spring, (d) summer and (e) autumn.

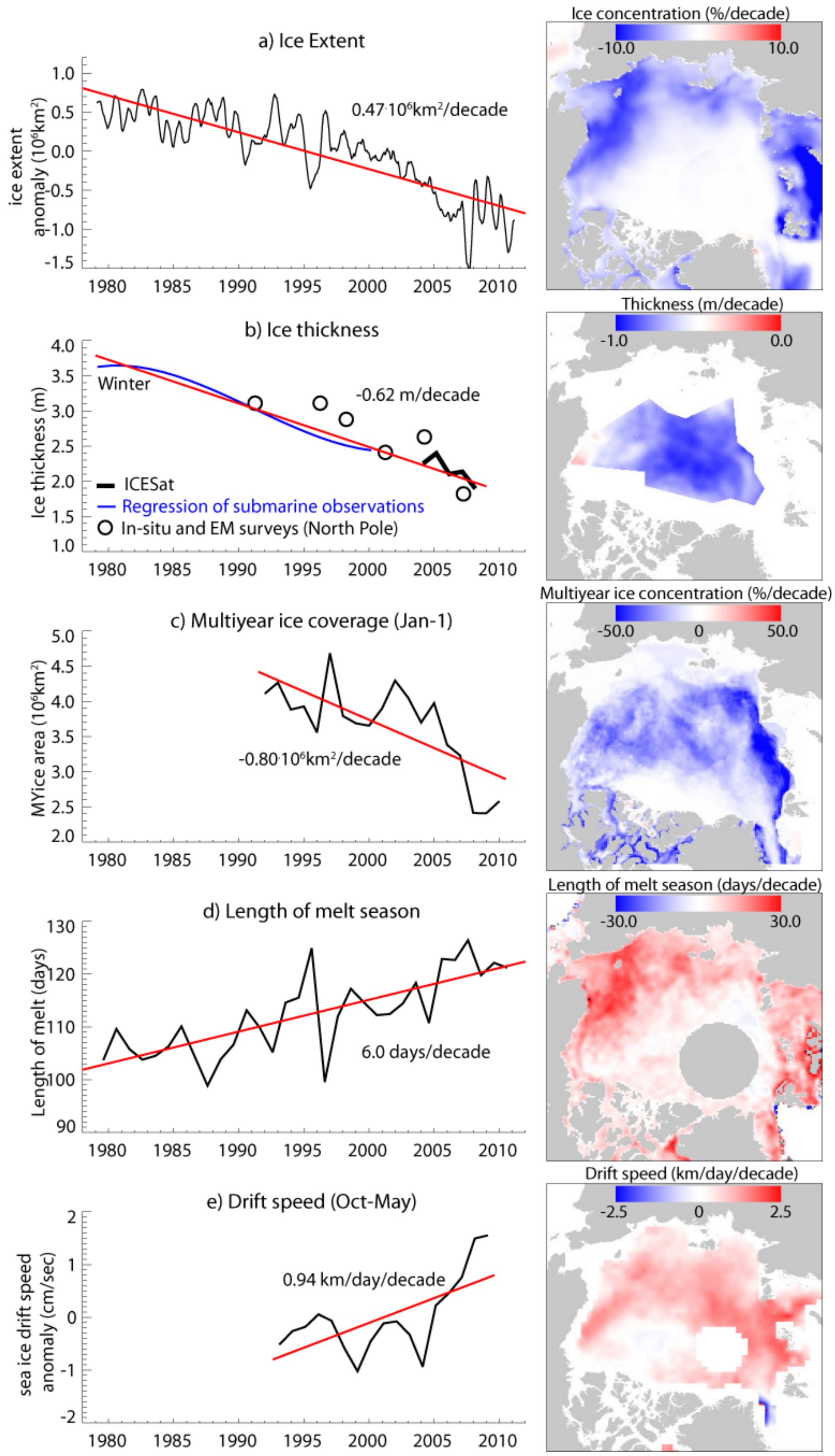

Figure 4.7: Summary of linear decadal trends (red) in: (a) Arctic ice extent and concentration from satellite passive microwave observations (Comiso and Nishio, 2008); (b) sea ice thickness from submarine (blue), satellites (black), and in-situ/EM surveys (circles); trend in submarine ice thickness is from multiple regression of available observations to separate the interannual changes, the annual cycle, and the spatial field of thickness within the data release area (Haas et al., 2008; Kwok and Rothrock, 2009); (c) multiyear sea ice coverage from analysis of QuikSCAT (Kwok et al., 2009); (d) length of melt season (Markus et al., 2009); and (e) satellite-derived drift speed (Spreen et al., 2011).

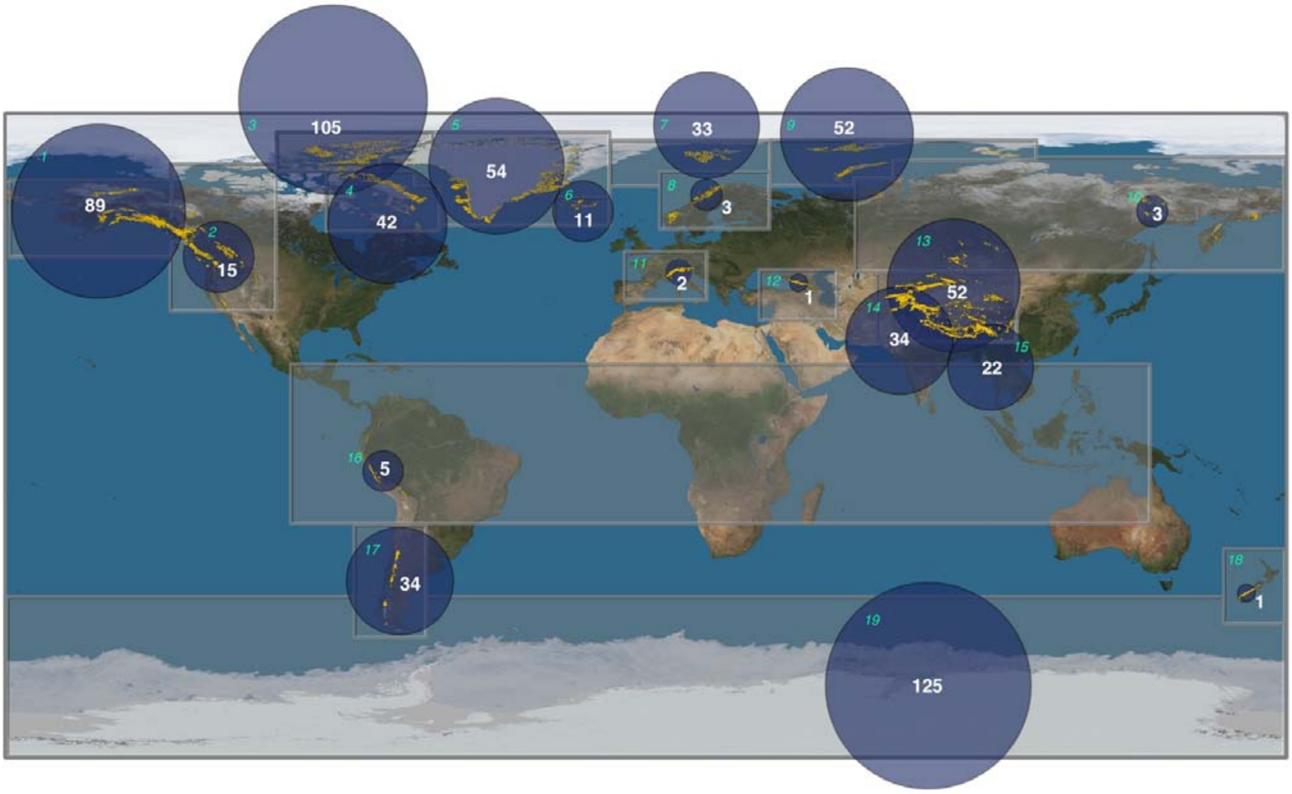

Figure 4.8: Total glacier area in 1,000 km^2 (white) subdivided into the 19 regions (green numbers in italics) used throughout the Section 4.3. The size of each circle is equivalent to the glaciated area in each region. The glacier areas are based on the new calculations (Arendt et al., 2011). The regions are: 1 Alaska, 2 Western Canada and US, 3 Arctic Canada (North), 4 Arctic Canada (South), 5 Greenland, 6 Iceland, 7 Svalbard, 8 Scandinavia, 9 Russian Arctic, 10 North Asia, 11 Central Europe, 12 Caucasus and Middle East, 13 Central Asia (North), 14 Central Asia (West), 15 Central Asia (South), 16 Low-Latitudes, 17 Southern Andes, 18 New Zealand, and 19 Antarctic and Sub-Antarctic. Yellow dots illustrate schematically locations of glaciers. The total area for region 19 is derived from various sources (Arendt et al., 2011) but data for digital overlay on this map are not yet available.

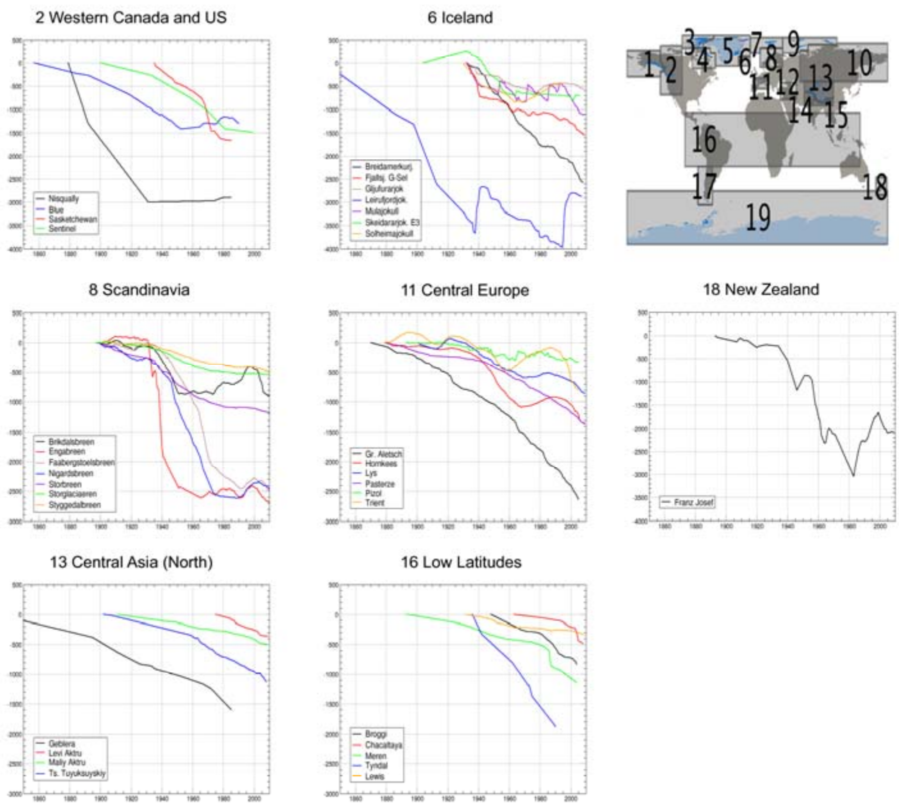

Figure 4.9: Cumulative glacier length changes as measured in the field for seven different regions. Data from WGMS (2008).

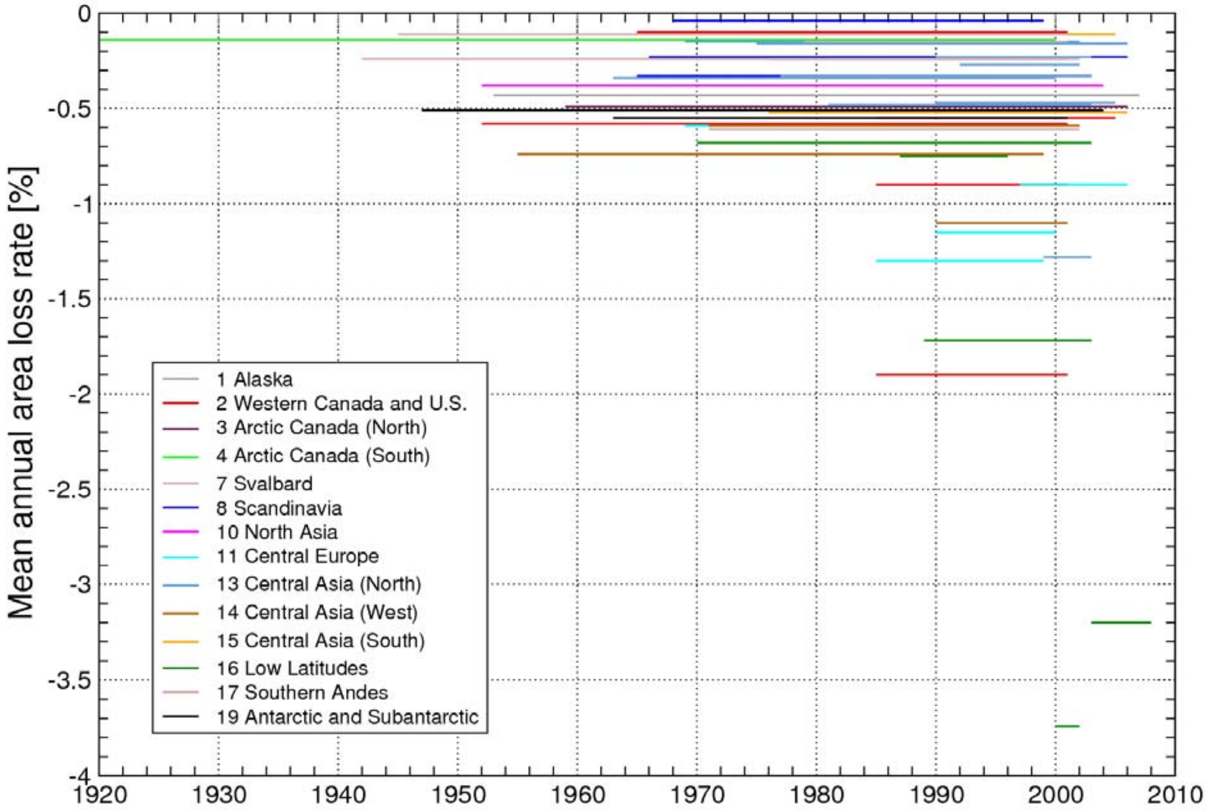

Figure 4.10: Mean annual area-loss rates for 14 out of the 19 regions depicted in Figure 4.8. Each line refers to the observed relative area loss from a specific publication and its length is related to the period used for averaging. The publications considered for each subregion (in brackets) are: (**1**) Le Bris et al., 2011; (**2**) Bolch et al., 2010a; Debeer and Sharp, 2007; Jiskoot et al., 2009; (**3**) Huss et al., 2008; (**4**) Paul and Kaab, 2005; (**7**) Kaab, 2008; (**8**) Andreassen et al., 2008; Paul and Andreassen, 2009; (**10**) Shahgedanova et al., 2010; (**11**) Abermann et al., 2009; Lambrecht and Kuhn, 2007; Paul et al., 2004; (**13**) Aizen et al., 2007; Bolch et al., 2010b; Cia et al., 2005; Kutuzov and Shahgedanova, 2009; Li et al., 2006; Surazakov et al., 2007; Wang et al., 2009; Ye et al., 2006a; Ye et al., 2006b; Zhou et al., 2009; (**14**) Bolch, 2007; Khromova et al., 2006; Narama et al., 2006; (**15**) Bolch et al., 2008; Kulkarni et al., 2007; Nie et al., 2010; (**16**) Cullen et al., 2006; Klein and Kincaid, 2006; Peduzzi et al., 2010; Racoviteanu et al., 2008; Silverio and Jaquet, 2005; (**17**) Rivera et al., 2005; Rivera et al., 2007; Schneider et al., 2007; (**19**) Berthier et al., 2009; Thost and Truffer, 2008. Data compilation by Matthias Mahrer, University of Zurich.

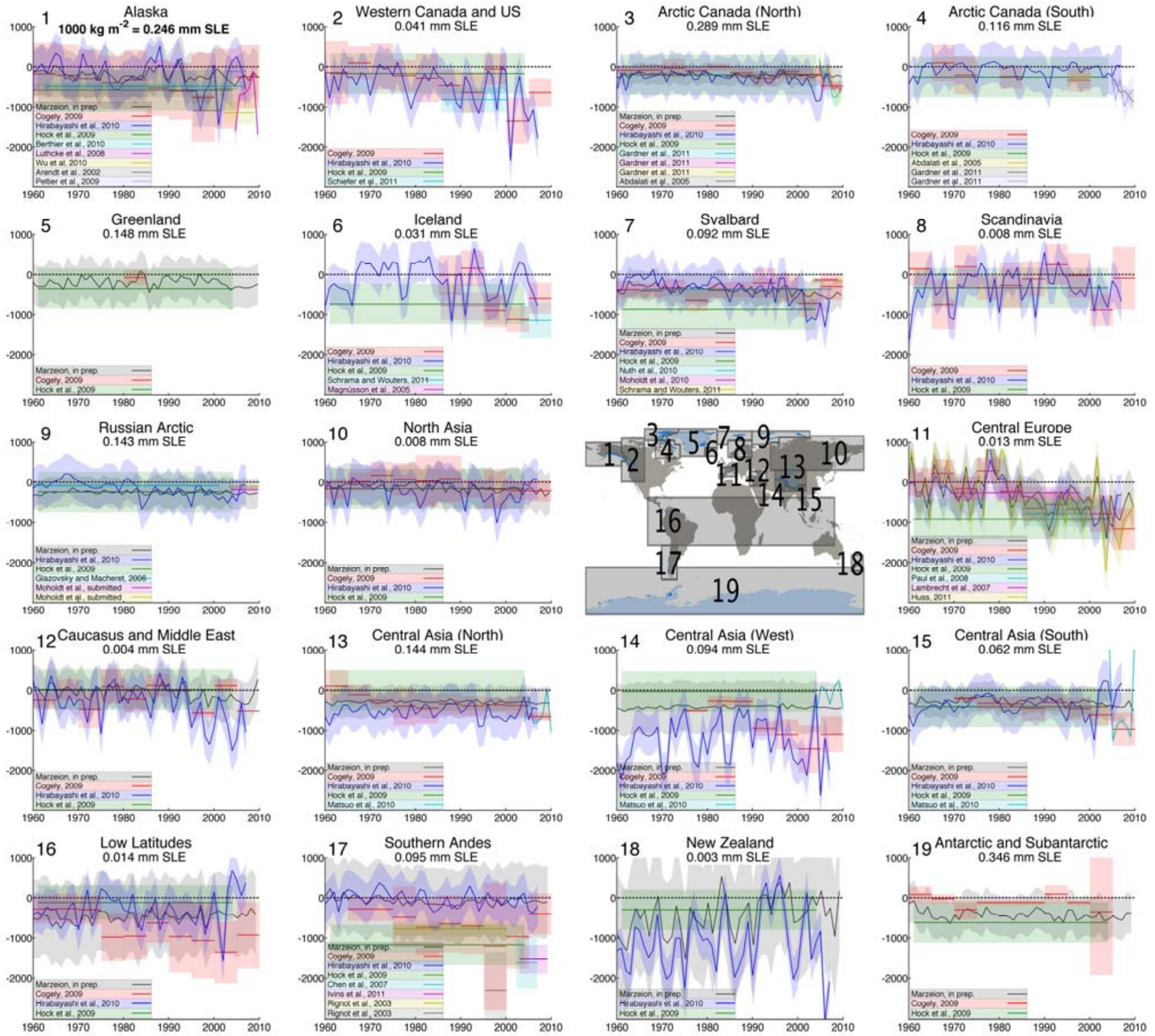

Figure 4.11: Glacier mass change rates in [kg m^{-2} yr^{-1}] for the 19 regions from Figure 4.8. Values are either from regional measurements (Abdalati et al., 2004; Arendt et al., 2002; Berthier et al., 2010; Chen et al., 2007; Gardner et al., 2011; Glazovsky and Macheret, 2006; Ivins et al., 2011; Luthcke et al., 2008; Magnusson et al., 2005; Matsuo and Heki, 2010; Moholdt et al., submitted; Moholdt et al., 2010; Nuth et al., 2010; Paul and Haeberli, 2008; Peltier, 2009; Rignot et al., 2003; Schiefer et al., 2007; Schrama and Wouters, 2011; Wu et al., 2010), extrapolation from single glacier measurements (Cogley, 2009c; Huss, 2011; Lambrecht and Kuhn, 2007), and modelling with atmospheric input variables (Hirabayashi et al., 2010; Marzeion et al., 2011). Incomplete regional measurements are up-scaled. Uncertainties, if not provided by the authors, are given as a random error of 500 kg m^{-2} for non-elevation difference studies and as a cumulative error of 5 m for elevation change studies. Conversions from area specific 1,000 kg m^{-2} into mm SLE are given for each region below the region names. Figure compilation: Alex S. Gardner, Atmospheric, Oceanic & Space Sciences, University of Michigan.

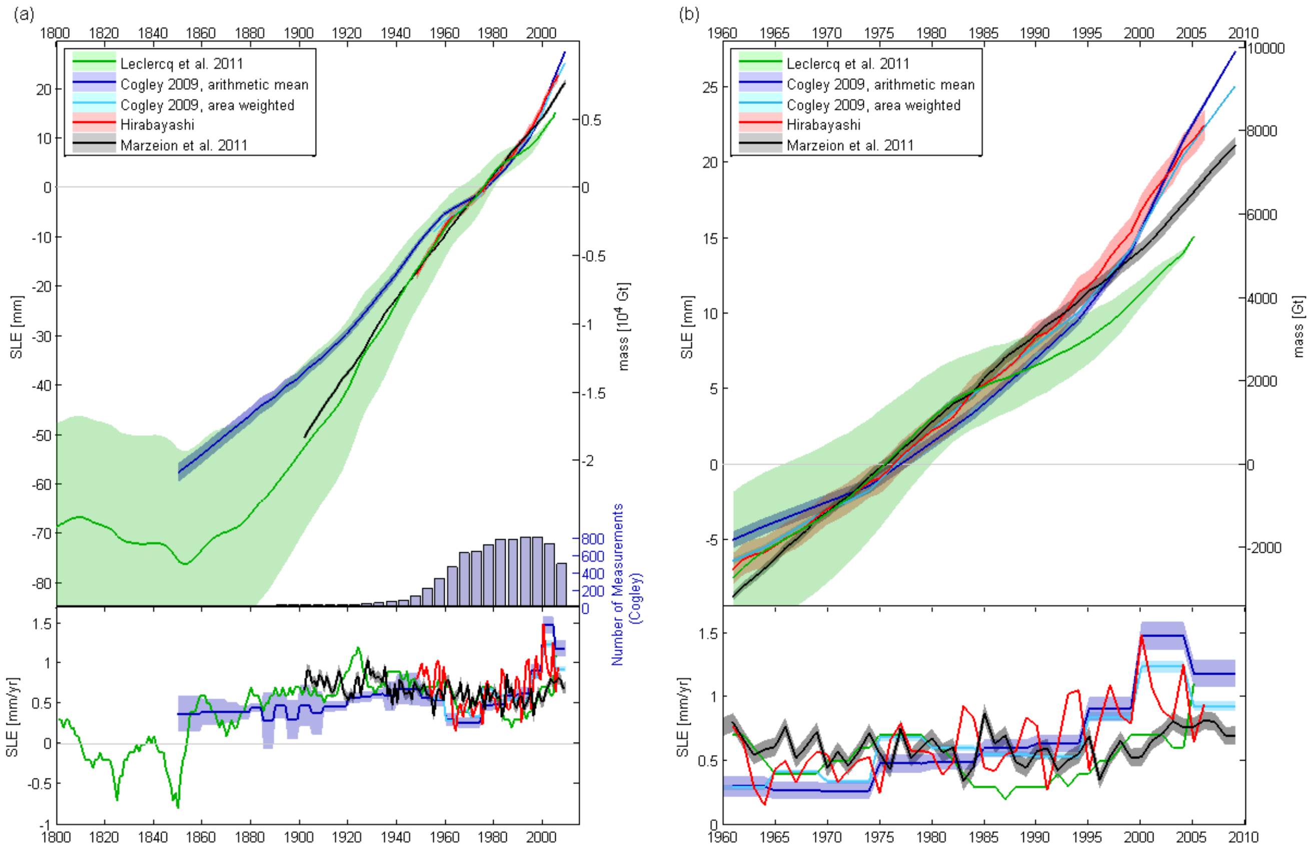

Figure 4.12: The global glaciers' cumulative (top graphs) and annual (lower graphs) mass change 1800–2010 and 1960–2010 in panel (a) and (b) respectively. Different cumulative estimates are all set to zero mm SLE with their 1961–1990 average. Estimates are from glacier length variations (Leclercq et al., 2011), from arithmetic means and area weighted extrapolations of individual glaciers directly and geodetically measured mass budgets (extended from Cogley, 2009c; Kaser, 2006), and modelling with atmospheric variables as input (Hirabayashi et al., 2010; Marzeion et al., 2011). Figure drawn by Ursula Blumthaler, Institute of Meteorology and Geophysics, University of Innsbruck.

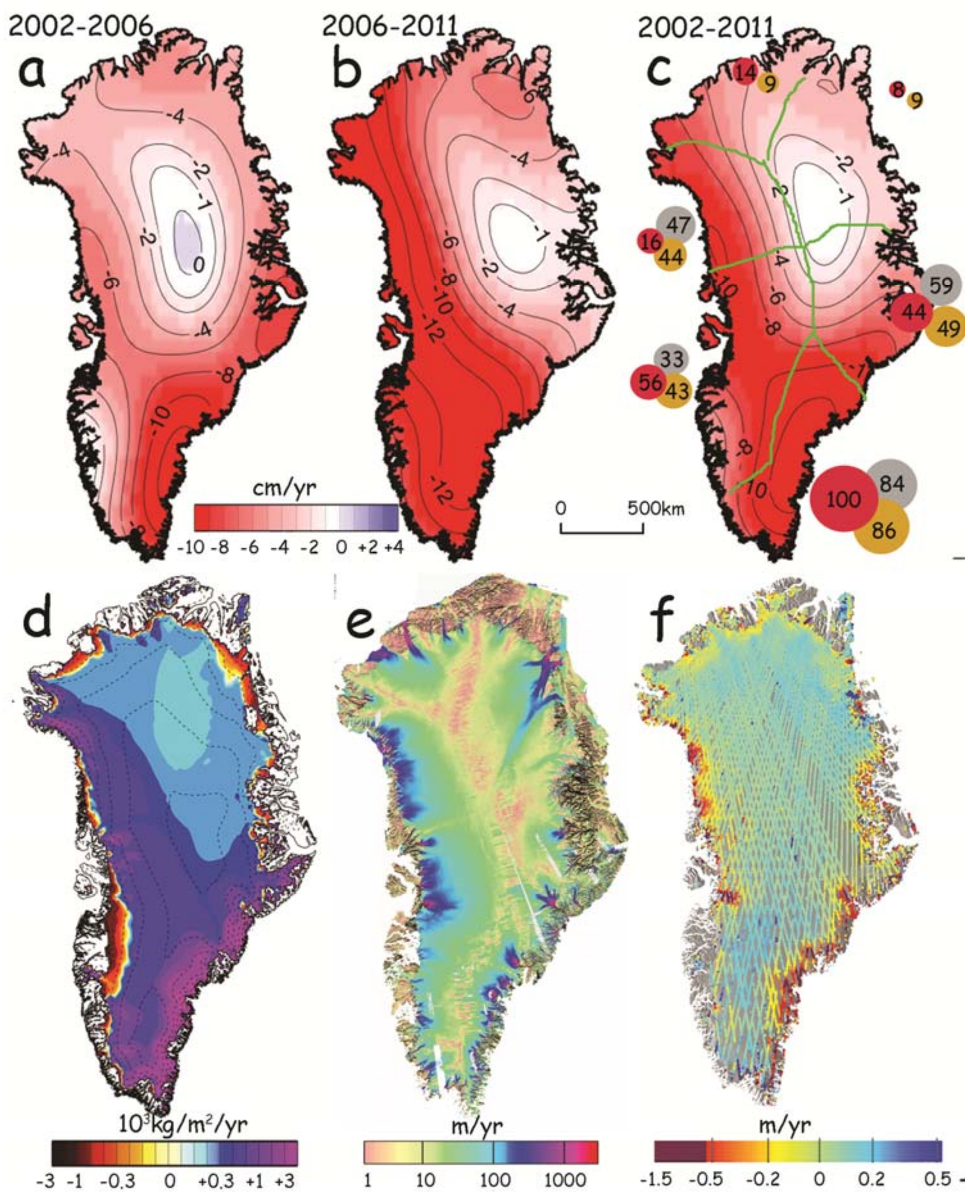

Figure 4.13: Temporal pattern of ice loss in Greenland from GRACE time-variable gravity in cm of water per year for the periods (a) 2002 to 2006, (b) 2006 to 2011 and (c) 2002 to 2011, color coded red (loss) to blue (gain) (Velicogna, 2009). Circles in c) indicate average ice loss (Gt/yr) from GRACE (red = mass budget (Rignot et al., 2011b); orange = GRACE (Velicogna, 2009); and blue = ICESat (Sorensen et al., 2011)); (d) surface mass balance for years 1957–2009 (Ettema et al., 2009); (e) ice velocity from satellite radar interferometry data for years 2007–2009, and (f) ice-thinning rates from ICESat data for years 2003–2008 (Pritchard et al., 2009).

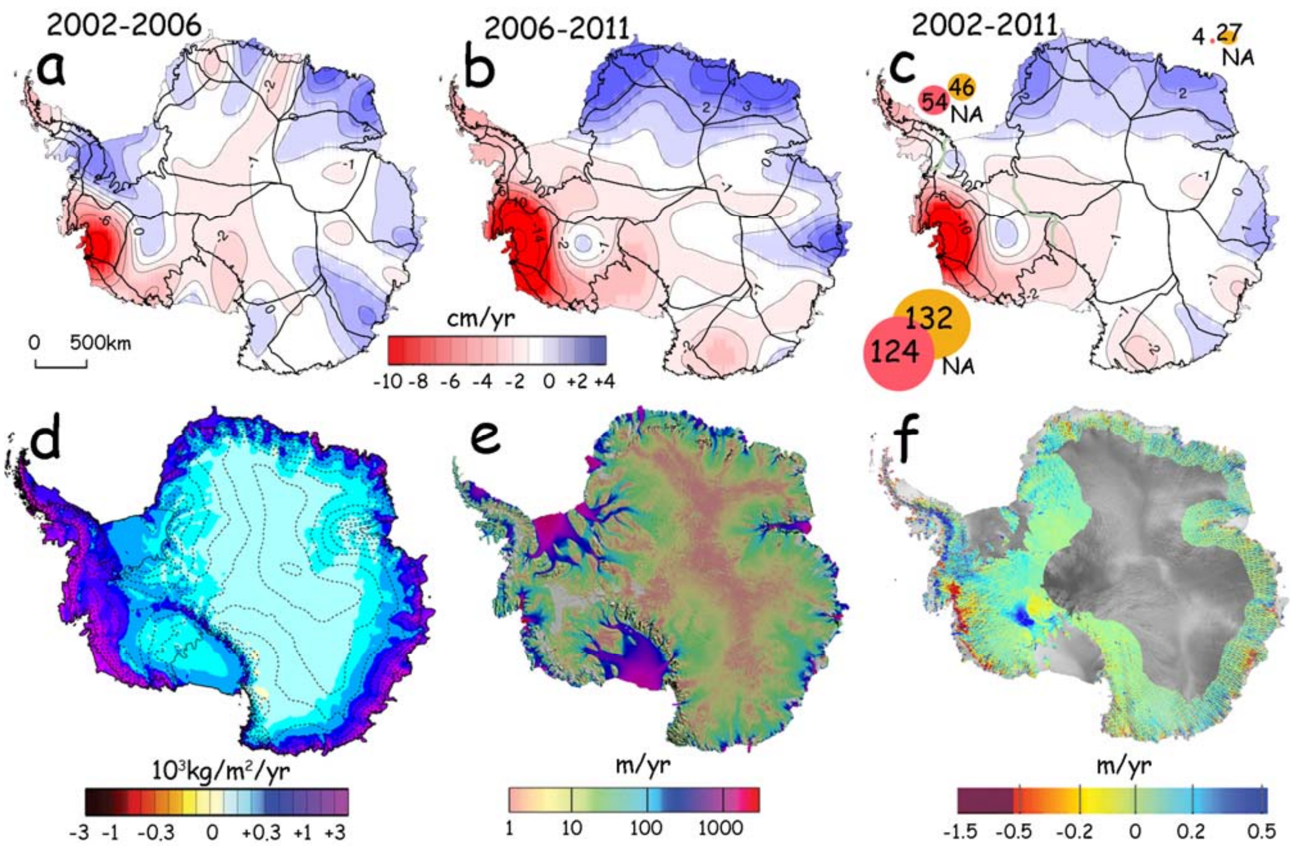

Figure 4.14: Temporal evolution of ice loss in Antarctica from GRACE time-variable gravity in cm of water per year for the periods (a) 2002 to 2006, (b) 2006 to 2011 and (c) 2002 to 2011, color coded red (loss) to blue (gain) (Velicogna, 2009). Circles in (c) indicate average ice loss (Gt/yr) for 2002–2011 for the Antarctic Peninsula (red = flux (Rignot et al., 2011b); orange = GRACE (Ivins et al., 2011)), the West Antarctic Ice Sheet (red = flux (Rignot et al., 2011b)), orange = GRACE (Velicogna, 2009) and East Antarctica (red = flux (Rignot et al., 2008b)), orange = GRACE (Chen et al., 2009)); no regional estimates are available from altimetry for that time period; (d) surface mass balance in Antarctica for years 1989–2004 (van den Broeke et al., 2006); (e) ice sheet velocity for 2007–2009 showing fastest flow in red, fast flow in blue, and slower flow in green and yellow (Rignot et al., 2011a); (f) ice thinning rates from ICESat for years 2003–2008 with thinning in red to thickening in blue (Pritchard et al., 2009).

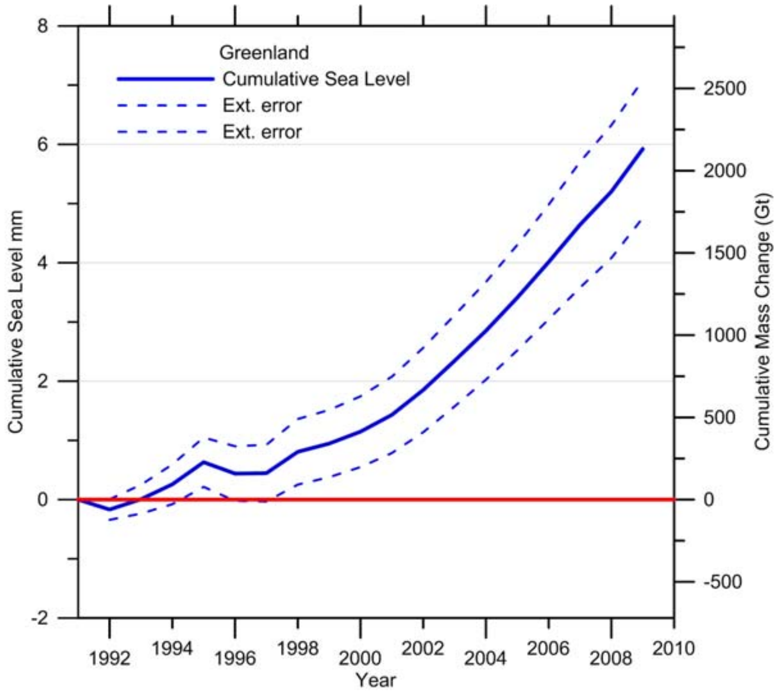

Figure 4.15: Cumulative sea level rise (and ice loss equivalent) from Greenland derived from the weighted average of 12 recent studies (see Table 4.5 and Appendix 4.A) (Baur et al., 2009; Cazenave et al., 2009; Chen et al., 2011; Pritchard et al., 2010; Rignot et al., 2011b; Sasgen and others, In review; Schrama and Wouters, 2011; Slobbe et al., 2009; Sorensen et al., 2011; Velicogna, 2009; Wu et al., 2010; Zwally et al., 2011). The studies selected are the latest made by 12 different research groups, for Greenland, and do not include earlier estimates from the same researchers when those have been updated by more recent analyses using extended data. In calculating the average, each estimate has been weighted based on an assessment of its reliability: High reliability = weighting of 1.0, Medium = 0.5, Low = 0.2. The number of estimates used in this composite varies with time, with only 2 per year in the 1990s and up to 12 per year after 2002. The plotted values are the cumulative sea level contribution at the end of the year on the x-axis, starting at an arbitrary zero on January 1st 1992. Since yearly estimates from different studies do not overlap within the uncertainties quoted by the authors, the errors shown are based on the maximum and minimum estimate for each year within uncertainty ranges cited in the original studies. The cumulative error is weighted by $1/\sqrt{n}$, where n is the number of years accumulated.

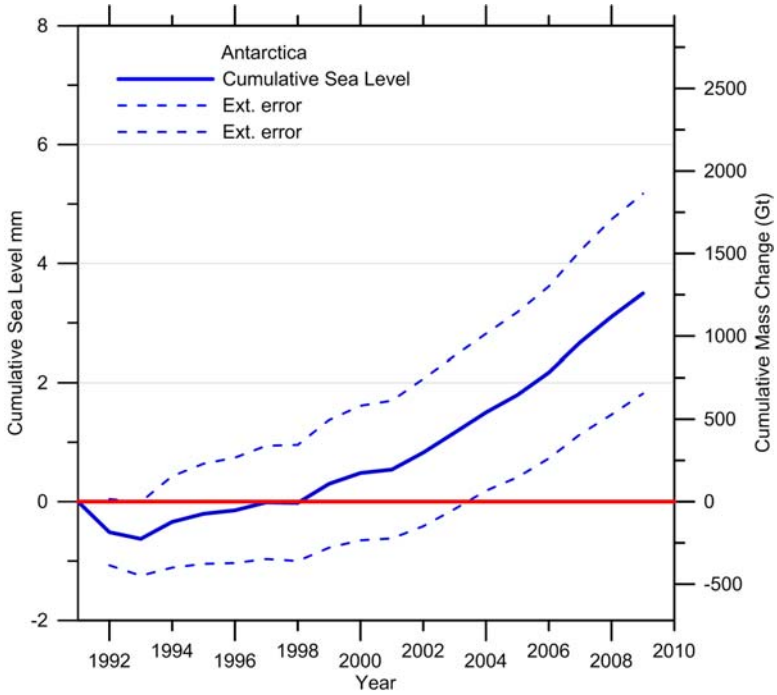

Figure 4.16: Assessment of the cumulative sea level contribution from Antarctica derived from the weighted average of 12 recent analyses (see Table 4.5 and Appendix 4.A) (Cazenave et al., 2009; Chen et al., 2009; Dong-Chen et al., 2009; Horwath and Dietrich, 2009; Ivins et al., 2011; Moore and King, 2008; Rignot et al., 2011b; Shi et al., 2011; Velicogna, 2009; Wingham et al., 2006a; Wu et al., 2010; Zwally et al., 2005). The studies selected are the latest made by 12 different research groups for Antarctica, and do not include earlier estimates from the same researchers when those have been updated by more recent analyses using extended data. In calculating the average, each estimate has been weighted based on an assessment of its reliability: High reliability = weighting of 1.0, Medium = 0.5, Low = 0.2. The number of estimates used in this composite varies with time, with only 2 per year in the 1990s and up to 12 per year after 2002. The plotted values are the cumulative sea level contribution at the end of the year on the x-axis, starting at an arbitrary zero on January 1st 1992. Since yearly estimates from different studies do not overlap within the uncertainties quoted by the authors, the errors shown are based on the maximum and minimum estimate for each year within uncertainty ranges cited in the original studies. The cumulative error is weighted by $1/\sqrt{n}$, where n is the number of years accumulated. See Section 4.4.2.2 for further details.

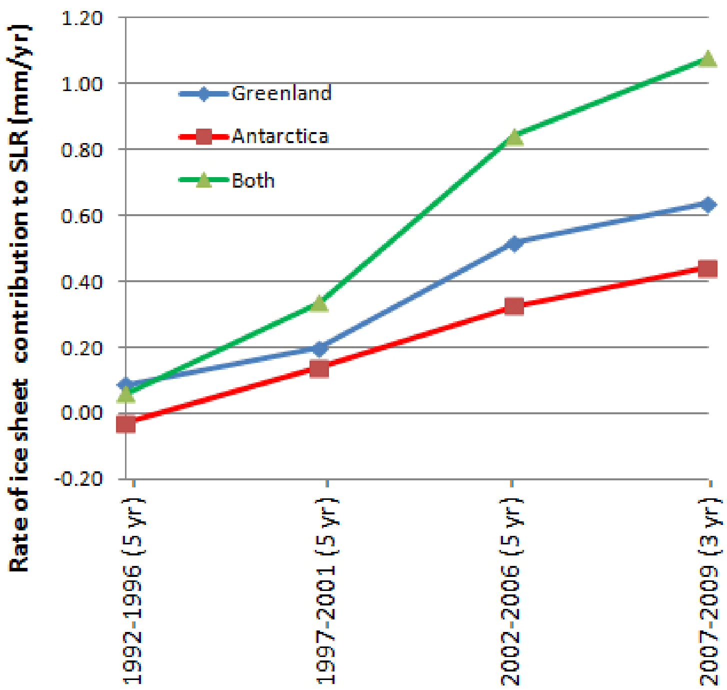

Figure 4.17: Rate of ice sheet contribution to sea level rise averaged over 5 year periods between 1992 and 2009 (the last period is only 3 years). These estimates are derived from the data in Figures 4.15 and 4.16.

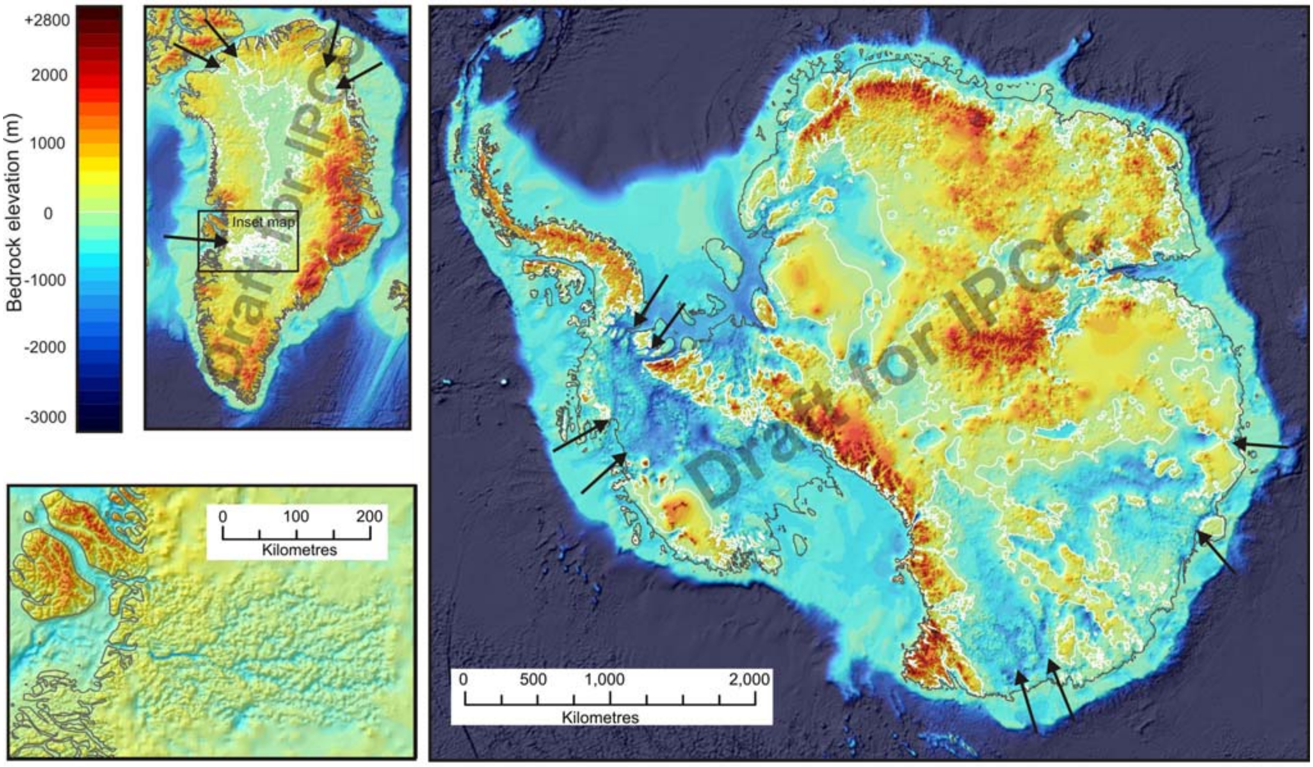

Figure 4.18: Bed topography for Greenland and Antarctica, derived from (Griggs and Bamber, 2011a; Pritchard et al., 2011) with marine-based parts of the ice sheet highlighted and arrows showing access routes for rapid discharge of marine-based sectors. Figure drawn by P. Fretwell, BAS.

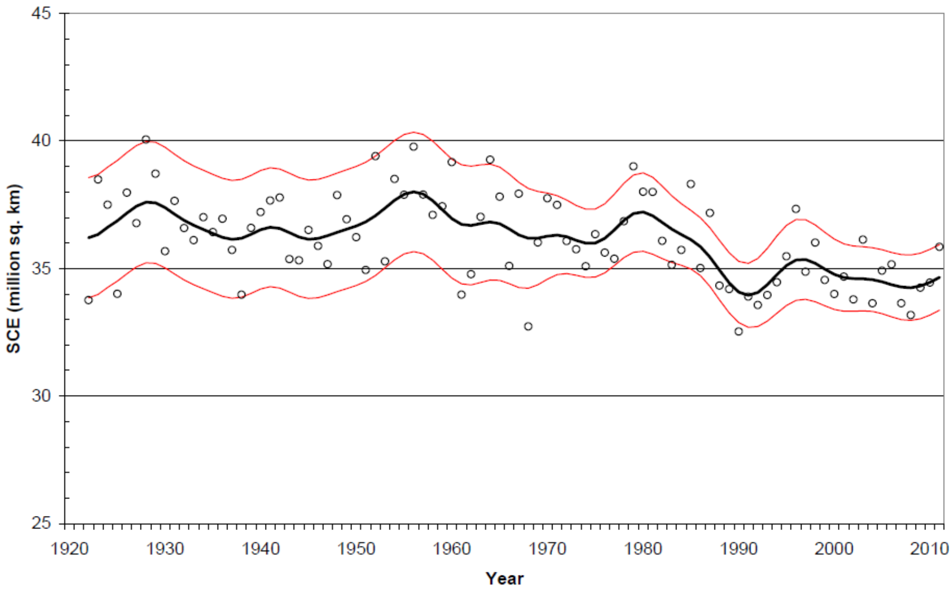

Figure 4.19: Variability April NH SCE over the period of available data with13-term filtered values of the mean and 95% confidence interval. The width of the smoothed confidence interval is also influenced by the interannual variability in SCE. From Brown and Robinson (2011), updated.

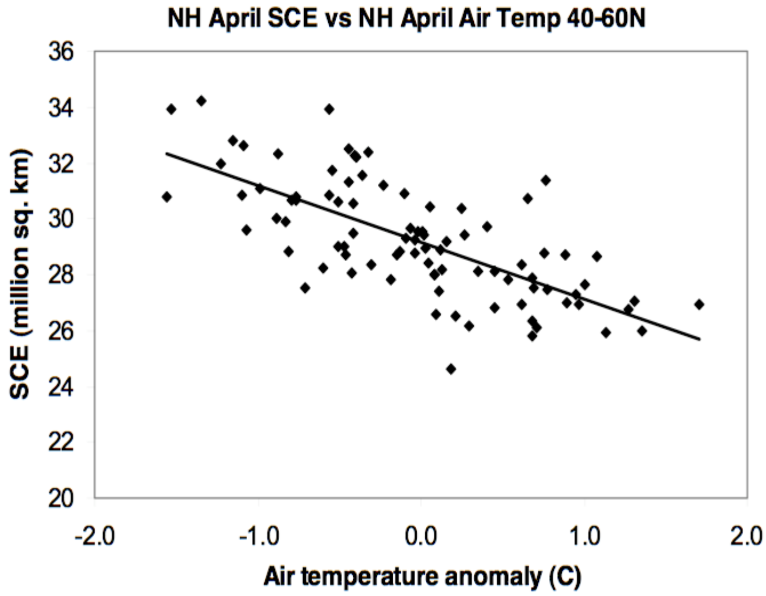

Figure 4.20: Relationship between NH April SCE and corresponding land area air temperature anomalies over 40°N–60°N from the CRU dataset. Air temperature explains 48.7% of the variance. From Brown and Robinson (2011).

Citation	Region	Metric	Period of study	Statistic	N	%< 0
Ishizaka 2004	Japan	SD Jan-Feb	1970-99 minus 1960-89		95	53
Bulygina 2011	northern Eurasia	Max SD	1966-2010	cm	675	33
Mote 2006	western N Amer.	1 Feb SWE	1950-2000		473	71
Christy 201X	regions of Calif	snowfall	1878-2011		18*	72
Skaugen 201X	s. Norway	max SWE	1961-2009	Sen	105	5
Micu 2009	Romania	mean SD	1961-2003		15	46
Petkova 2004	Bulgaria	max SD	~1931-2000		15	66
Valt 2010	Italy	snowfall	1960-2009		18	100
Marty 2011	Switzerland	max SD	1931-2010		18	35
Ishizaka 2004	Japan	SD Mar	1970-99 minus 1960-89		89	73
Bulygina 2011	northern Eurasia	#d SD>20cm	1966-2010	# days	675	31
Mote 2006	western N Amer.	1 Apr SWE	1950-2000		799	72
Christy 201X	regions of Calif	MAM snow	1878-2011		4*	50
Micu 2009	Romania	SCD	1961-2003		15	66
Petkova 2004	Bulgaria	SCD	~1931-2000		15	80
Valt 2010	Italy	SCD	1950-2009		18	100
Scherrer 2004	Switzerland	SCD	1958-99		106	90
Marty 2011	Switzerland	SCD	1948-2011		34	100

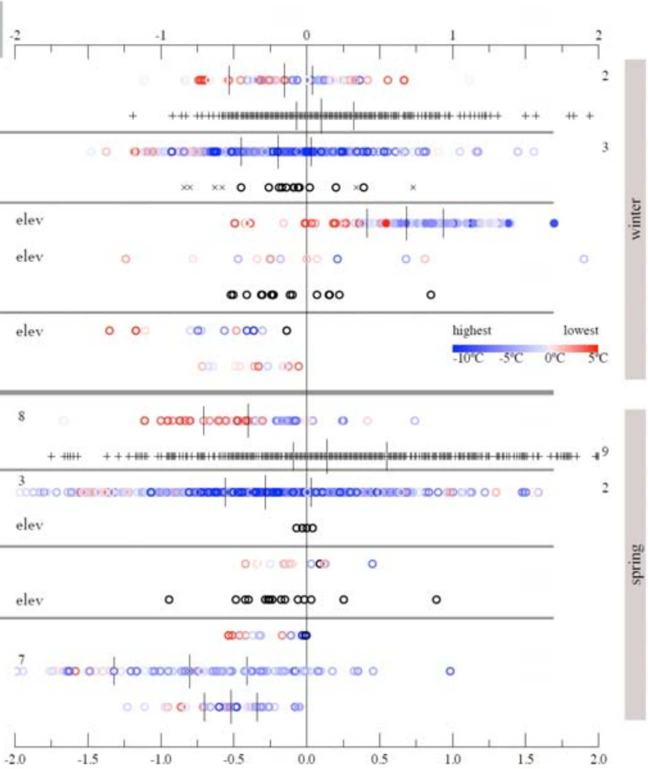

Figure 4.21: Summary of station trends in metrics of snow that, based on the work of Brown and Mote (2009), are (top half) more reflective of mid-winter conditions and (bottom half) more reflective of spring conditions. Where symbols are circles, the quantity plotted is the percentage change of a linear fit divided by the number of years of the fit. For the Bulygina study, the quantity plotted is the trend in cm yr^{-1} (top) and # days yr^{-1} (bottom). Solid circles in the Skaugen study were statistically significant. Christy (In submission) combined records from over 500 stations into 18 regions (hence the asterisk); none of the trends was statistically significant. He judged time series from some regions unsuitable for statistical analysis and these are indicated here by an 'x'. For studies with more than 50 sites, the median, 25th and 75th percentiles are shown with vertical lines. In a few cases, some plotted trends lie beyond the edges of the graph; these are indicated by a numeral at the corresponding edge of the graph, e.g., 2 sites >2% yr^{-1} for the Ishizaka study. Colours indicate temperature or, where indicated, elevation using the lowest and highest site to set the colour scale. Note the prevalence of negative trends at lower/warmer sites, especially in spring.

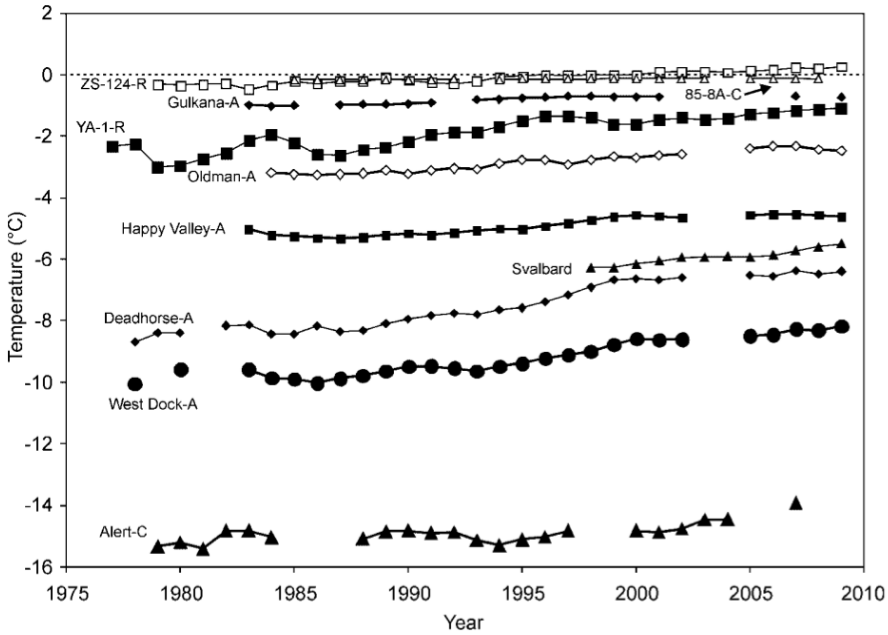

Figure 4.22: Time series of mean annual ground temperatures at depths between 10 and 20 m for boreholes throughout the circumpolar northern permafrost regions (Romanovsky et al., 2010b). Data sources for North American, Russian and Nordic sites are Smith et al. (2010), Romanovsky et al. (2010a) and Christiansen et al. (2010), respectively. **C** Canadian site; **A** Alaskan site; **R** Russian site. The Svalbard site is Janssonhaugen (PACE-10) (Isaksen et al., 2007). Measurement depth for Russian boreholes and 85–8A is 10 m, Gulkana, Oldman and Alert are 15 m, and 20m for all other boreholes. Borehole locations are: ZS-124 – 67.48°N 063.48°E; 85-8A – 61.68°N 121.18°W; Gulkana – 62.28°N 145.58°W; YA-1 – 67.58°N 648°E; Oldman – 66.48°N 150.68°W; Happy Valley – 69.18°N 148.88°W; Svalbard – 78.28°N 016.58°E; Deadhorse –70.28°N 148.58°W; West Dock – 70.48°N 148.58°W; Alert – 82.58°N 062.48°W.

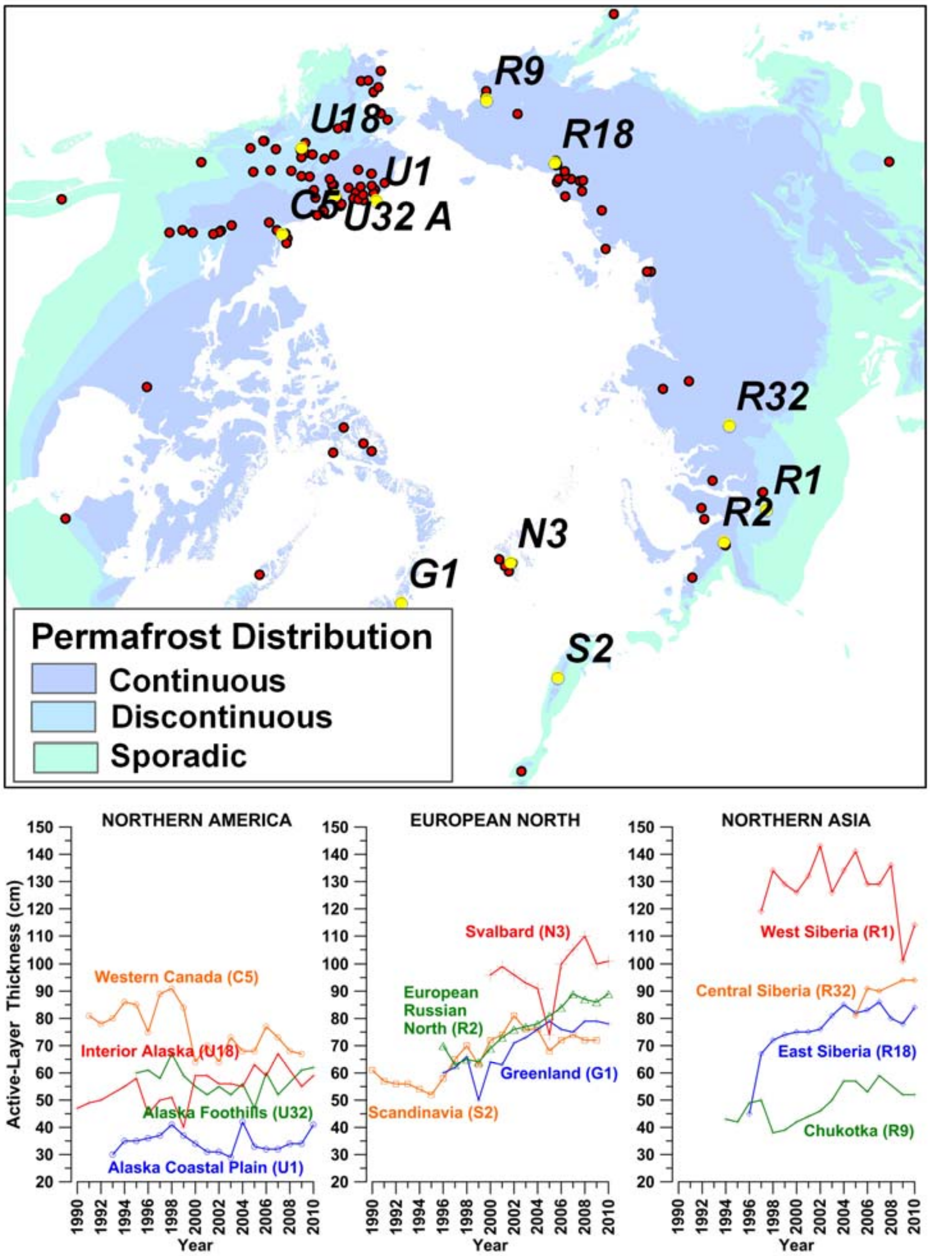

Figure 4.23: Locations for the Circumpolar Active Layer Monitoring (CALM) sites (top) and changes in active layer thickness (bottom) from Shiklomanov et al. (2010).

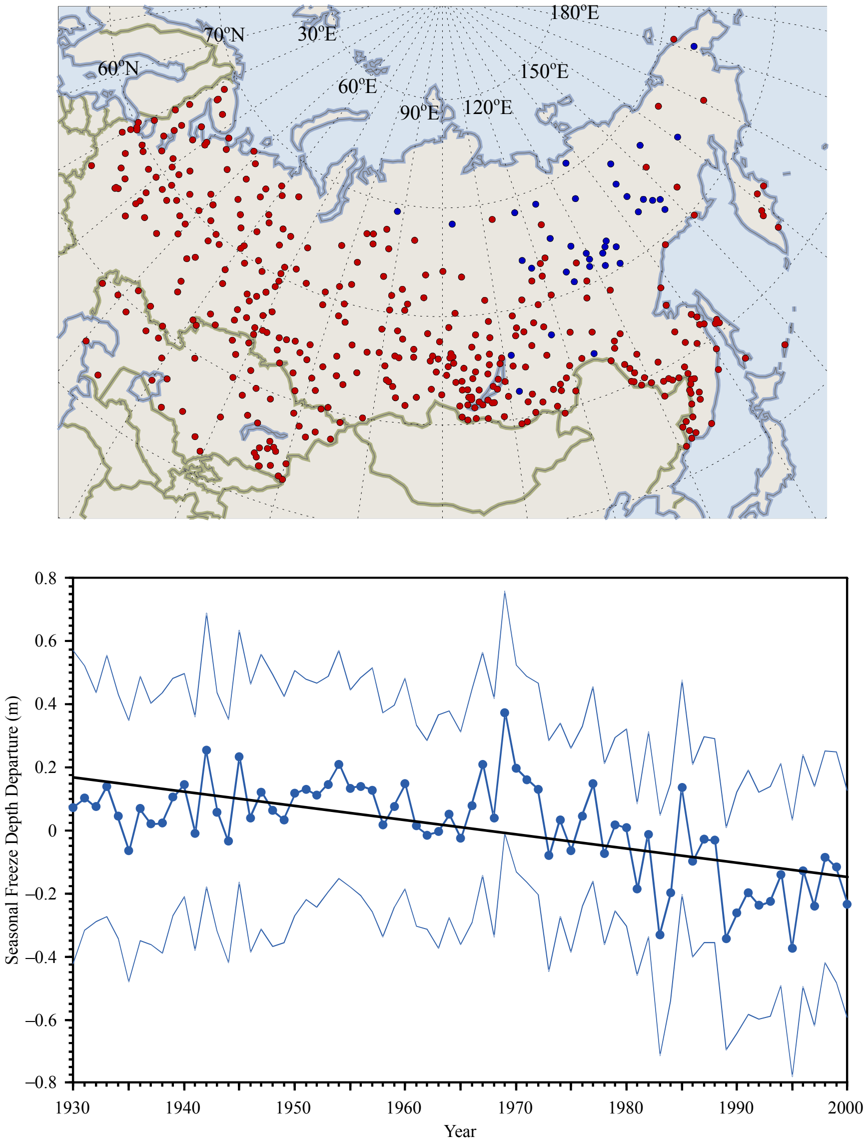

Figure 4.24: Top: distribution of hydrometeorological stations across Russia; bottom: changes in thickness of seasonally frozen ground (From Frauenfeld and Zhang, 2011).

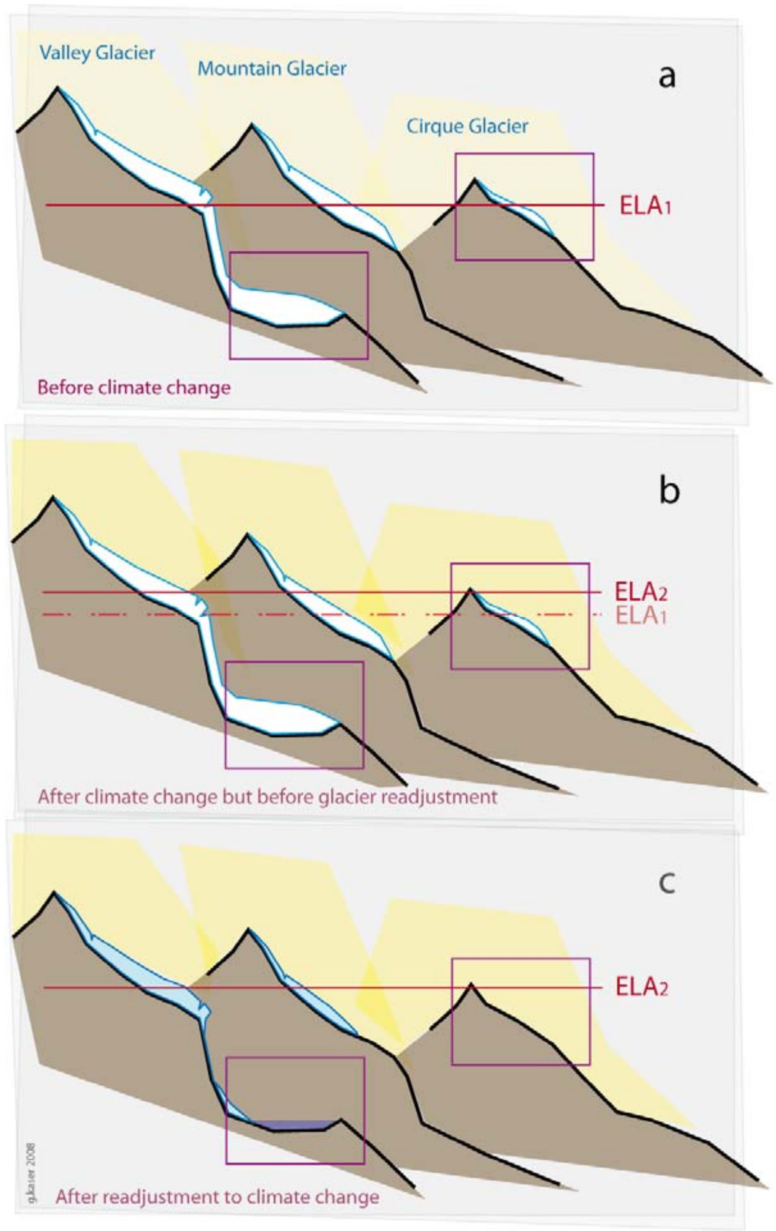

FAQ 4.1, Figure 1: Schematic of three types of glaciers located at different elevations and their response to an upward shift of the equilibrium line altitude ELA. (a) For a given climate, the EL has a specific altitude (ELA1) and all glaciers have a specific size. (b) Due to a temperature increase the ELA shifts upwards to a new altitude ELA2, initially resulting in reduced accumulation and larger ablation areas for all glaciers. (c) After glacier size has adjusted to the new ELA, the valley glacier (left) has lost its tongue and the small cirque glacier (right) has disappeared entirely.

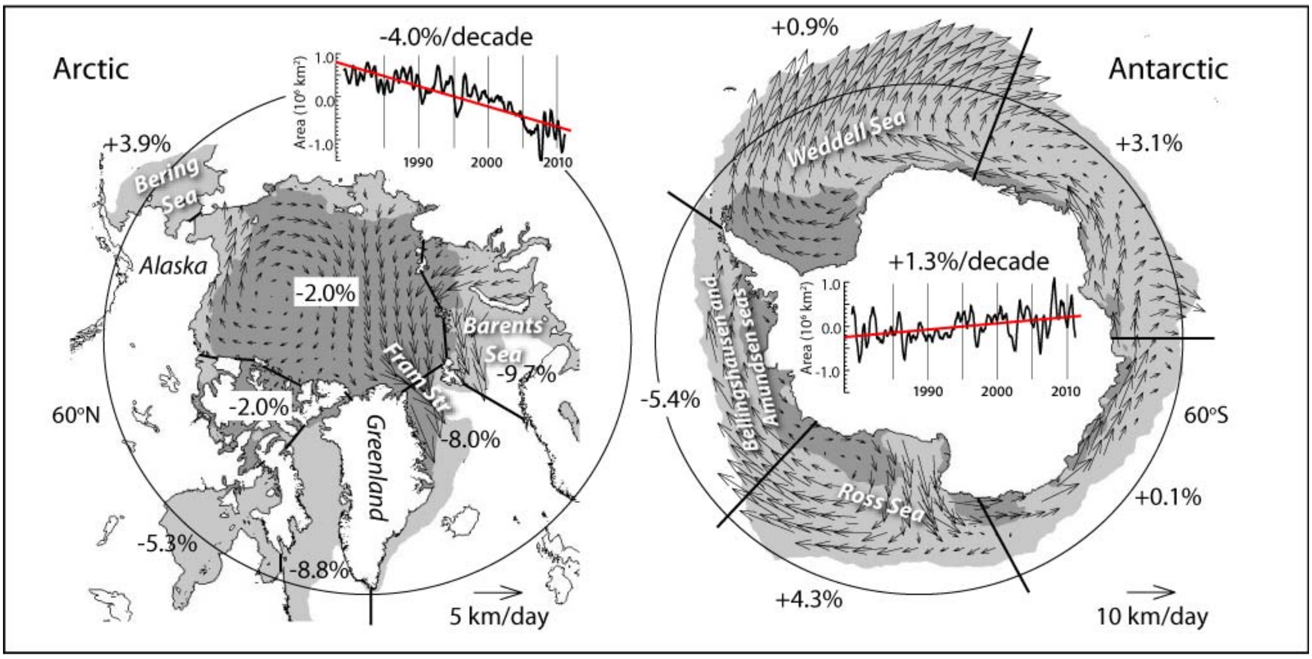

FAQ 4.2, Figure 1: The mean circulation pattern of sea ice and the decadal trends (%) in annual average ice extent in different sectors of the Arctic and Antarctic. The average sea ice cover for the period 1979–2010, from satellite observations, at maximum (minimum) extent is shown as light (dark) grey shading.